Measurements of 1st, 2nd and 3rd azimuthal anisotropy in $\sqrt{s_{NN}}$=200GeV Cu+Au collisions at RHIC-PHENIX

RHIC-PHENIX実験における$\sqrt{s_{NN}}$**=200GeV** 銅・金衝突での**1**次、**2**次、**3**次方位角異方性の測定

中込宇宙

博士論文本審査 **2016**年**12**月**19**日

Outline

✓Introduction

- Quark Gluon Plasma(QGP)
- Azimuthal anisotropy
- CuAu collisions

✓Experiment/Analysis

- PHENIX
- centrality, event plane
- Simulation

✓Results/Discussions

- v_n at mid, forward/backward rapidities
- Initial model study

✓Summary

Introduction

Quark Gluon Plasma(QGP)

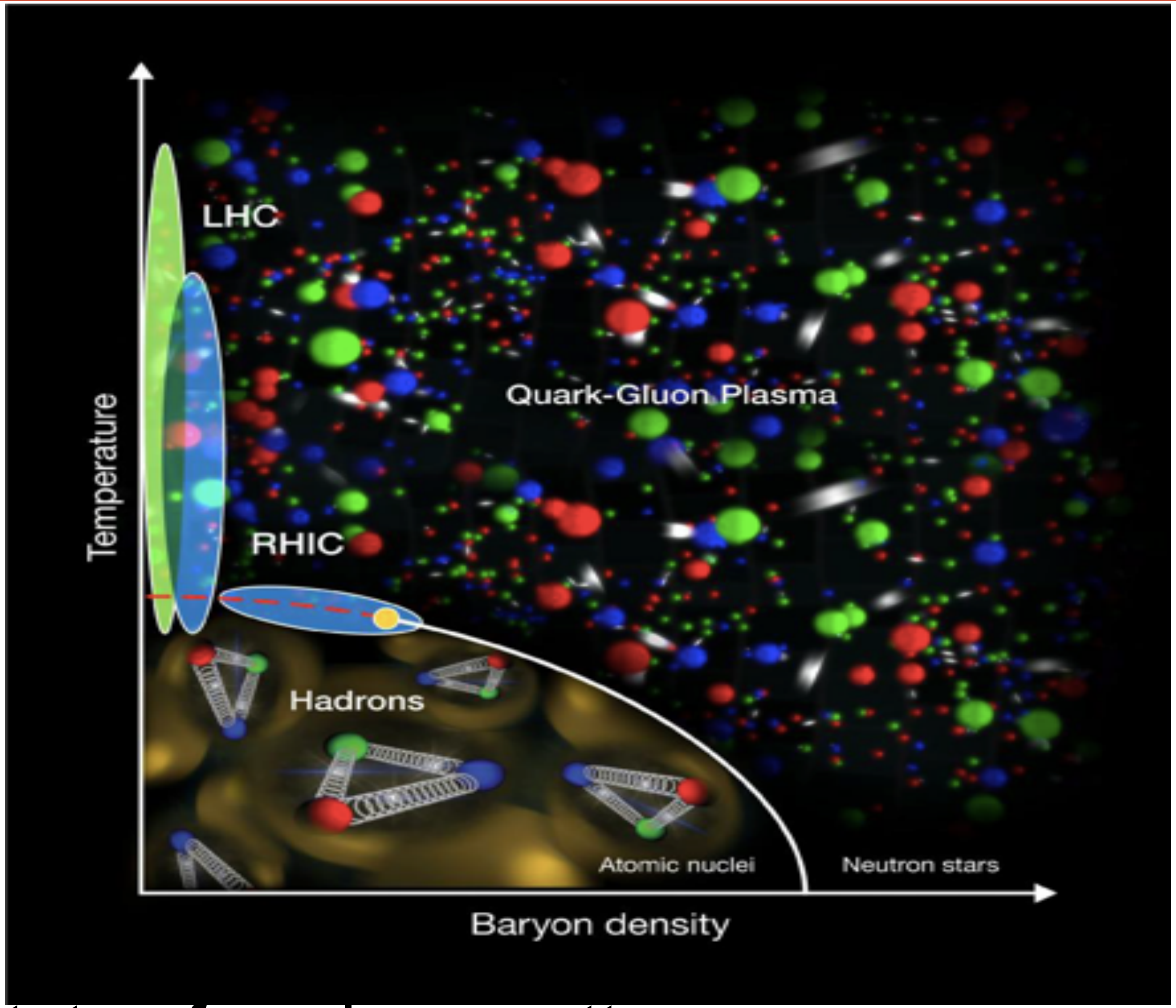

QGP is a state of nuclear matter

- extremely high temperature, density
- consist of asymptotic free quarks and gluons
- Almost perfect liquid

Predicted phase transition ε_c and T_c by Lattice QCD calculation

- $T_c \sim 170$ MeV
- $\varepsilon_c \sim 1$ [GeV/fm^3]

Relativistic Heavy Ion Collider(RHIC)

Species	Energies
Au+Au	200, 130, 62.4GeV 39, 27, 22.4GeV 19.6 14.6, 7.7GeV
Cu+Cu	200, 62.4, 22.4GeV
U+U	193GeV
Cu+Au	200GeV
3He+Au	200GeV
d+Au	200GeV
p+Au	200GeV
p+Al	200GeV
p+p	510, 500, 200GeV 62.4GeV

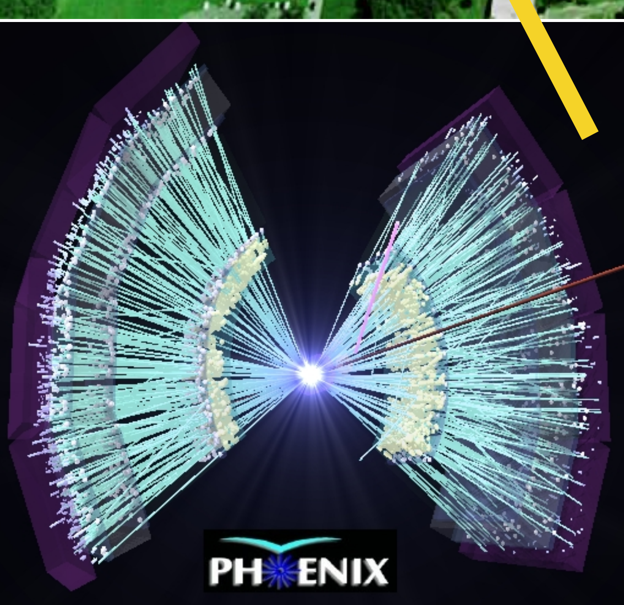

✓ Wide range of species and energies

Relativistic heavy ion collision is unique tool to form QGP

Au+Au 200GeV@RHIC

- $\varepsilon_{Bj} \sim 5$ [GeV/fm^3] > ε_c

Azimuthal anisotropy:Elliptic flow

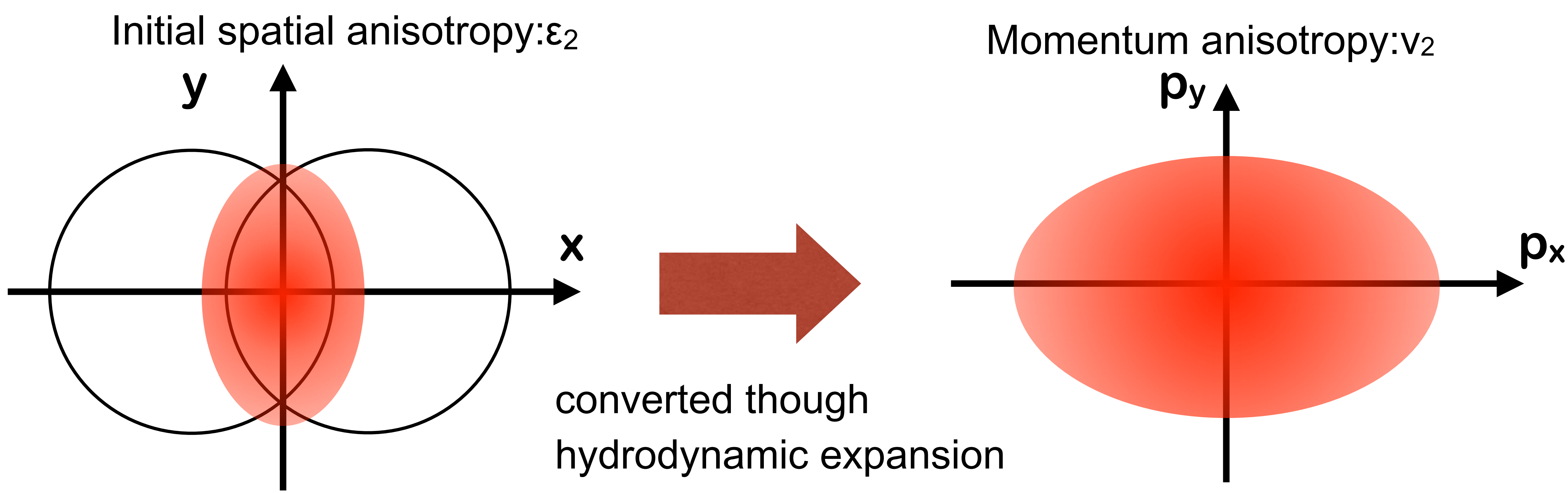

✓Initial spatial anisotropy ε_2 -> Final momentum anisotropy v_2

- Non-isotropic pressure gradient
- Larger initial energy density makes larger v_2

✓Azimuthal anisotropy is strong probe!

- Clear origin -> initial spatial geometry
- Influenced by hydrodynamic expansion

Azimuthal anisotropy:Directed,Triangular flow

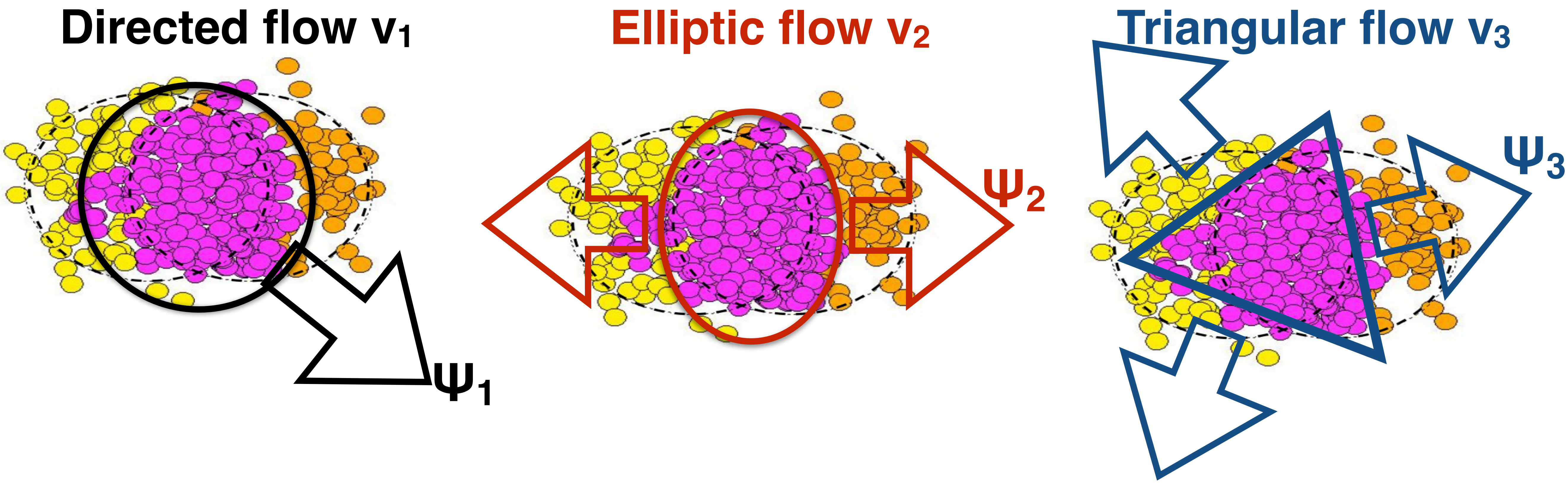

✓Initial geometry is not smooth picture!

- Event by event, initial participant is fluctuated

✓Coefficients in Fourier expansion of particle distribution

$$v_n = < \cos[n(\phi - \Psi_n)] >$$

$$\frac{dN}{d\phi} \propto 1 + \sum_{n=1} 2v_n \cos[n(\phi - \Psi_n)]$$

v_n constrain initial condition & viscosity

v2, v3 theory comparison

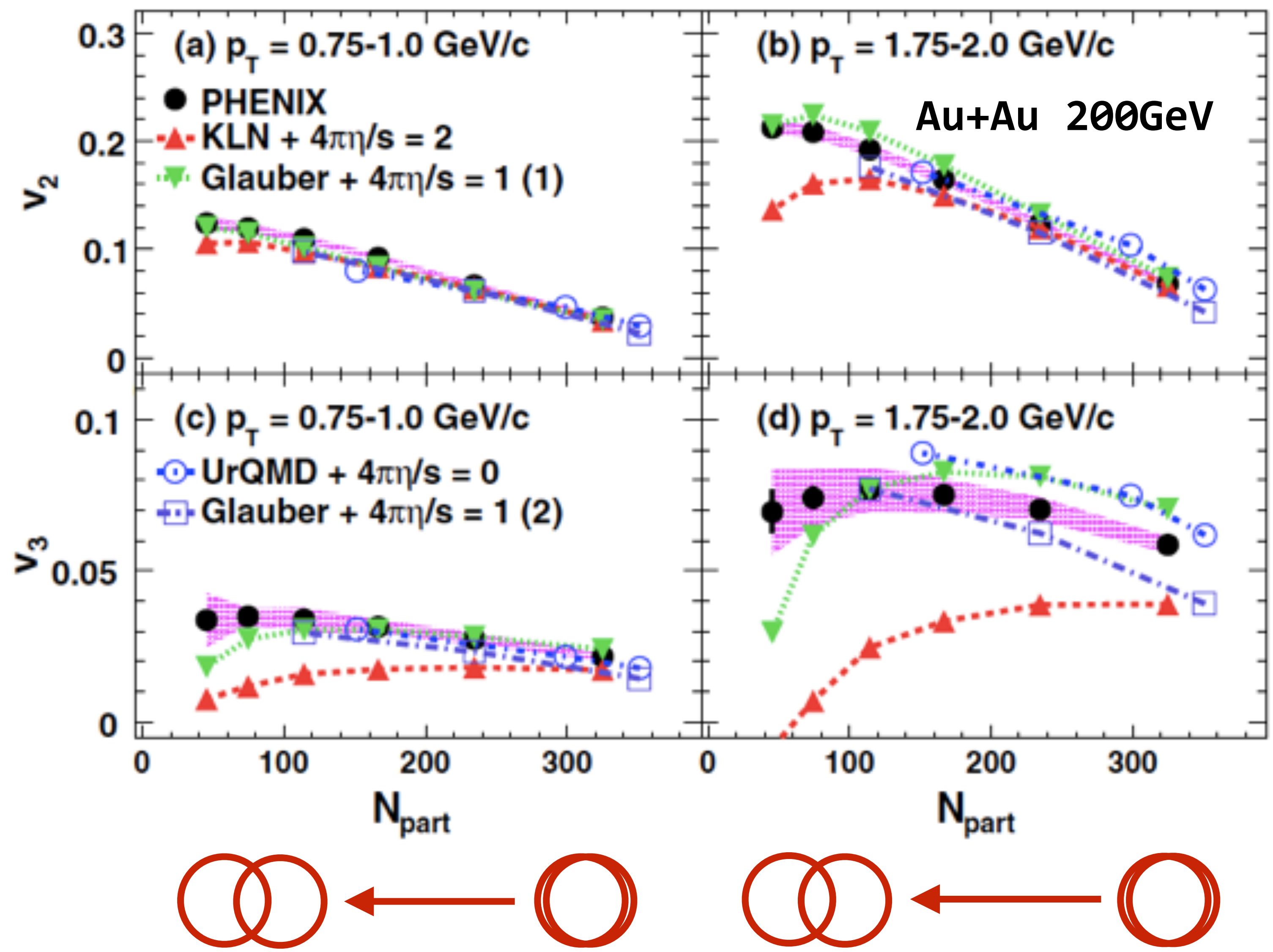

✓v_2, v_3 are sensitive to initial condition and viscosity of QGP

- Theoretically, initial condition and viscosity have uncertainty

➡v_n are good constraint of the initial geometry and viscosity

η dependence of v_2

Initial geometry after the collisions

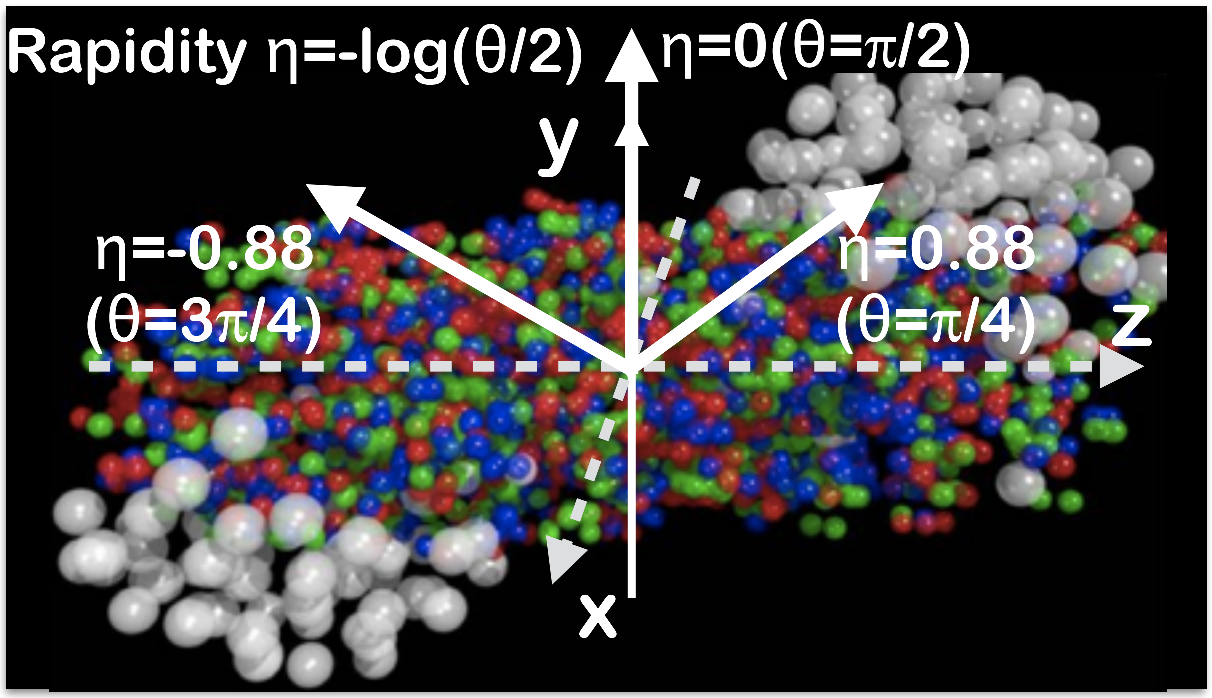

Final momentum anisotropy

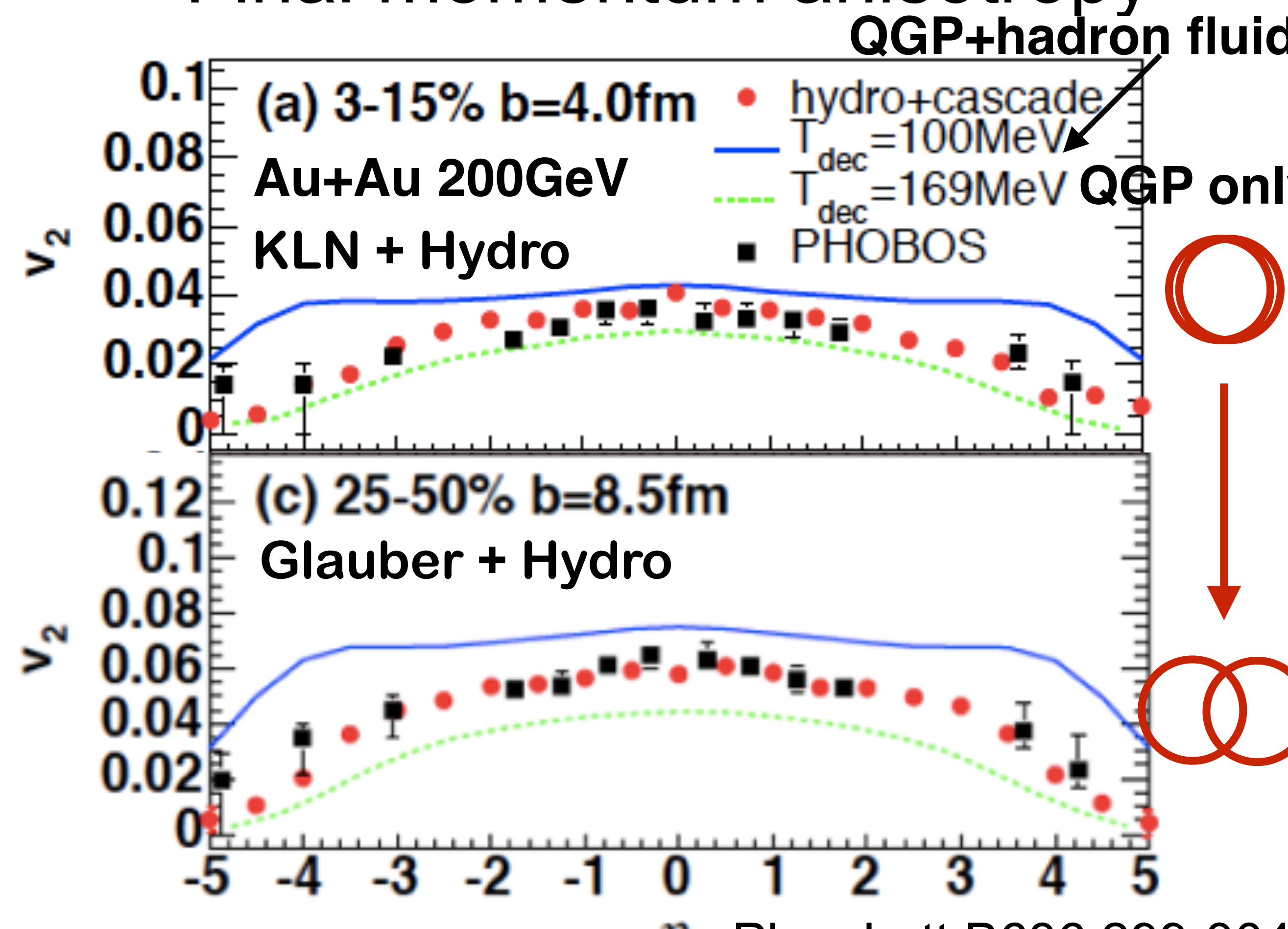

Phys.Lett.B636:299-304

✓At mid-η, v_2 is largest and f/b-η, v_2 becomes small

- Larger dN/dη at mid-η and smaller dN/dη at f/b-η
- Understand η dependence of initial geometry is important

✓v_2(η) depends on initial condition

-Not strong η dependence of initial geometry

-Mid-central:Glauber, Central:KLN

Rapidity dependence of initial condition

Initial geometry $\varepsilon_{2,B} < \varepsilon_{2,F}$

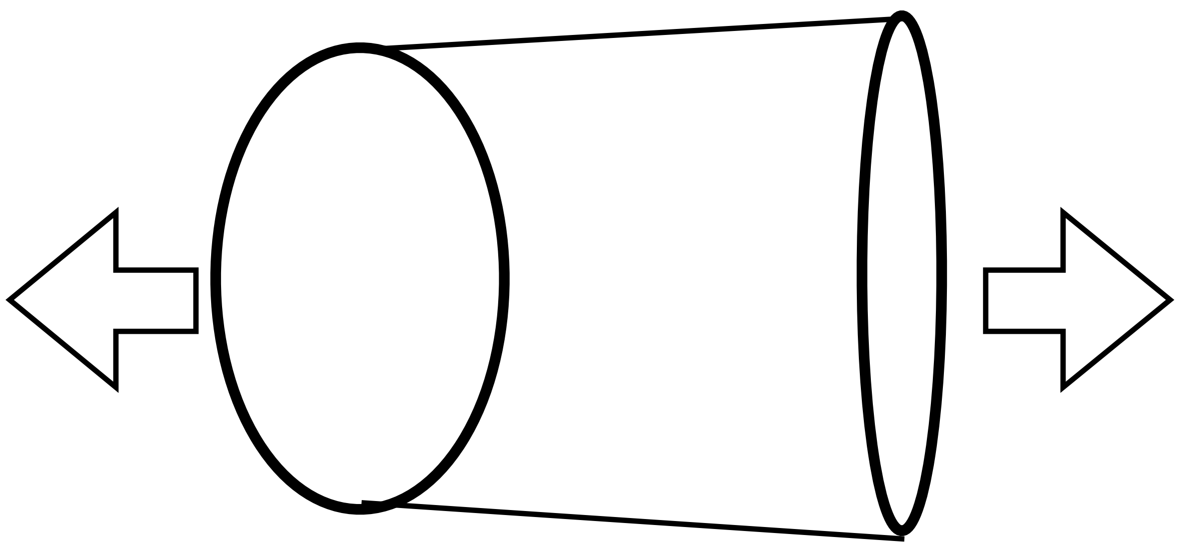

PhysRevC.90.034915

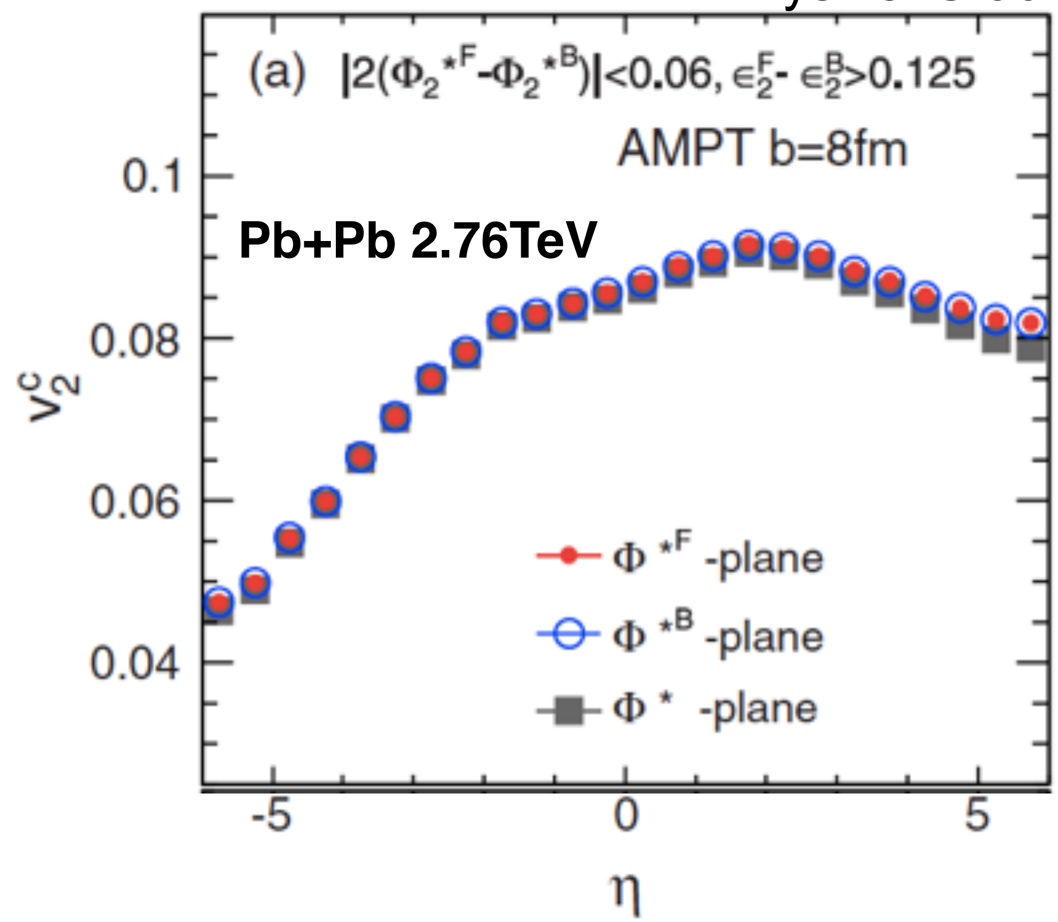

✓Initial geometry has been considered to be rapidity independent

✓Event by event, forward/backward v_n might be asymmetric

- initial participant geometries of the two nuclei would be different
- $\varepsilon_{n,B} < \varepsilon_{n,F}$ ➡ $v_{n,B} < v_{n,F}$

➡ Initial geometry has strong rapidity dependence

Motivation: Why Cu+Au is analyzed ?

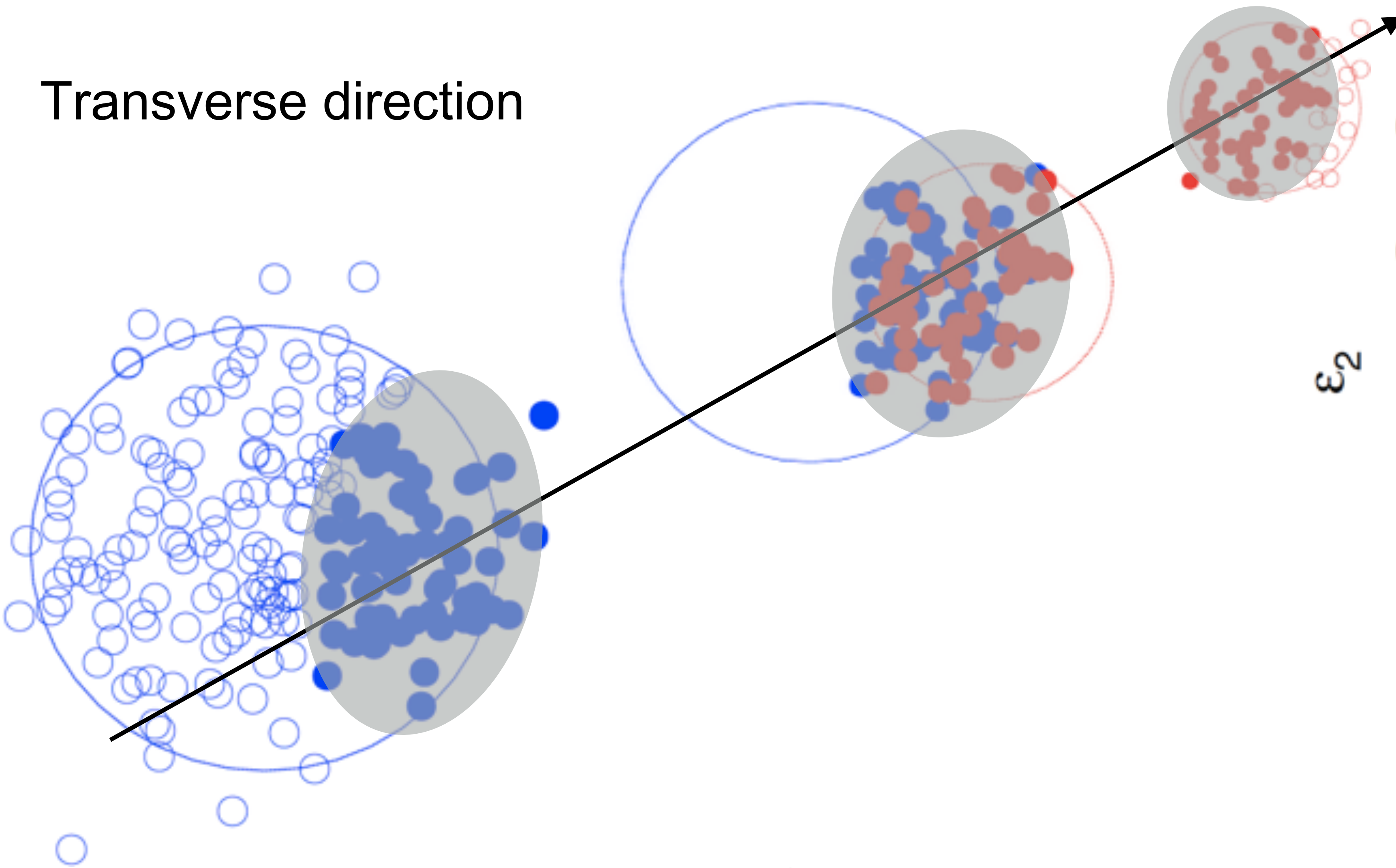

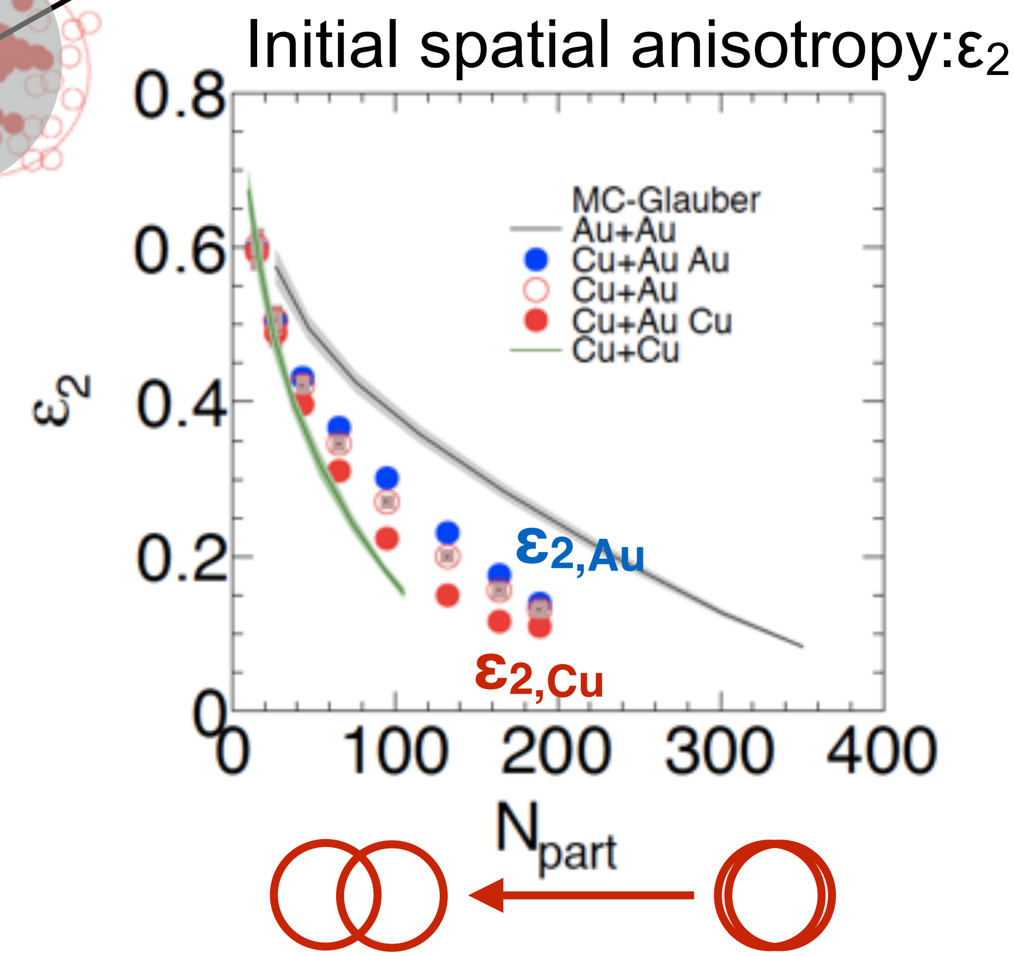

✓First asymmetric Cu+Au collisions were operated in 2012

✓Asymmetric initial condition provides

-Different left/right pressure gradient -> v_1

-Different Forward/Backward density and geometry

-> Rapidity asymmetric v_n

-> Measurements of v_n in asymmetric system could be good study of initial condition

My activity

M1~M2 (2011~2013)

Repair VTX @BNL

JPS Spring & Fall (Talk)

QM2012 (poster)

ATHIC 2012 (Talk)

Au+Au flow analysis using VTX

D1(2013~2014)

Repair VTX @BNL

Shift taking & detector expert for Run 13, Run14

Cu+Au flow analysis

D2 (2014~2015)

QM2014(Talk)

JPS-DNP(Talk)

Shift taking & detector expert for Run 14, Run15

D3(2015~2016)

QM2015(Poster)

TGSW2015 (Talk)

WWND2016(Talk)

D4 (2016~)

Cu+Au flow paper is accepted by PRC

PRC 94, 054910

Domestic conference

International conference

Hardware and shift

Analysis

Experiment

Analysis

PHENIX detectors

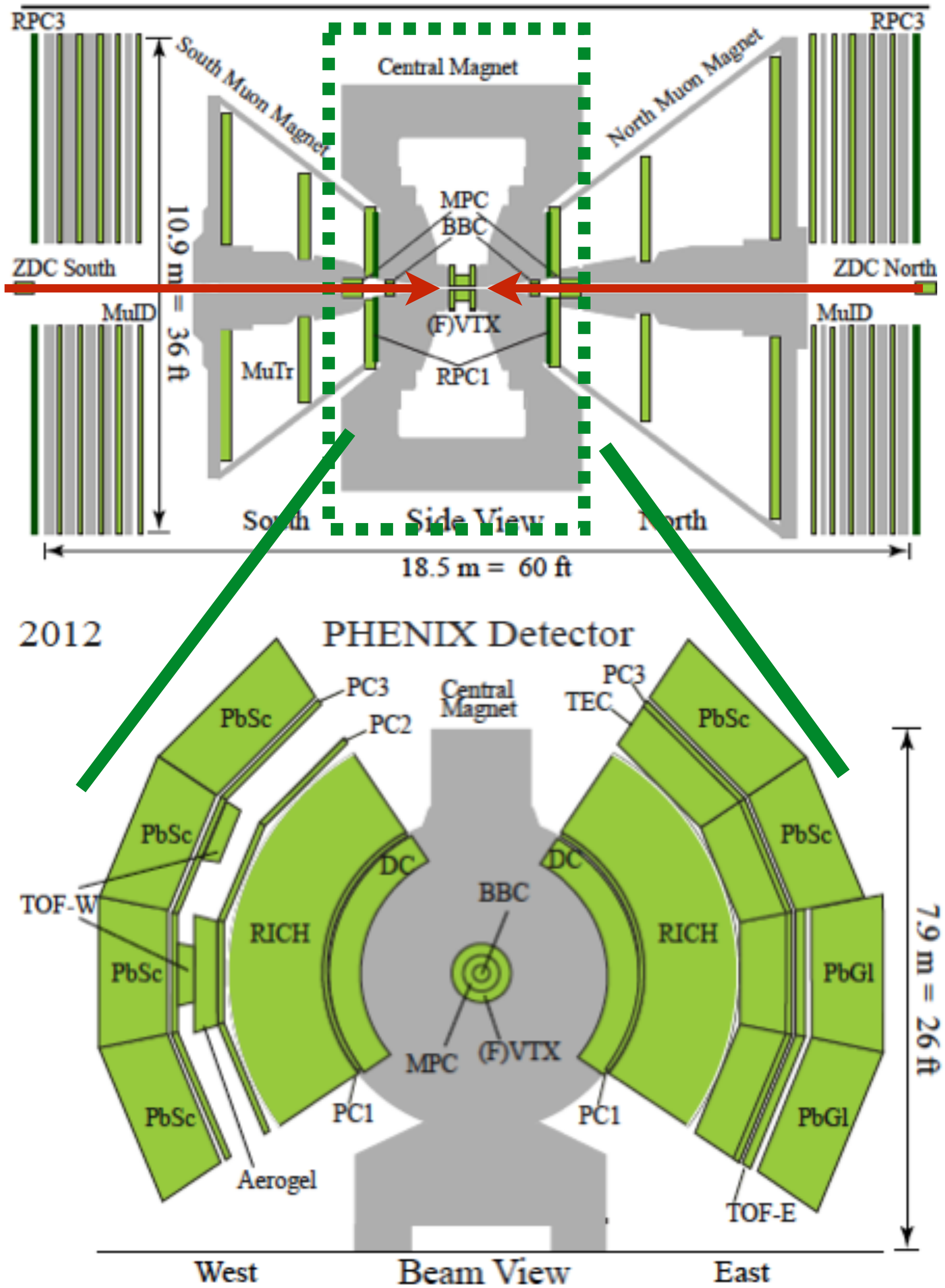

Trigger, centrality, collision vertex
Event plane
-Beam Beam counter(BBC)
(3<|η|<4)
Event plane
-Zero degree calorimeter
-Shower max detector

Charged particle Tracking
-Drift Chamber(DC) (|η|<0.35)
- Momentum
-Pad Chamber(PC) (|η|<0.35)
- Hit position
-Electro magnetic calorimeter(EMC) (|η|<0.35)
- Hit position

N_{part} & Centrality

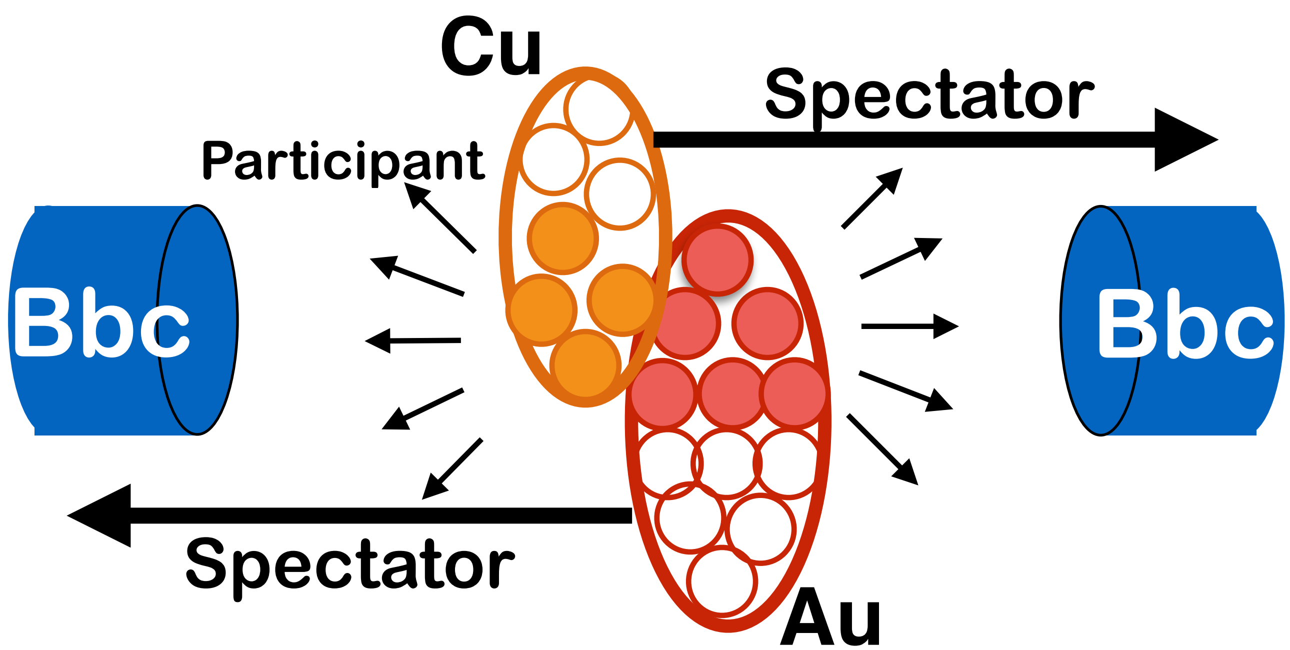

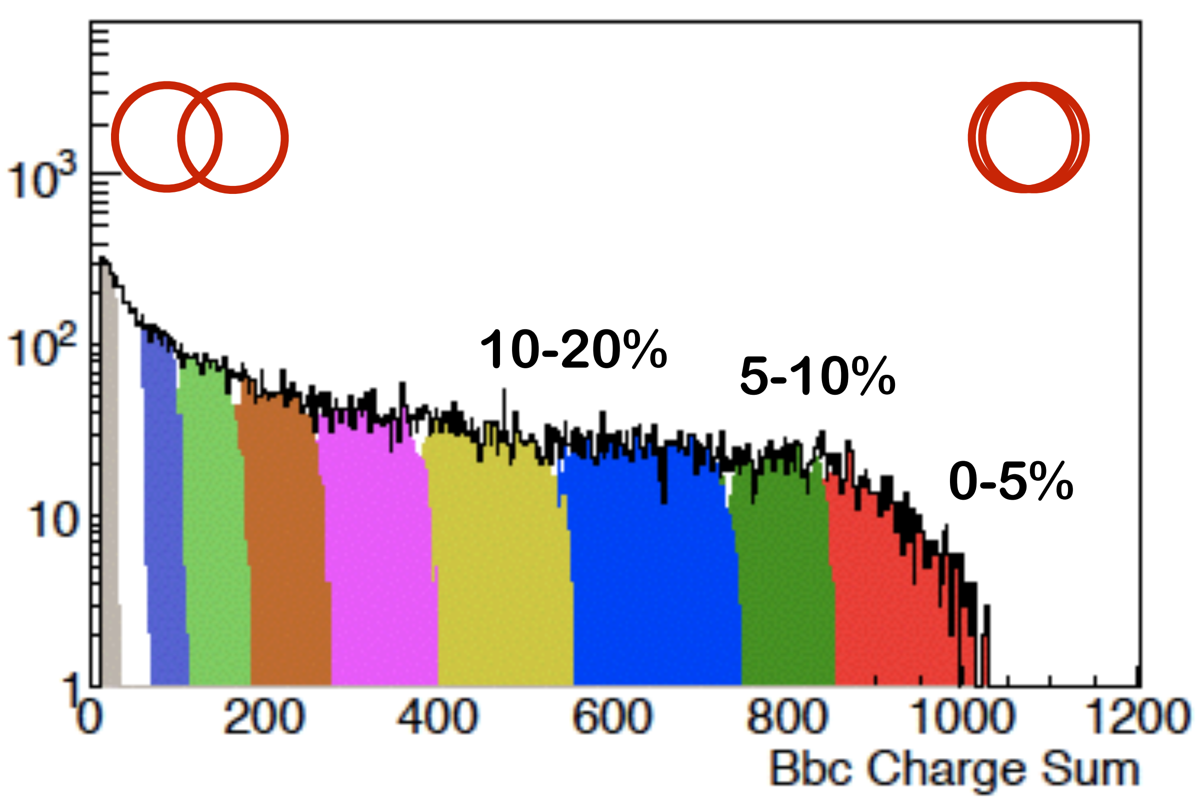

N_{part}

✓Number of participants
- e.g. Cu 4 , Au 6

✓Estimated by Glauber model
- nucleon base

Centrality

✓Fraction of events in terms of total geometrical cross section

-Overlap zone of two nuclei∝ Multiplicity

✓ Experimentally, overlap zone is classified by multiplicity in Bbc

- Multiplicity in Bbc ∝ Overlap zone

✓0%(central) 100%(peripheral)

Anisotropy measurement via Event Plane method

Event plane(EP) method

- one of the flow measurement methods
- produced particles are measured with respect to EP
- EP is the azimuthal direction most particles are emitted to
- observed v_n is corrected by EP resolution

$$v_n = \frac{< \cos(n[\phi - \Psi_n^{obs}]) >}{\mathrm{Res}\{\Psi_\mathrm{n}^\mathrm{obs}\}}$$

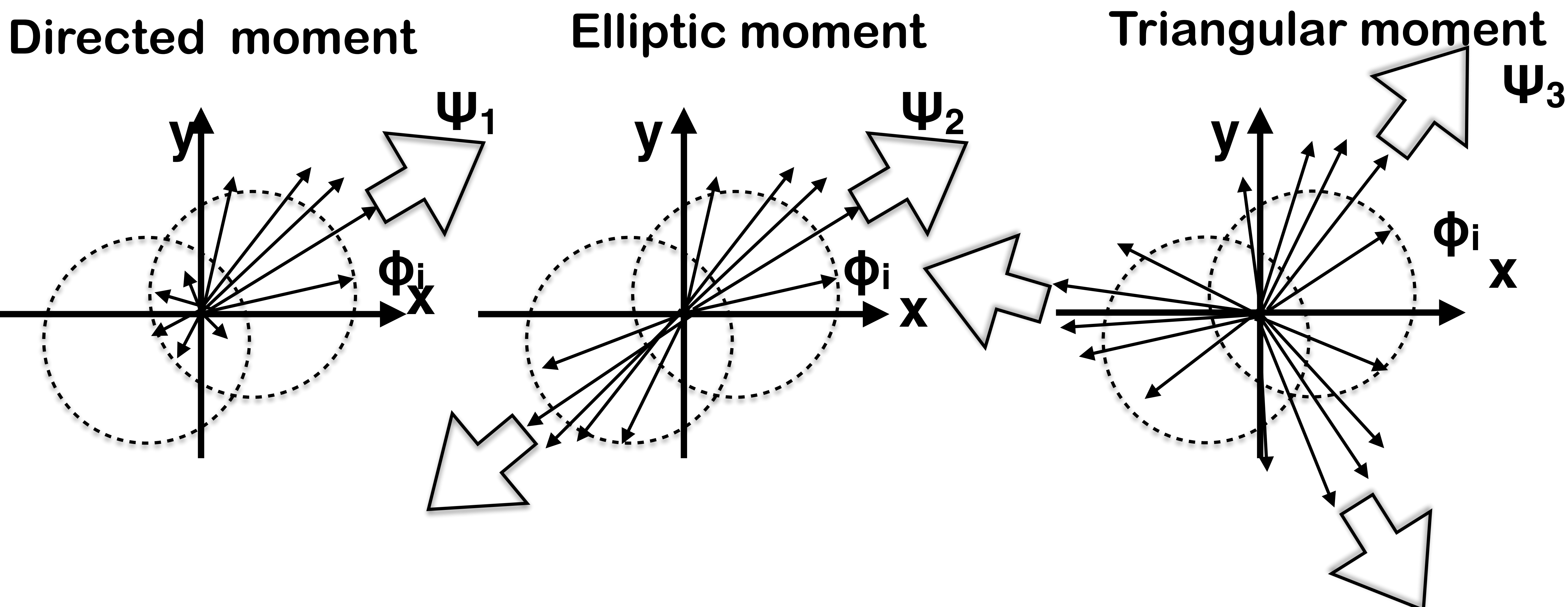

Event plane detectors and resolutions

Event Plane detectors

- 2nd, 3rd Event plane
  - Bbc, Cnt
- 1st Event plane
  - Bbc, Smd

PHENIX η acceptance

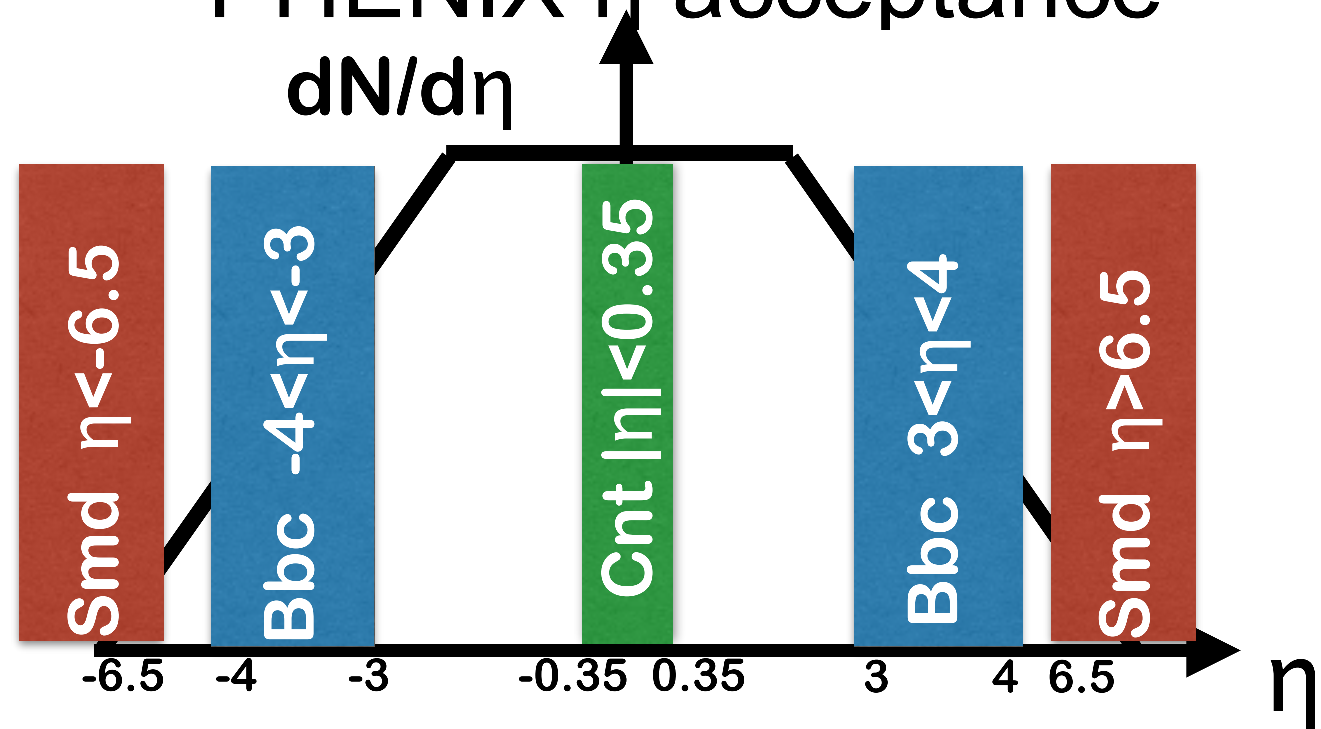

Event Plane resolution

$$\mathrm{Res}\{\Psi_n^{\mathrm{obs}}\} =< \cos(n[\Psi_n^{\mathrm{obs}} - \Psi_n^{\mathrm{true}}]) >$$

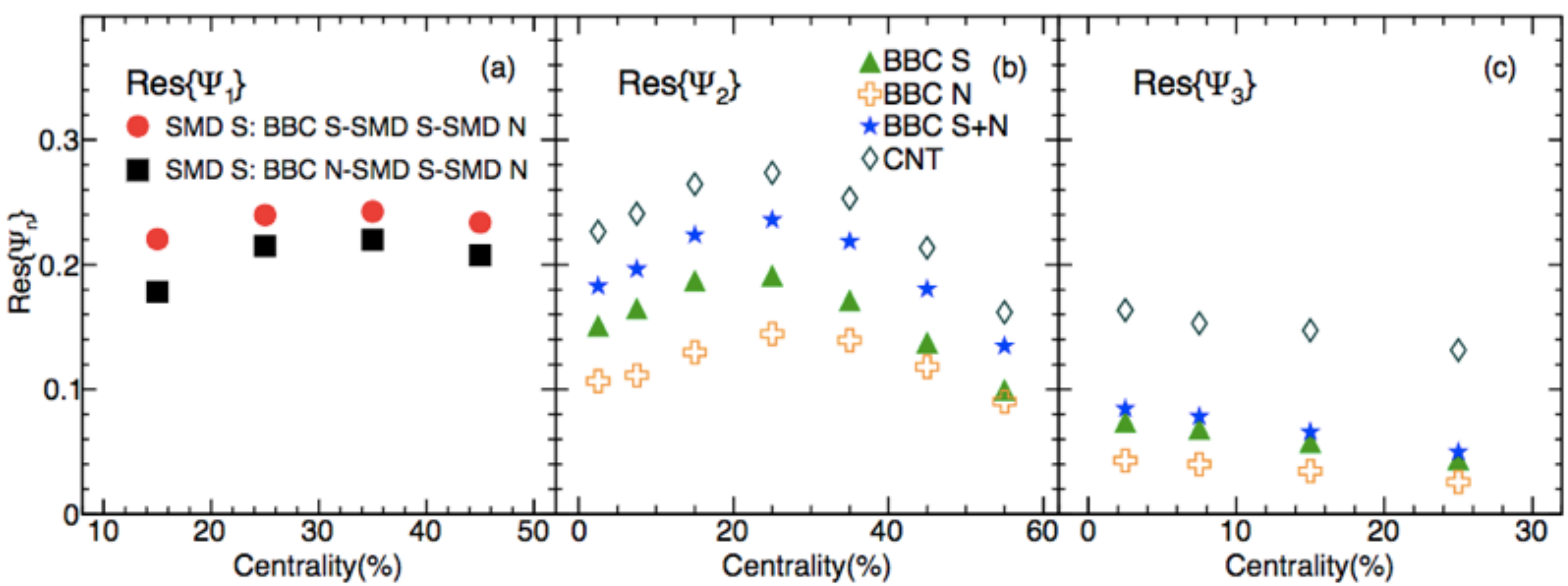

v_n measurement at Bbc($3<|\eta|<4$)

✓ v_n is measured using 64 Bbc pmts

- Bbc can not reconstruct tracks
- Measured v_n include back ground

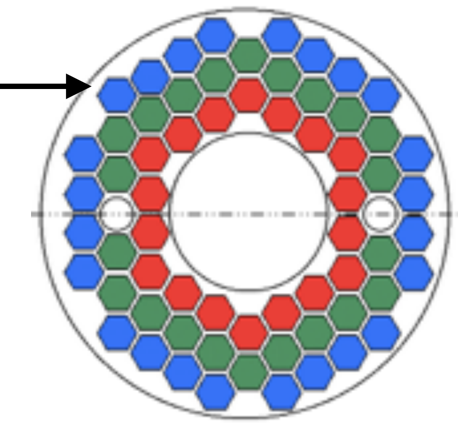

✓ Full Geant simulation with PHENIX configuration

- Measured v_n -> True v_n

$$v_n^{\text{true}} = \frac{v_n^{\text{mes}}}{R_n} \qquad R_n = \frac{v_{n,\text{output}}^{\text{Sim}}}{v_{n,\text{input}}^{\text{Sim}}}$$

$v_{n,\text{input}}^{\text{Sim}}$ **Input v_n from particle simulation**

$v_{n,\text{output}}^{\text{Sim}}$ **Output v_n from Geant simulation**

✓ Correction factor R_n

- R_2 : 0.74
- R_3 : 0.66

✓ Systematic study

- $dN/d\eta$
- p_T spectra
- v_n (pt)
- v_n (eta)

Comparison of v_2 to PHOBOS's results

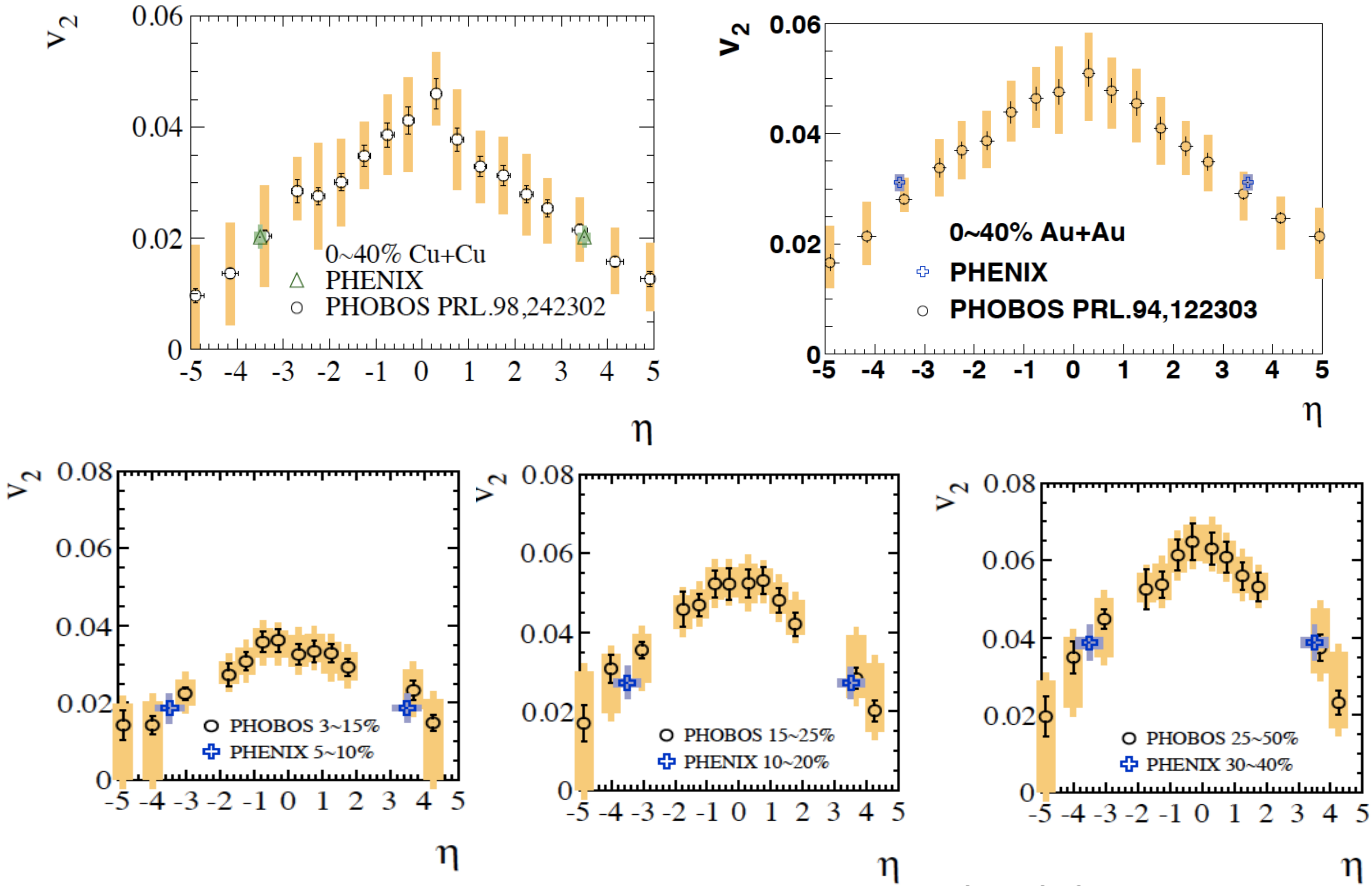

✓My results are consistent with PHOBOS's results

$dN_{ch}/d\eta$ measurements at Bbc

Like v_n measurements, correction factors is estimated from Geant simulation

$$\frac{dN_{ch}}{d\eta} = R * ADC^{\mathrm{obs}}$$

$$R = \frac{2}{3}\frac{1}{ADC^{\mathrm{sim}}_{\mathrm{output}}}$$

2/3:+-π/(+-π,π0)

$ADC^{\mathrm{sim}}_{output}$

R ~0.5

Comparison to PHOBOS

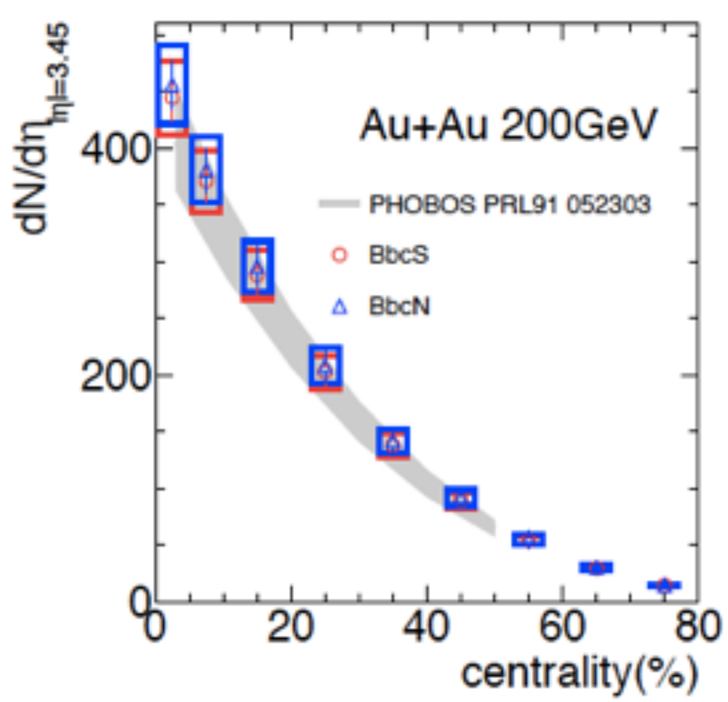

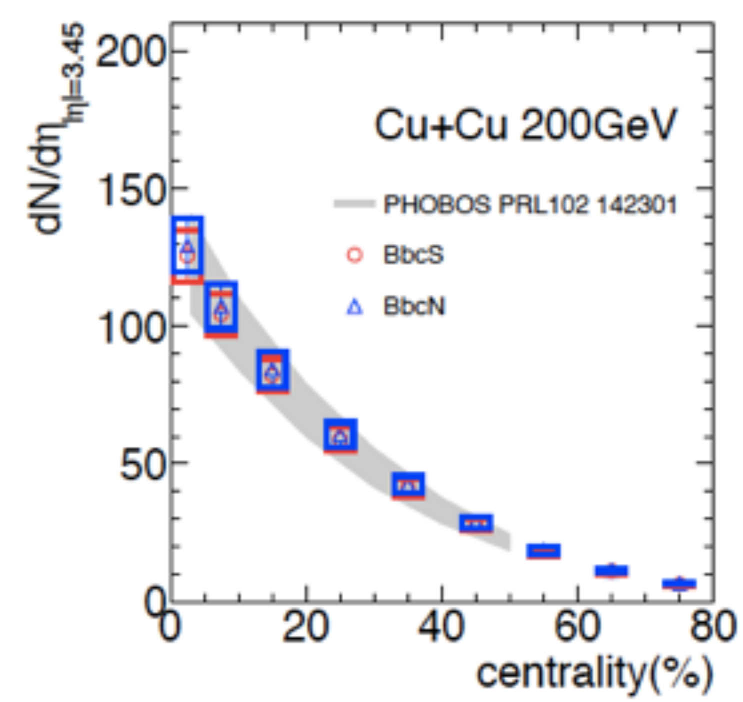

My results are consistent with PHOBOS's results

Systematic sources

✓v_n at mid-η
- East and West arm difference
- CNT track cut
- Event Plane difference
- Event Plane resolution difference

✓v_n at F/B-η
- Event Plane difference
- Geant simulation
  - dN/dη distribution
  - p_T distribution
  - p_T dependence of v_n
  - η dependence of v_n

✓dN/dη at F/B-η
- Geant simulation
  - dN/dη distribution
  - p_T distribution

Results

Discussions

- v_1, v_2, v_3 at mid-η
- Multiplicity at F/B-η
- v_2, v_3 at F/B-η

Charged hadron $v_1(p_T)$ in Cu+Au collisions

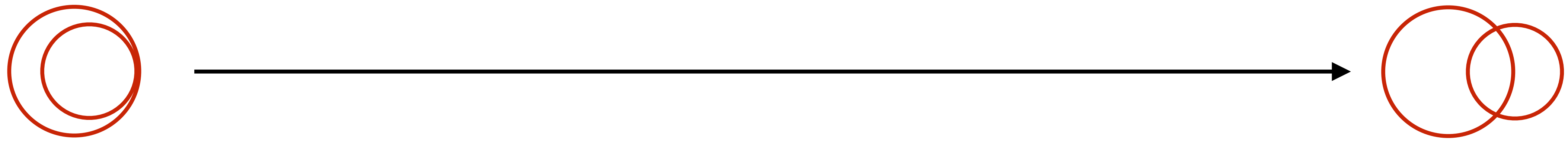

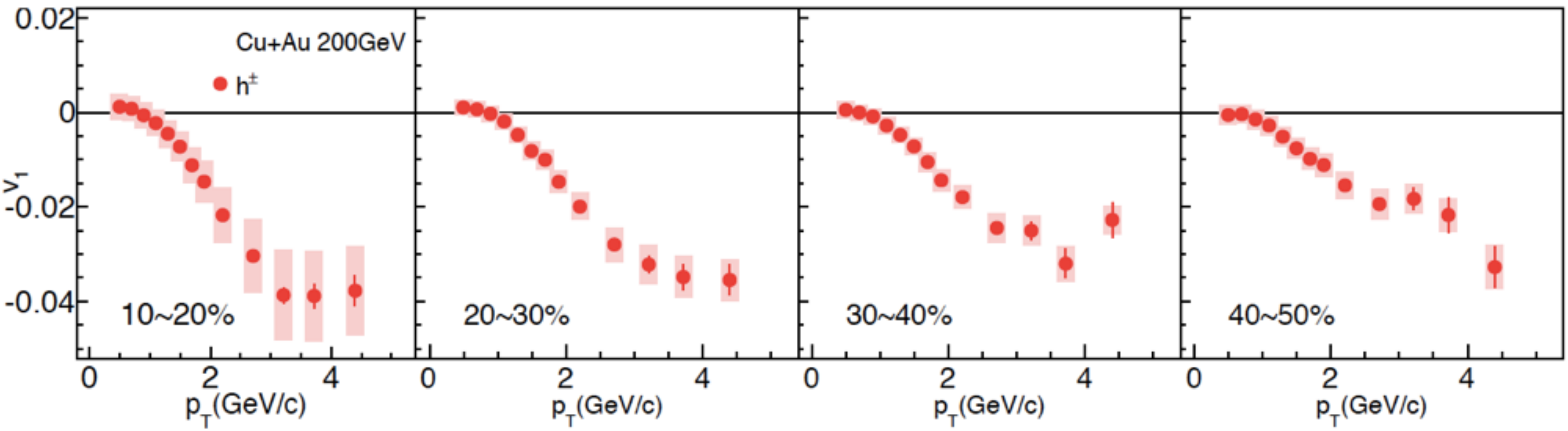

✓v_1 at mid-rapidity is observed with respect to Au spectator for 10-50%

- sigh of v_1 is flipped toward Cu nucleus side

✓Negative v_1 indicates high p_T particle are emitted to Au side

- -Magnitude decreases from central to more peripheral events
- -In peripheral events, Left/Right path length becomes similar

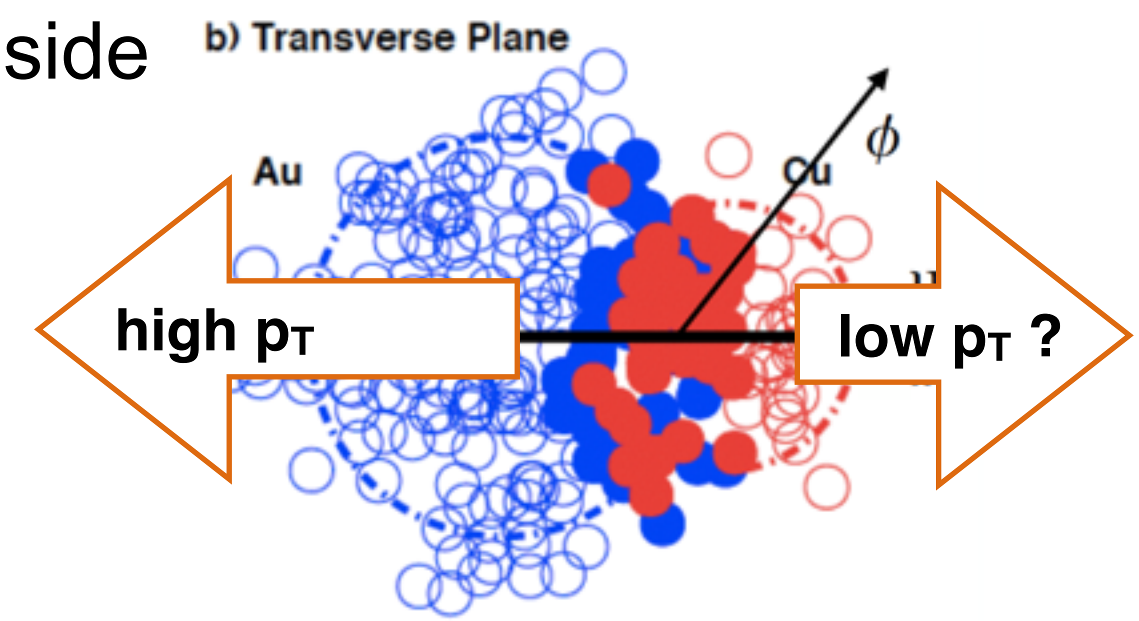

Interpretation of negative $v_1(p_T)$ at higher p_T

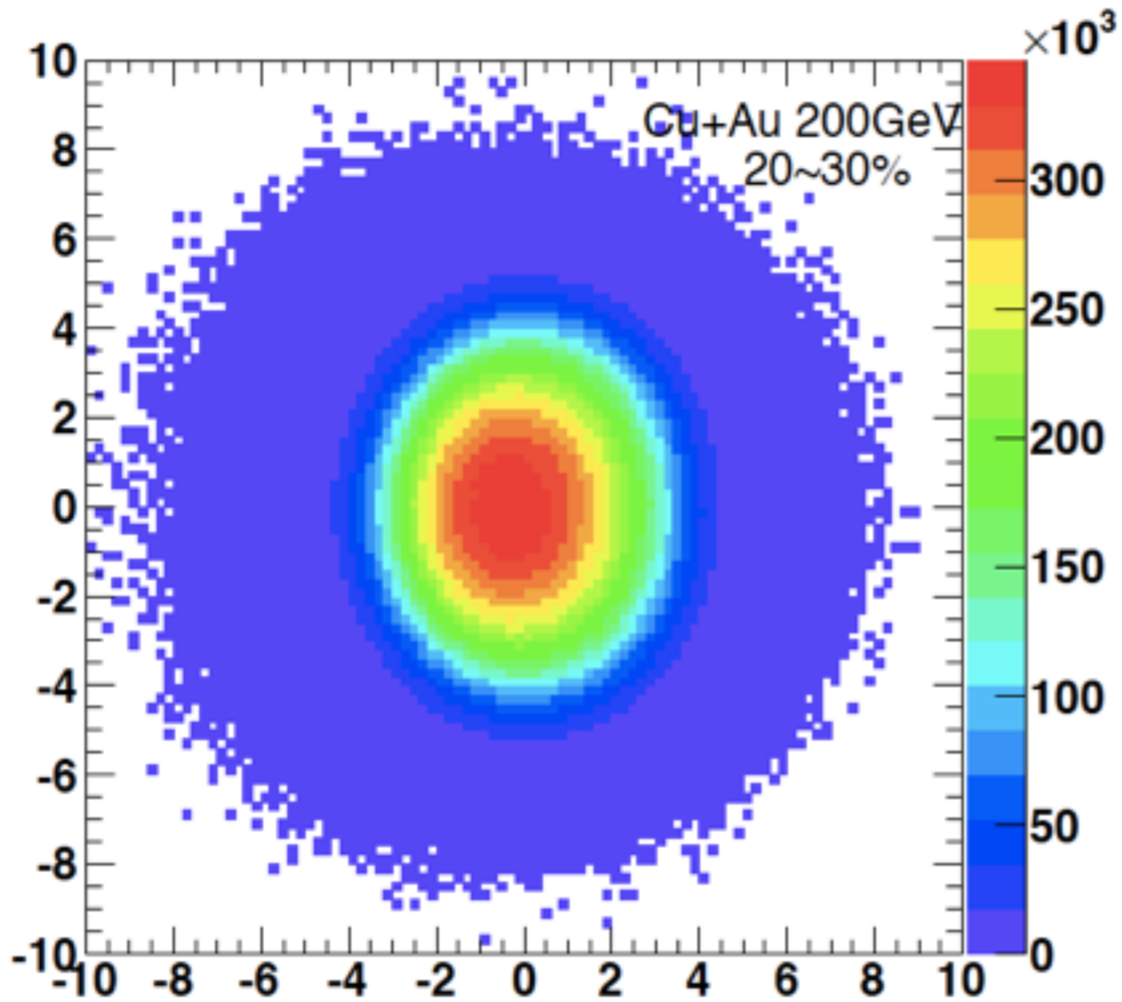

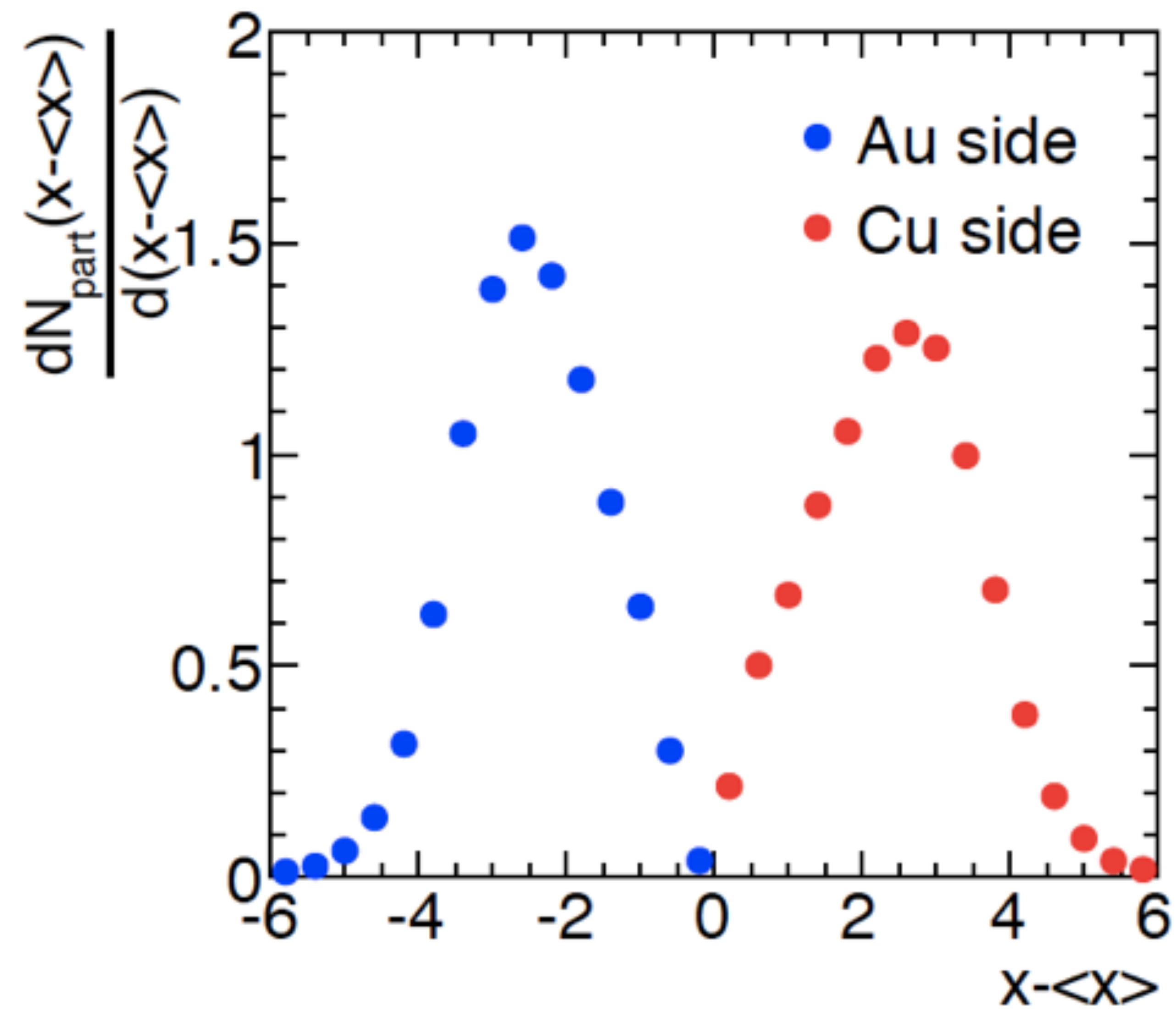

✓Density gradient is larger in Au nucleus side

✓Larger pressure gradient pushes particles to high p_T

-Density gradient induce pressure gradient

- Many high p_T particles are emitted toward Au side

Charged hadron $v_2(p_T)$ in Cu+Au collisions

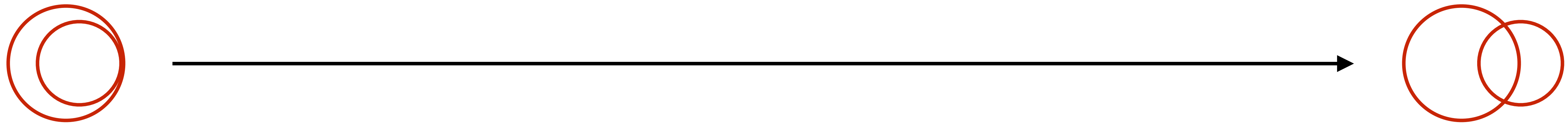

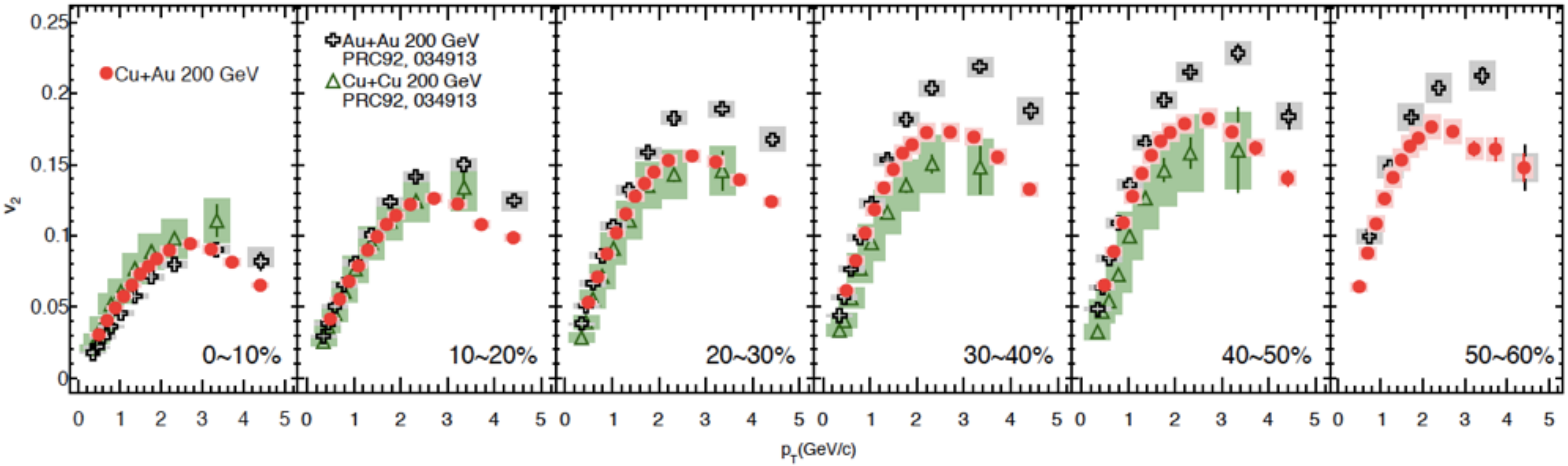

✓Similar p_T and centrality dependence of v_2 as seen in symmetric collisions

- v_2 is measured with respect to Bbc

-Strong centrality dependence, magnitude increase from central to peripheral

-Cu+Au v_2 is between symmetric Au+Au and Cu+Cu collisions

Charged hadron $v_3(p_T)$ in Cu+Au collisions

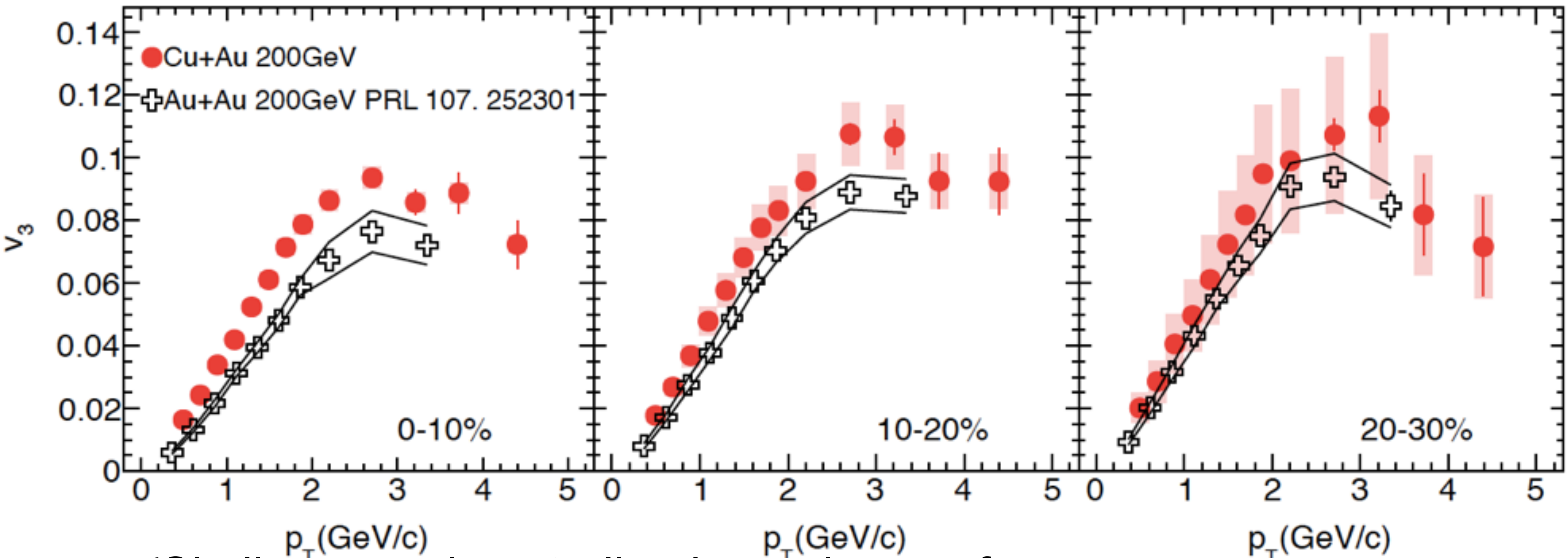

✓Similar p_T and centrality dependence of v_3 as seen in symmetric collisions

- v_3 is measured with respect to Bbc
- Weak centrality dependence, magnitude slightly increase from central to peripheral
- Cu+Au v_3 shows larger values than Au+Au results

System size dependence of $v_n(N_{part})$

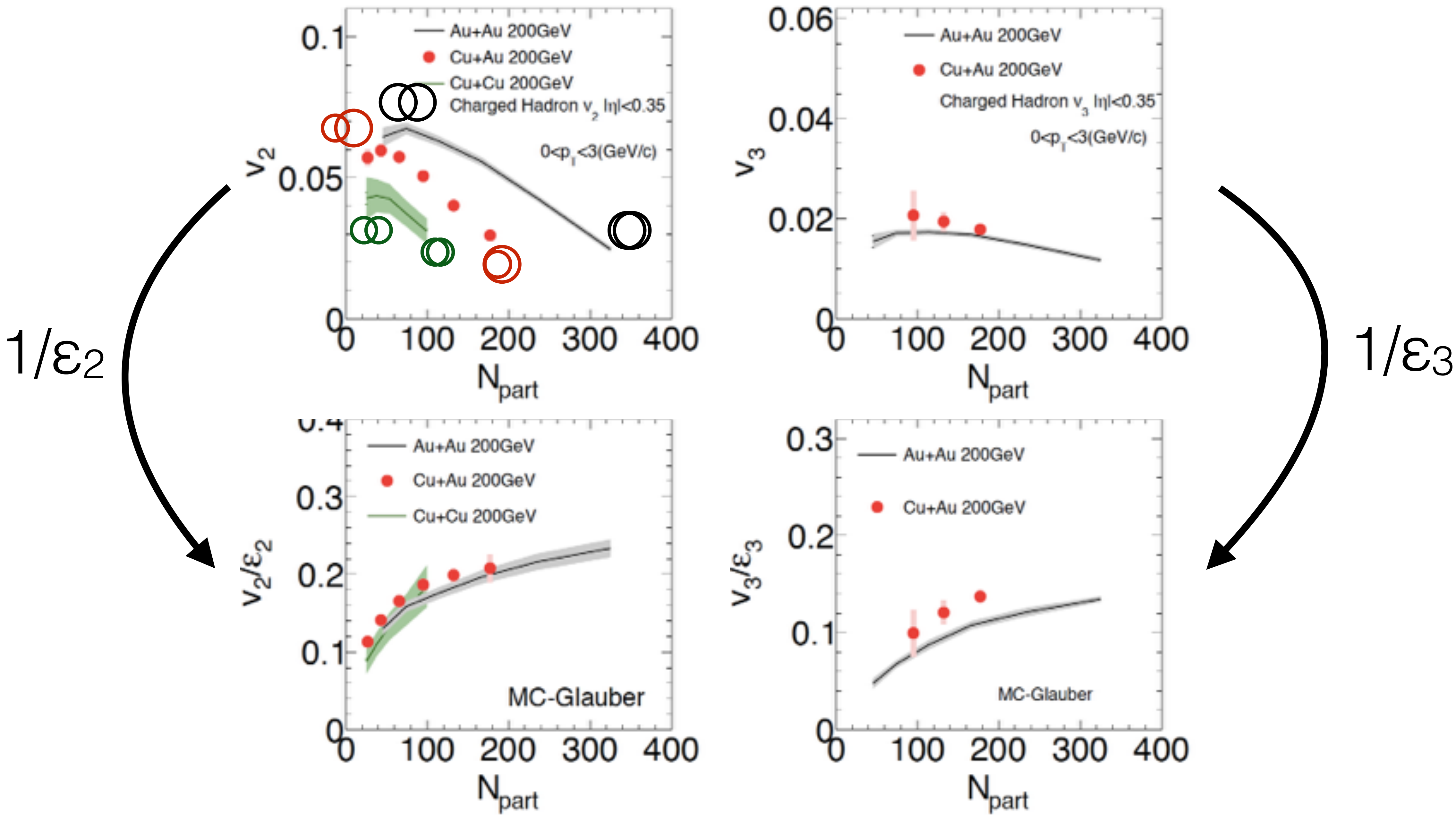

✓Cu+Au v_2/ε_2 is consistent with Au+Au and Cu+Cu results

✓Unlike v_2, Cu+Au v_3 is consistent with Au+Au v_3

✓Cu+A v_3/ε_3 is not consistent with Au+Au results

- MC-Glauber might not reproduce ε_3 correctly

Results

Discussions

- v_1, v_2, v_3 at mid-η
- Multiplicity at F/B-η
- v_2, v_3 at F/B-η

η dependence of charged particle multiplicity

Au-going side ⟷ Cu-going side

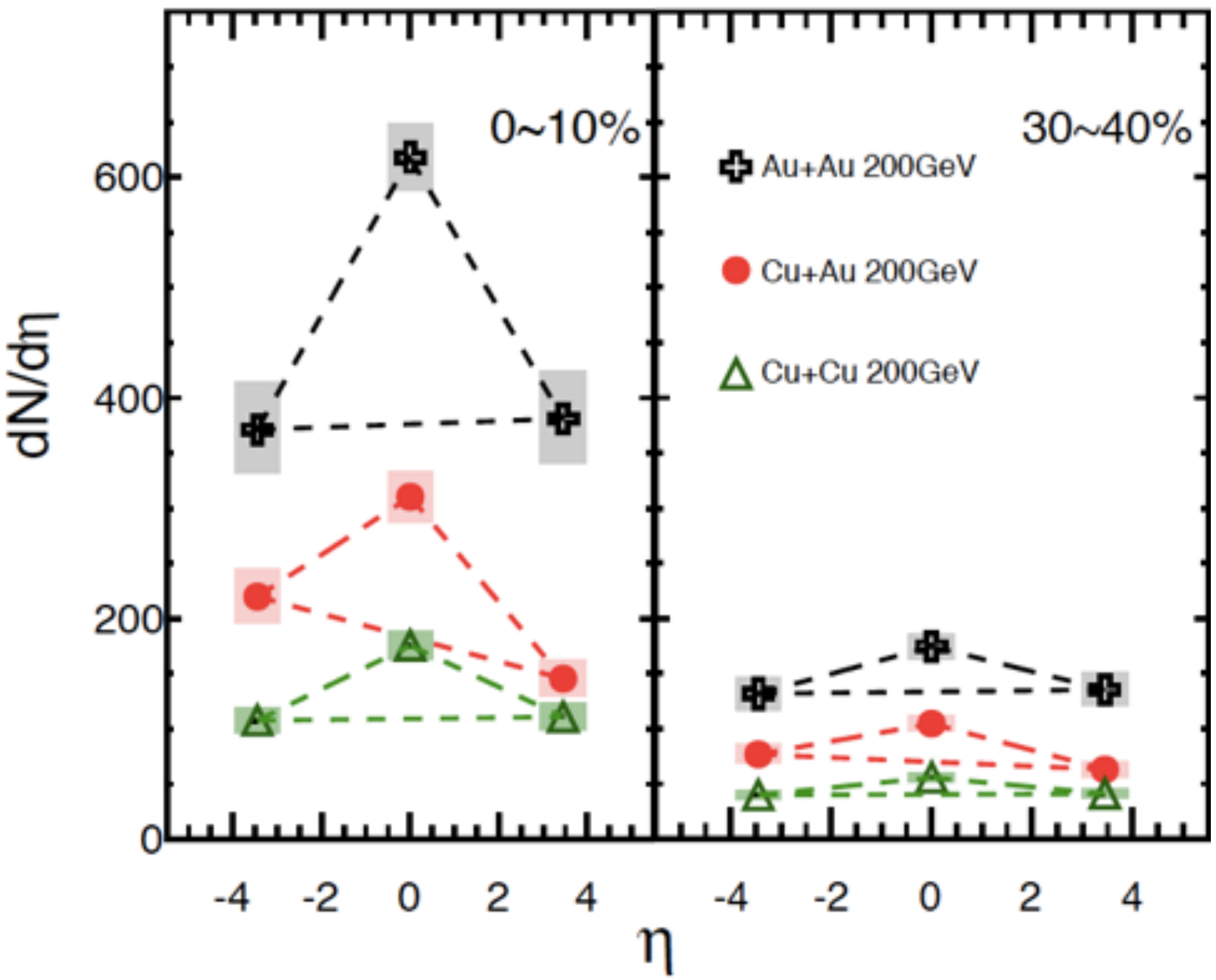

✓Au-going side dN/dη > Cu-going side dN/dη

- Number of participants in Au > Number of participants in Cu

✓Larger collision system dN/dη > smaller collision system dN/dη

- Au+Au > Cu+Au > Cu+Cu

Study of relative contribution from $N_{part,Au}$ and $N_{part,Cu}$

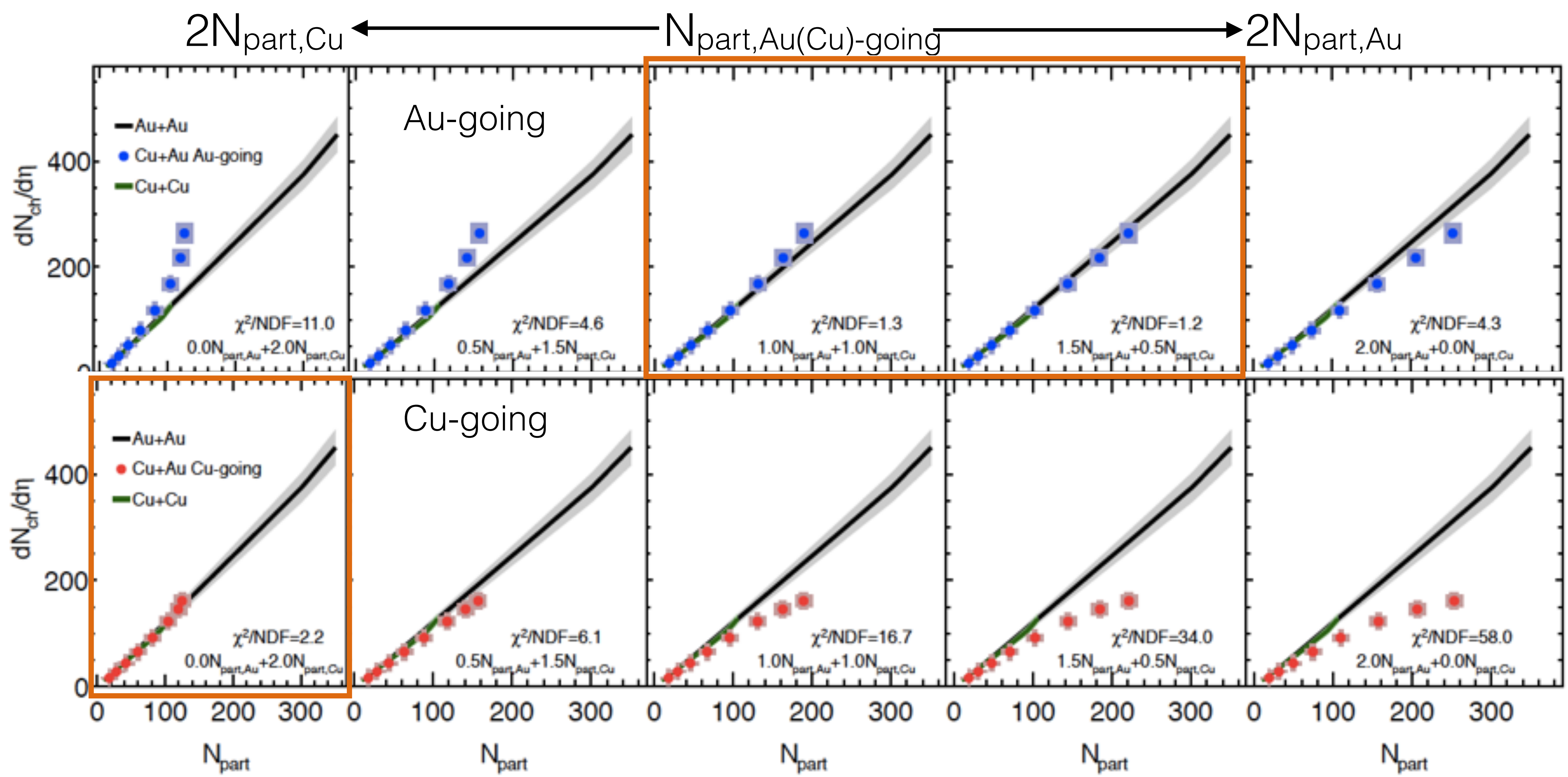

✓Weighted N_{part} scaling for CuAu dN/dη

- $N_{part,Au}$ and $N_{part,Cu}$ are participants in Au and Cu, respectively
- $N_{part,Au(Cu)\text{-}going} = wN_{part,Au}+(2-w)N_{part,Cu}$ ($2N_{part,Cu} < N_{part,Au(Cu)\text{-}going} < 2N_{part,Au}$)

✓Au-going side -> $N_{part,Au}$ and $N_{part,Cu}$, Cu-going side -> $N_{part,Cu}$

χ^2/NDF for the difference of $dN_{ch}/d\eta$ between Cu+Au and Au+Au

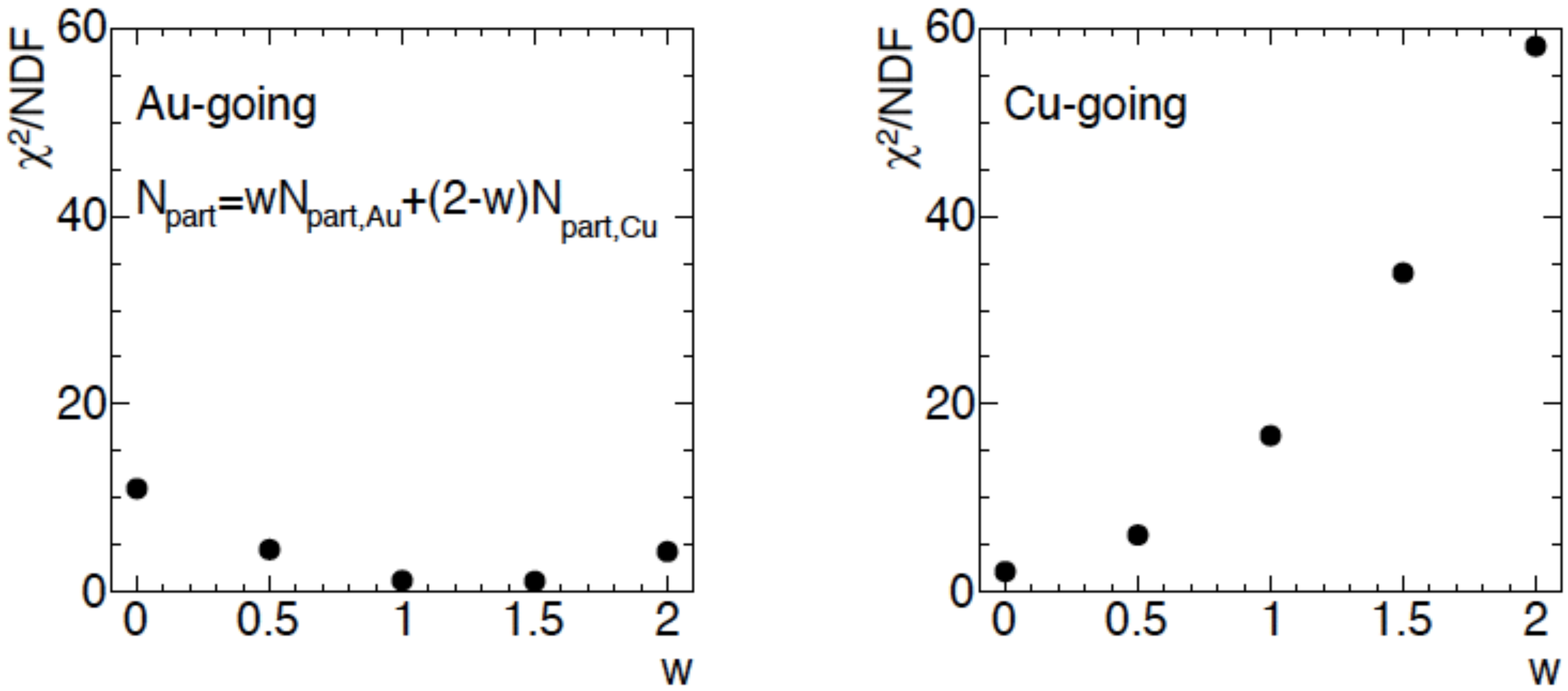

✓Au-going side is determined from $N_{part,Au}$ and $N_{part,Cu}$

- χ^2/NDF become small around w = 1~1.5

✓Cu-going side is determined from mainly $N_{part,Cu}$

- χ^2/NDF become small around w = 0

Results

Discussions

- v_1,v_2,v_3 at mid-η
- Multiplicity at F/B-η
- v_2,v_3 at F/B-η

Rapidity dependence of v_n in Cu+Au collisions

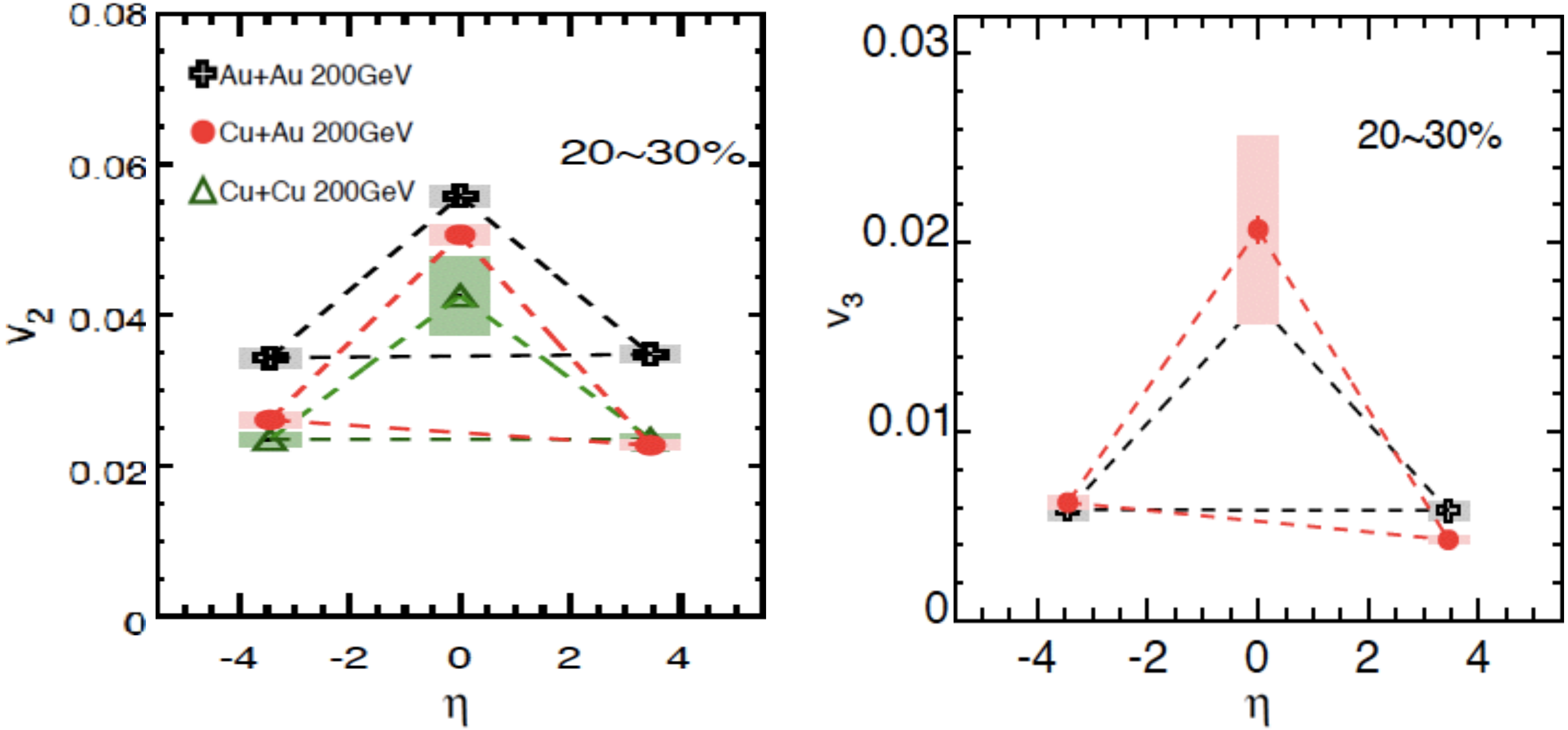

✓In Cu+Au collisions, F/B asymmetry of v_n is observed.

-v_n is measured with respect Cnt

-v_2(Au-going) > v_2(Cu-going)

-v_3(Au-going) > v_3(Cu-going)

->caused by different initial geometries in Au and Cu ?

✓Unlike v_2 , Au-going v_3 in Cu+Au show similar values of Au+Au v_3

Multiplicity dependence of v_n in Cu+Au collisions

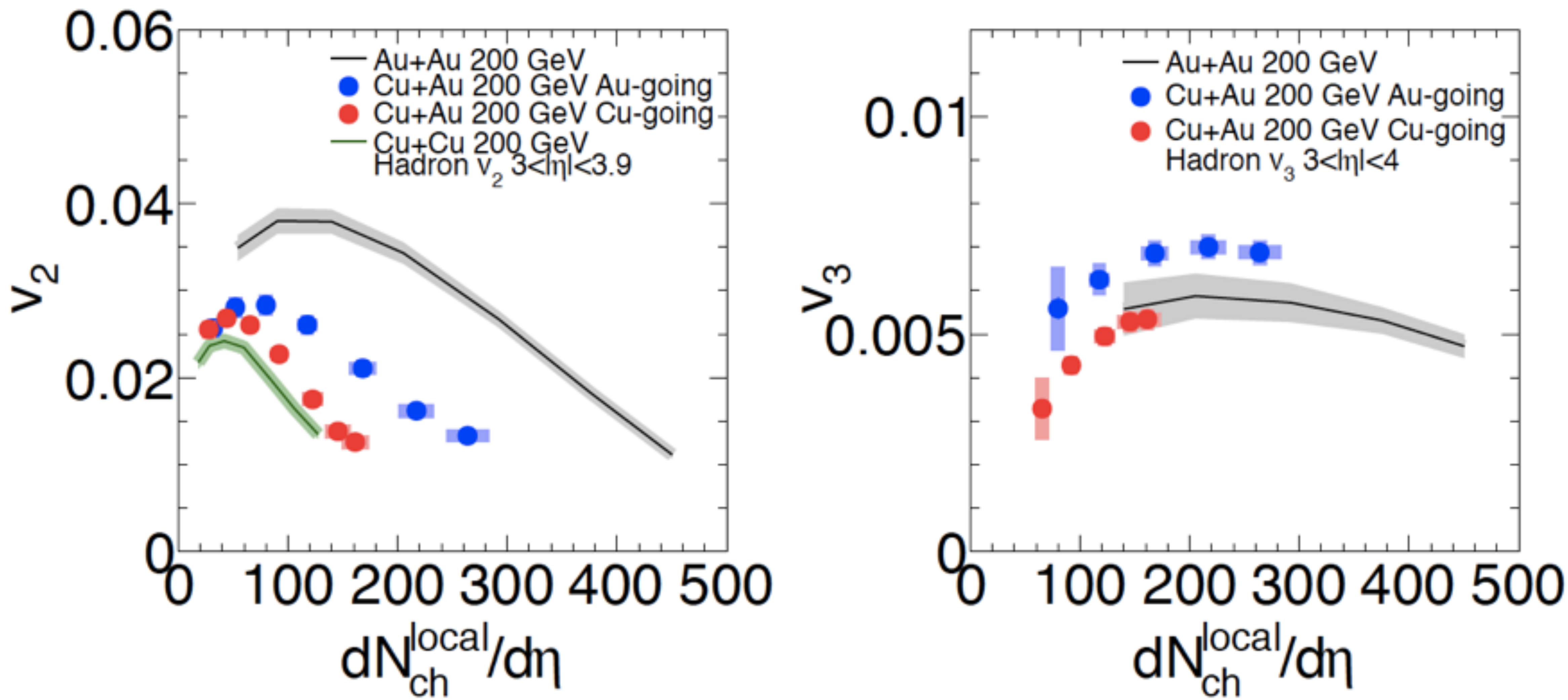

✓In Cu+Au collisions, F/B asymmetry of v_n is observed.

- plotted as a measured dN/dη at F/B-rapidity

-v_2(Au-going) > v_2(Cu-going)

-v_3(Au-going) > v_3(Cu-going)

->caused by different initial geometries in Au and Cu ?

Study of ε_2 in Cu+Au collisions at F/B-rapidity

$\varepsilon_{2,Au} \leftarrow \varepsilon_{2,Au\text{-}going} \rightarrow \varepsilon_{2,Cu}$

$\varepsilon_{2,Cu} \leftarrow \varepsilon_{2,Cu\text{-}going} \Rightarrow \varepsilon_{2,Au}$

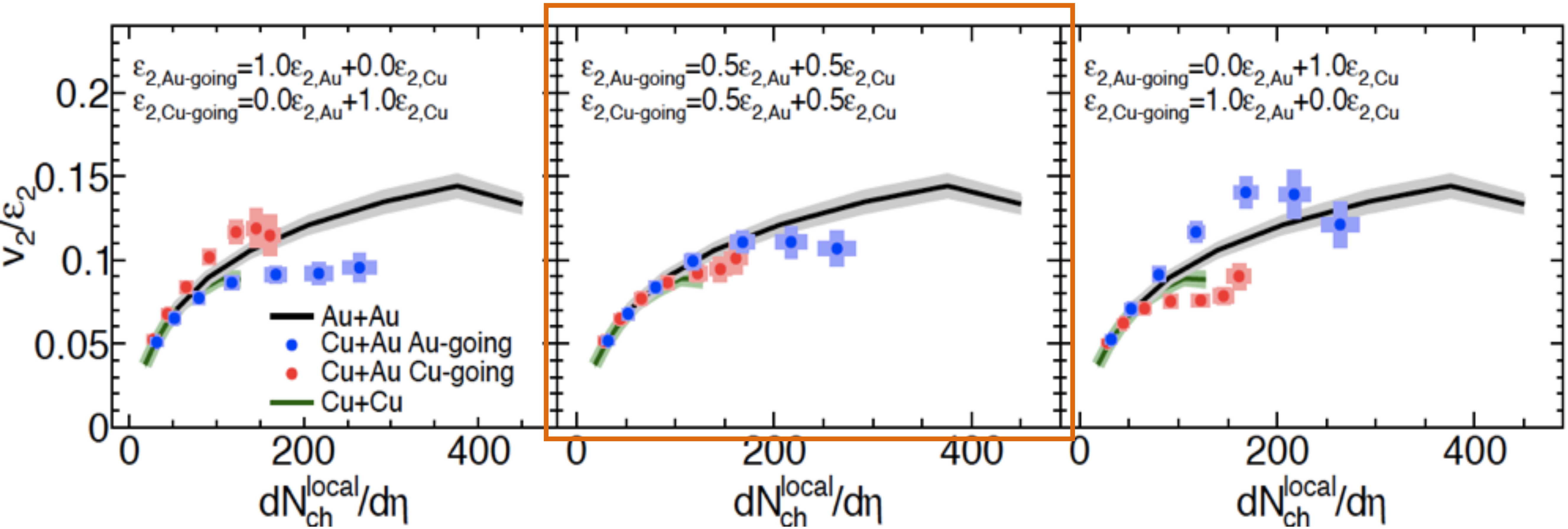

✓Weighted ε_2 scaling of v_2 ($dN/d\eta$) at ($3<|\eta|<3.9$)

-$\varepsilon_{2,Au}$ and $\varepsilon_{2,Cu}$ are give by Au and Cu, respectively

-$\varepsilon_{2,Au(Cu)\text{-}going} = w_{Au(Cu)\text{-}going}\varepsilon_{2,Au}+(1-w_{Au(Cu)\text{-}going})\varepsilon_{2,Cu}$

($\varepsilon_{2,Cu} < \varepsilon_{2,Au(Cu)\text{-}going} < \varepsilon_{2,Au}$)

➡common $\varepsilon_{2,Au\text{-}going} = \varepsilon_{2,Cu\text{-}going}$ is favored

Study of ε_3 in Cu+Au collisions at F/B-rapidity

$\varepsilon_{3,Au} \leftarrow \varepsilon_{3,Au\text{-}going} \rightarrow \varepsilon_{3,Cu}$

$\varepsilon_{3,Cu} \leftarrow \varepsilon_{3,Cu\text{-}going} \rightarrow \varepsilon_{3,Au}$

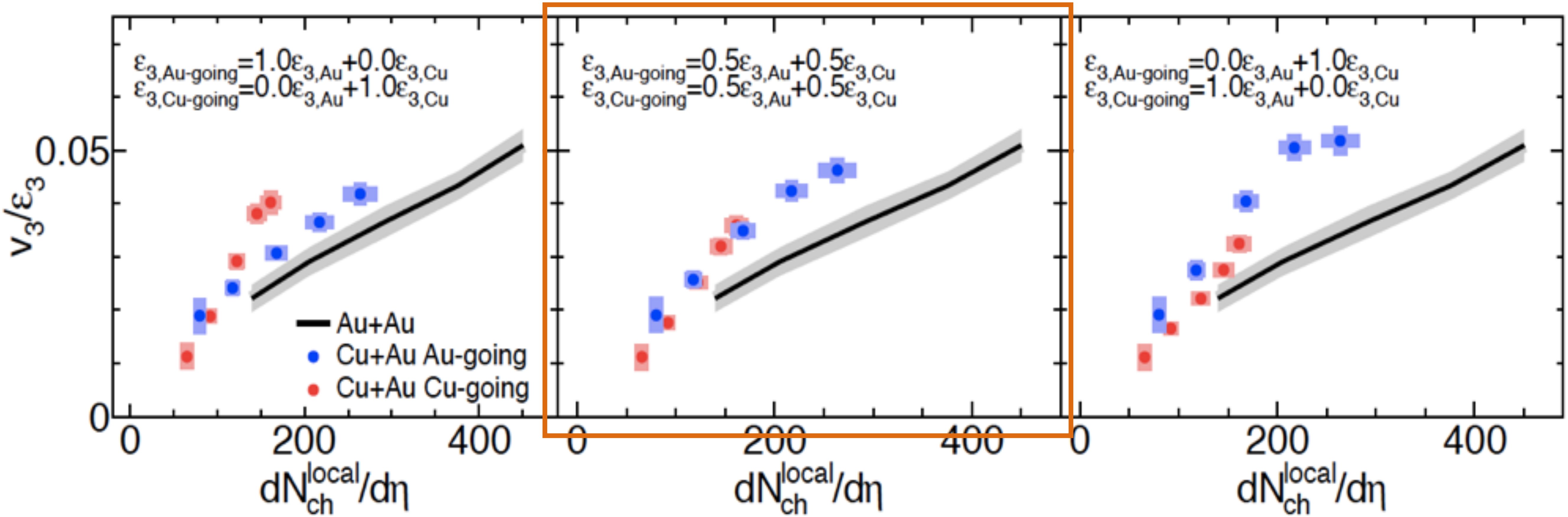

Weighted ε_3 scaling of v_3 (dN/dη) at (3<|η|<3.9)

-$\varepsilon_{3,Au}$ and $\varepsilon_{3,Cu}$ are give by Au and Cu, respectively

->$\varepsilon_{3,Au(Cu)\text{-}going} = w_{Au(Cu)\text{-}going}\varepsilon_{3,Au}+(1-w_{Au(Cu)\text{-}going})\varepsilon_{3,Cu}$ ($\varepsilon_{3,Cu} < \varepsilon_{3,Au(Cu)\text{-}going} < \varepsilon_{3,Au}$)

✓Like mid-rapidity v_3, MC-Glauber can not describe system size dependence?

✓common $\varepsilon_{3,Au\text{-}going} = \varepsilon_{3,Cu\text{-}going}$ is favored

χ^2/NDF for the difference of v_n/ε_n between Au-going and Cu-going

2nd order harmonics

3rd order harmonics

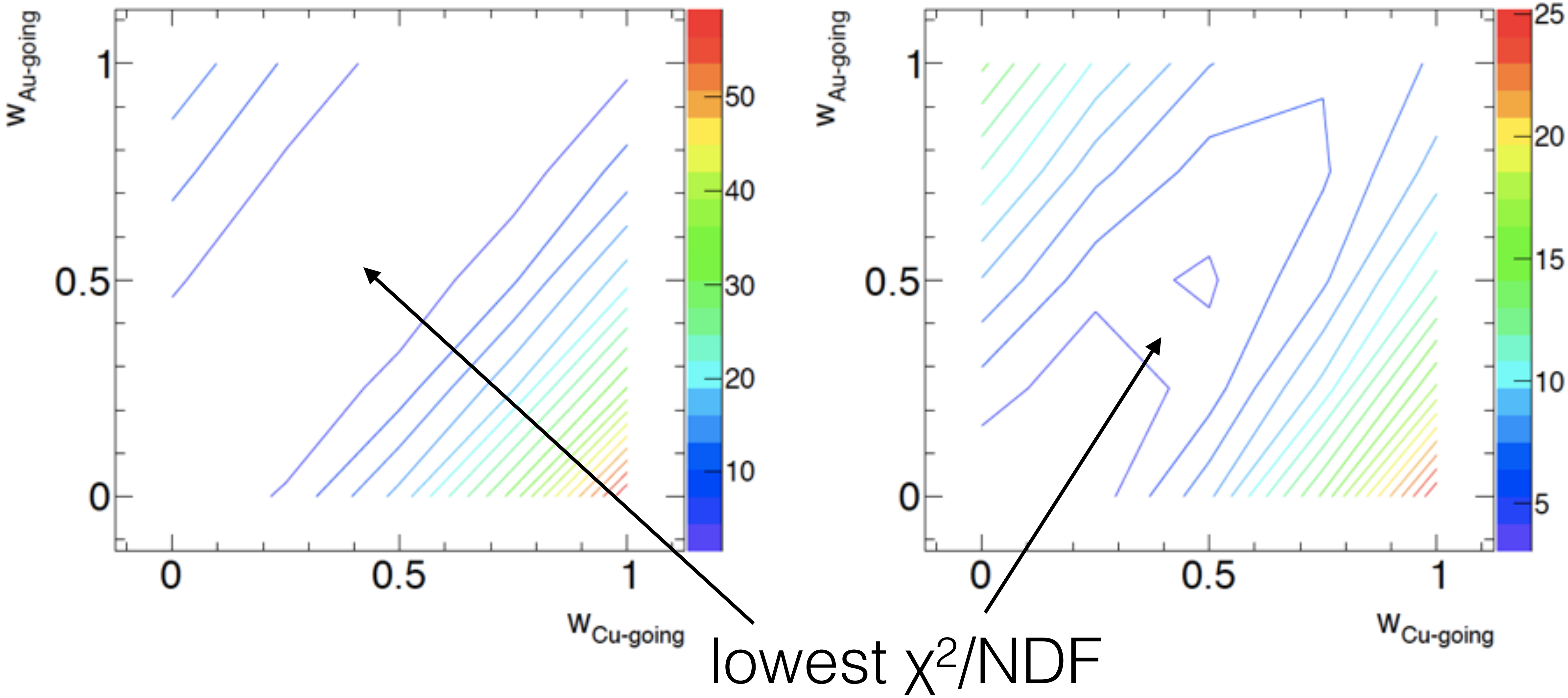

✓ χ^2/NDF for $w_{Au\text{-}going}$ vs $w_{Cu\text{-}going}$

- $\varepsilon_{n,Au(Cu)\text{-}going} = w_{Au(Cu)\text{-}going}\varepsilon_{n,Au} + (1 - w_{Au(Cu)\text{-}going})\varepsilon_{n,Cu}$

✓ Common $\varepsilon_{n,Au\text{-}going} \sim \varepsilon_{n,Cu\text{-}going}$ is favored by v_2 and v_3

- $w_{Au\text{-}going} \sim w_{,Cu\text{-}going}$

χ^2/NDF for the difference of v_n/ε_n between Cu+Au and Au+Au

2nd order harmonics

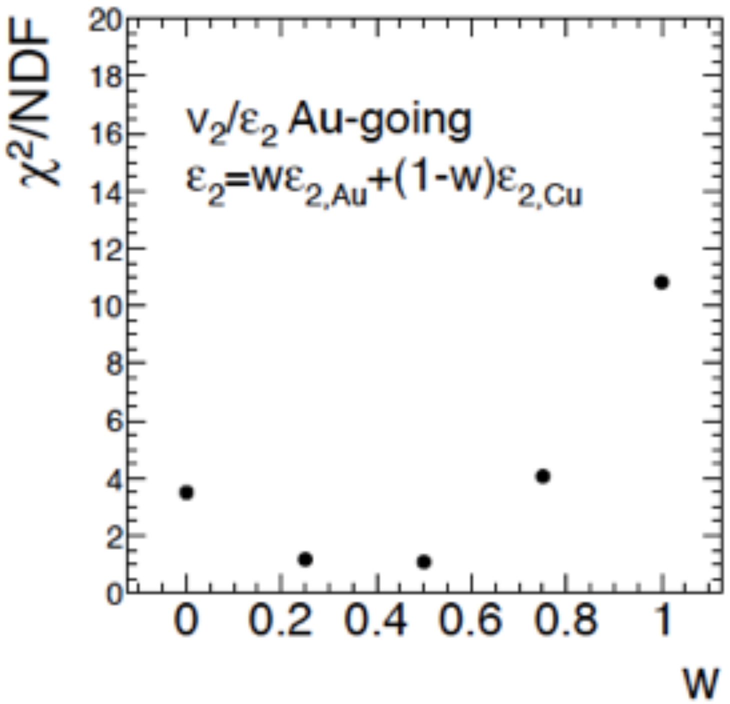

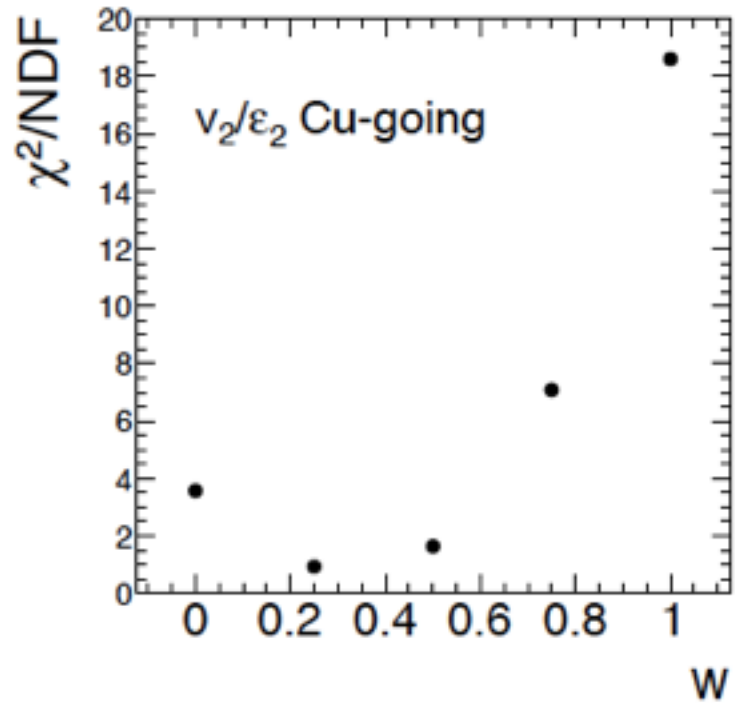

- ✓ $\varepsilon_{2,\text{Au-going}} \sim \varepsilon_{2,\text{Cu-going}}$
  - $\varepsilon_{2,Au}$ and $\varepsilon_{2,Cu}$ are similar contribution
  - Both χ^2/NDF become small around w = 0.2 ~ 0.5

3rd order harmonics

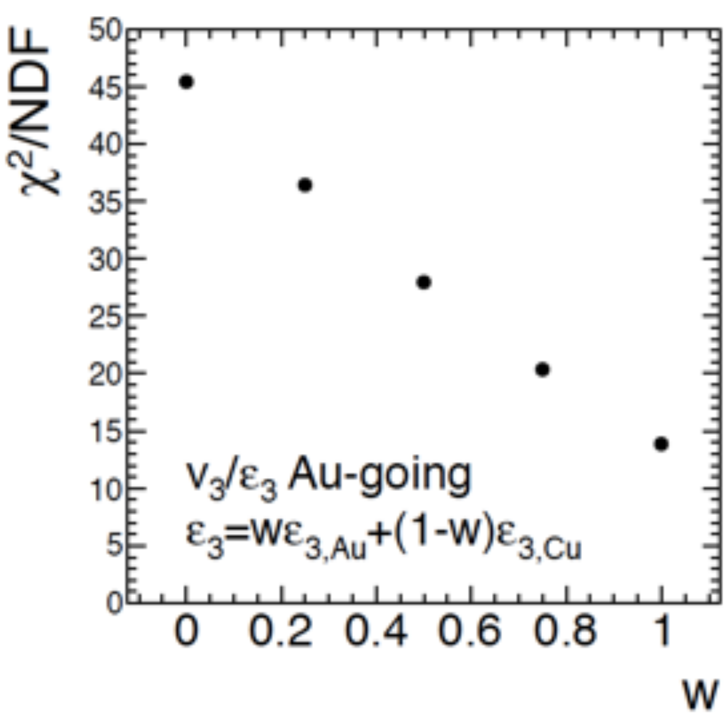

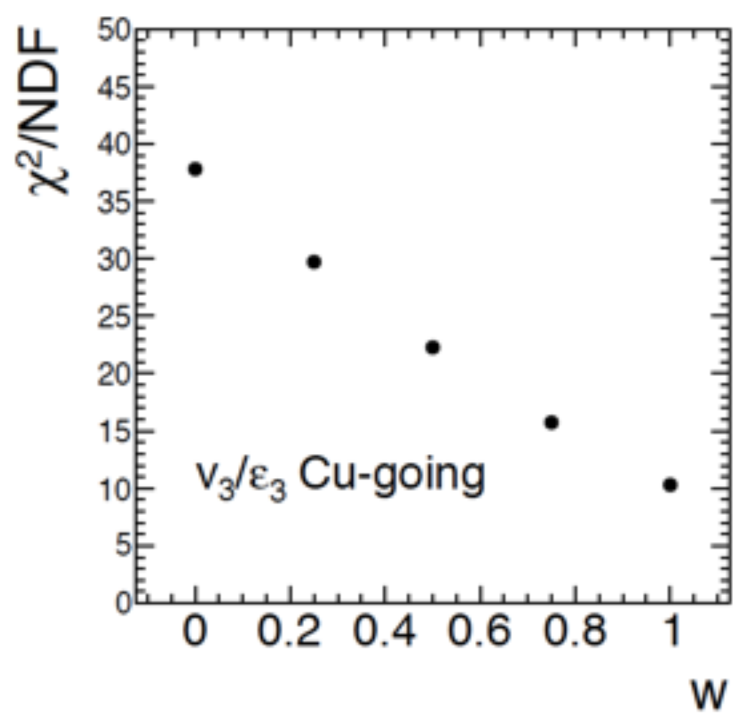

- ✓ Glauber does not describe ε_3
  - Compared to v_2/ε_2, χ^2/NDF is large
  - Both χ^2/NDF become small around w = 1

Summary 1 : Mid-rapidity

✓First order flow harmonic

- High p_T particles are emitted to Au side
- Magnitude decrease from central to peripheral
- Larger density gradient in Au nucleus side push particle to high p_T

✓Second order flow harmonics

- Similar centrality and p_T dependence as seen in symmetric collisions
- Glauber model well described initial geometry

✓Third order flow harmonics

- Similar centrality and p_T dependence as seen in symmetric collisions
- Glauber model is not favored by the third oder initial geometry

Summary 2 : Forward/Backward rapidity

✓Charged particle multiplicity
- Au-going side is higher than Cu-going side
- Au-going side is determined by both of $N_{part,Au}$ and $N_{part,Cu}$
- Cu-going side is determined by mainly $N_{part,Cu}$

✓Second order flow harmonics
- Au-going side is higher than Cu-going side for mid central
- Au-going side is close to Cu-going side for central and peripheral
- Au-going and Cu-going side are scaled well by common eccentricity

✓Third order flow harmonics
- Au-going side is higher than Cu-going side for central and mid central
- Like v_2 Au-going and Cu-going side are scaled well by common eccentricity
- Like mid-rapidity v_3 , Glauber model does not describe initial geometry in Au+Au and Cu+Au.

Conclusion

By studying azimuthal anisotropy and particle multiplicity in Cu+Au collisions,

✓Initial geometry

- Left / Right asymmetry in transverse direction
- Initial geometry at Forward/Backward is common

✓Initial energy density

- Au-going side is determined by both of $N_{part,Au}$ and $N_{part,Cu}$
- Cu-going side is determined by mainly $N_{part,Cu}$

Back Up

Interpretation of negative $v_1(p_T)$ at higher p_T

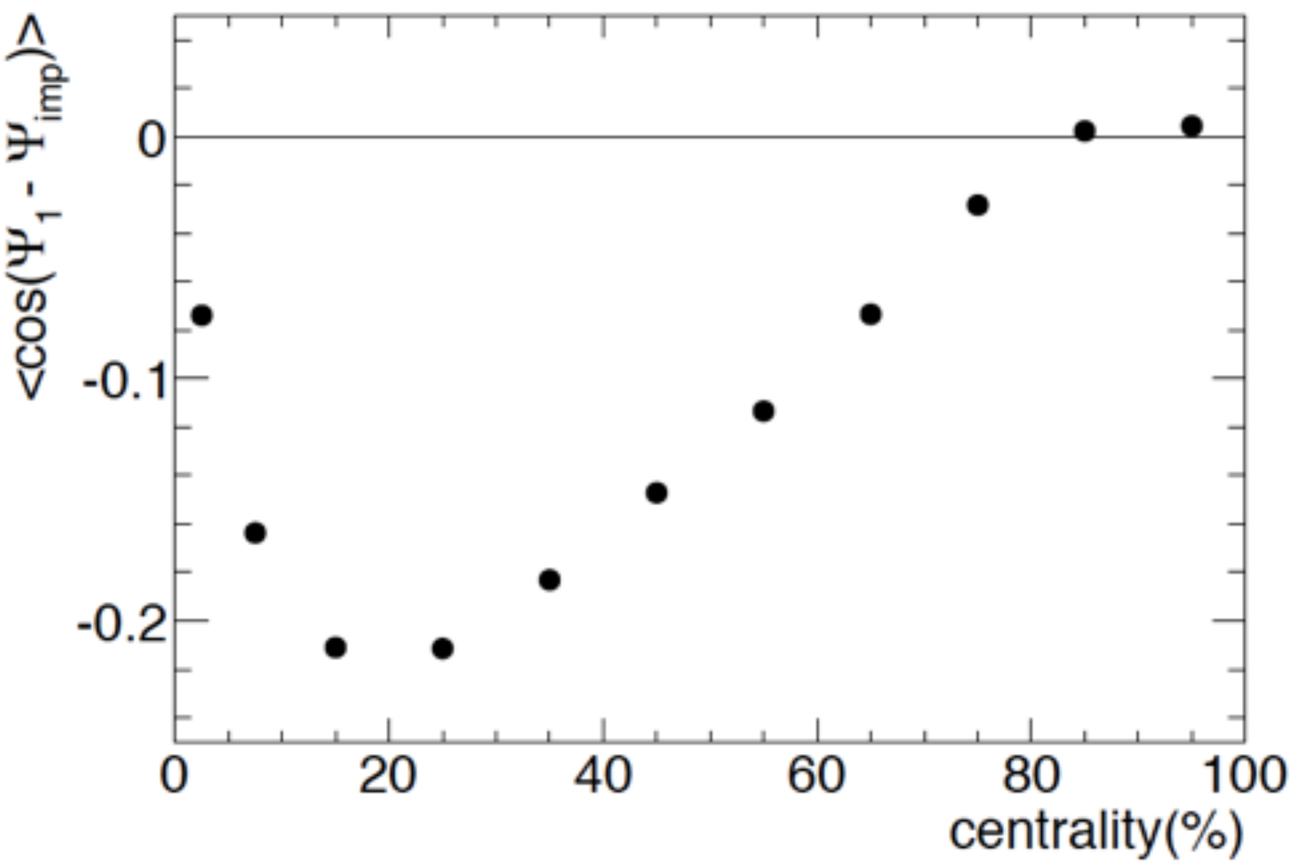

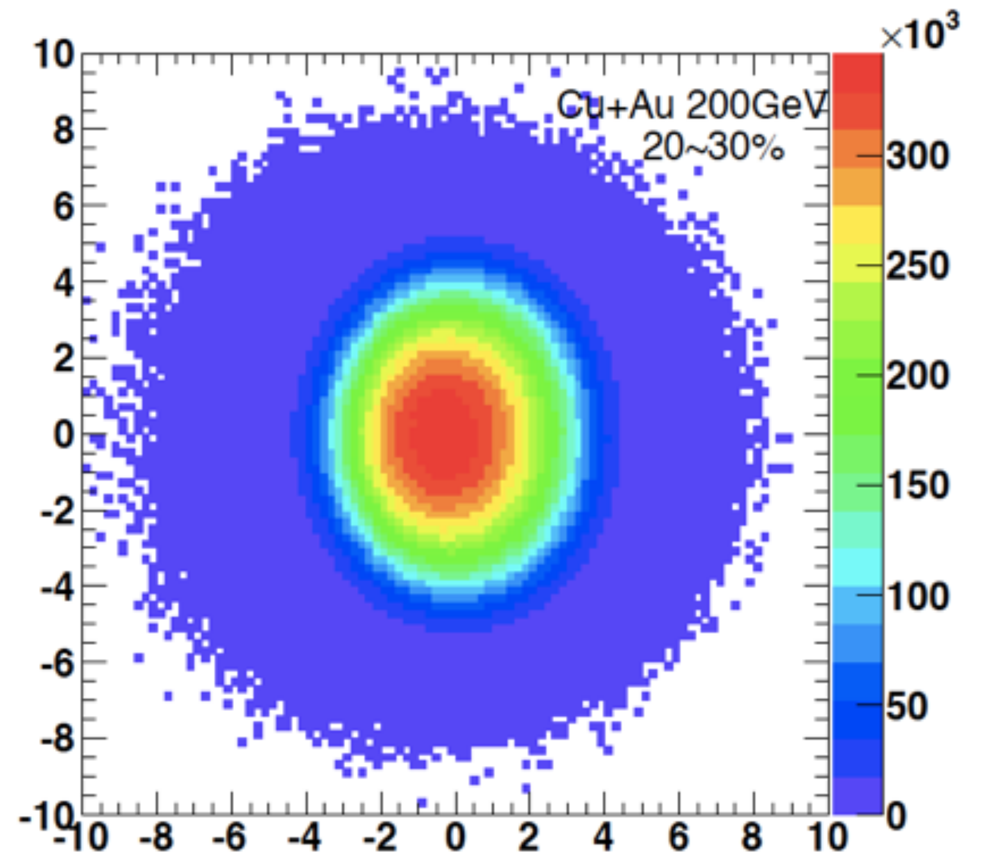

✓Density gradient is larger in Au nucleus side

Rapidity dependence of initial condition

PhysRevC.90.034915

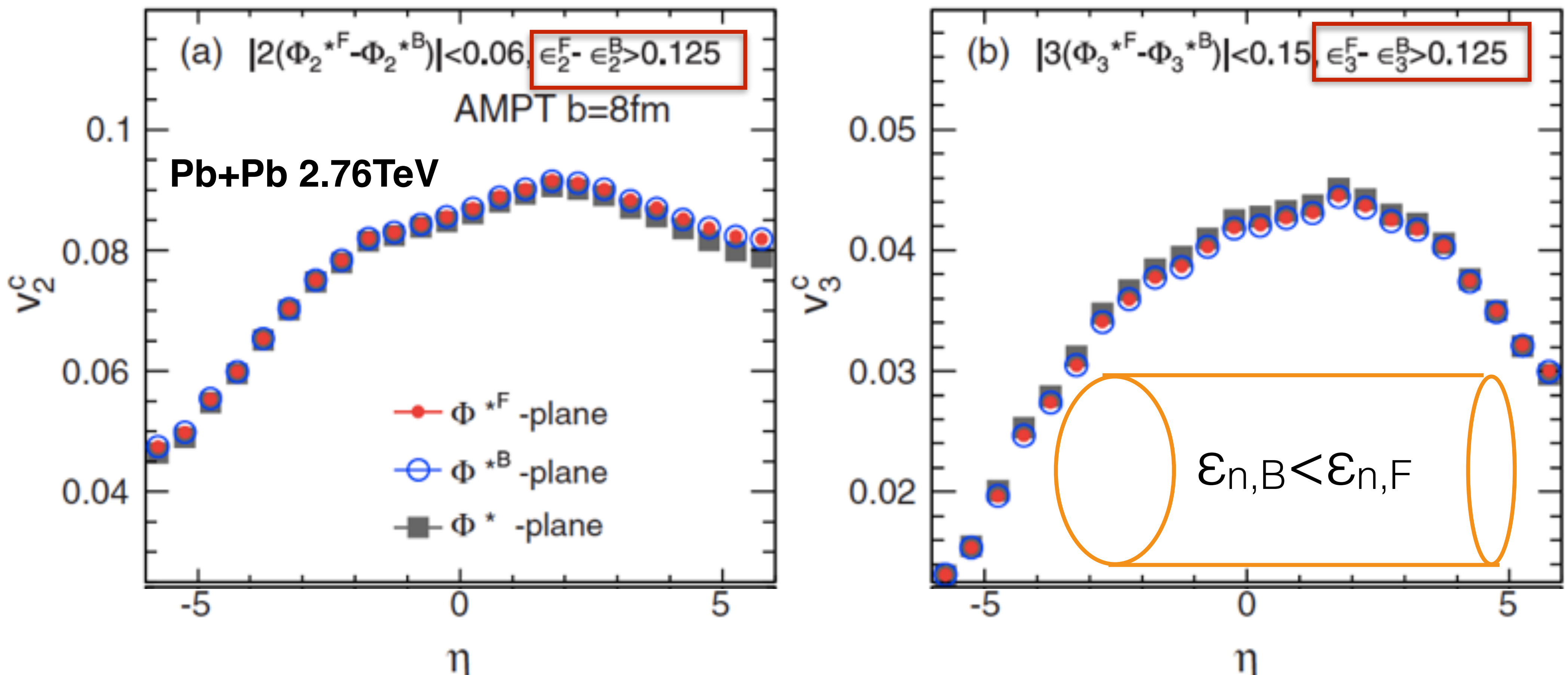

✓initial geometry has been considered to be **rapidity independent**

✓Initial conditions on target and projectile nuclei are not same event

$\varepsilon_n(+\eta) > \varepsilon_n(-\eta)$ ➡ $v_n(+\eta) > v_n(-\eta)$

✓ Initial geometry has strong rapidity dependence

➡ $\varepsilon_n(\eta) = \alpha\varepsilon_n(+\eta) + \beta\varepsilon_n(-\eta)$

Results
Discussions

- v_1,v_2,v_3 at mid-η
- v_2,v_3 at F/B-η
- Initial condition study
- v_1,v_2,v_3 theory comparison

Parton cascade and hydro $v_n(p_T)$

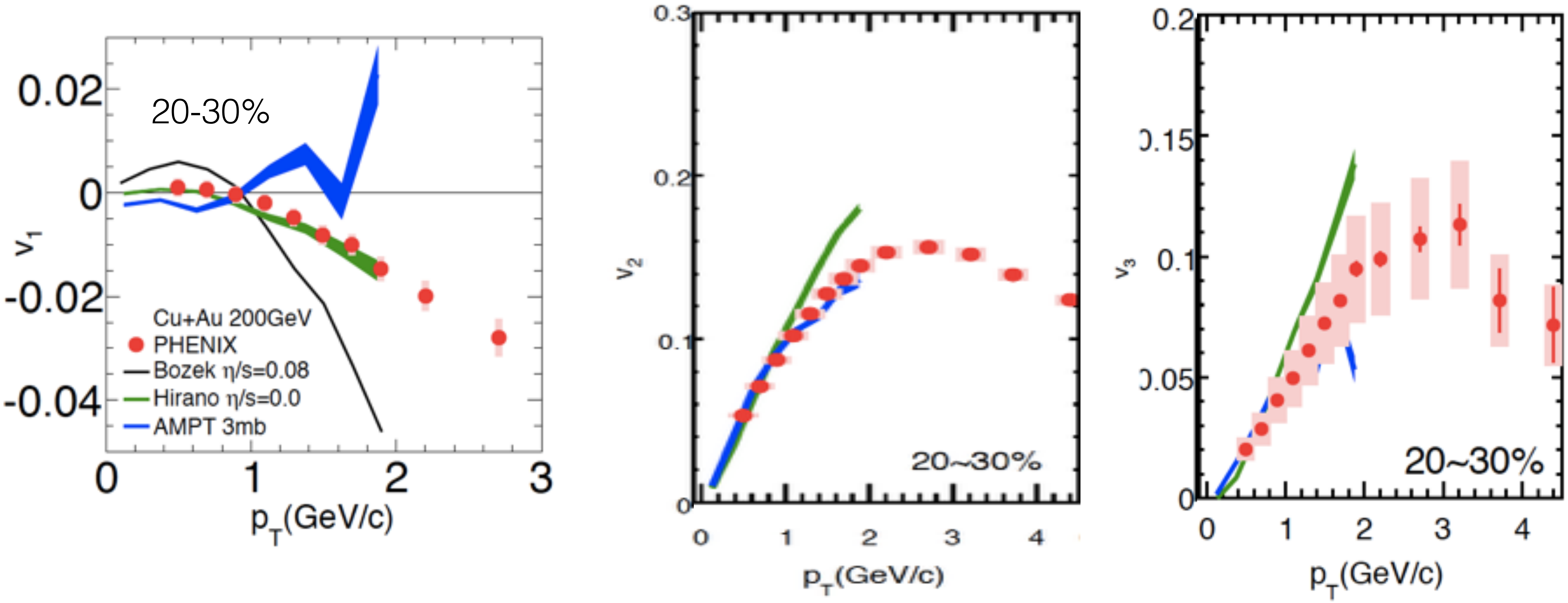

- Hydro(Bozek):Glauber + hydro
- Hydro(Hirano):Glauber + hydro + hadron cascade
- AMPT :Glauber + parton cascade + hadron cascade

✓Hydrodynamic reproduce v_n
✓AMPT model well reproduce v_2 and v_3 , but shows opposite sign of v_1

Parton cascade and hydro $v_n(\eta)$

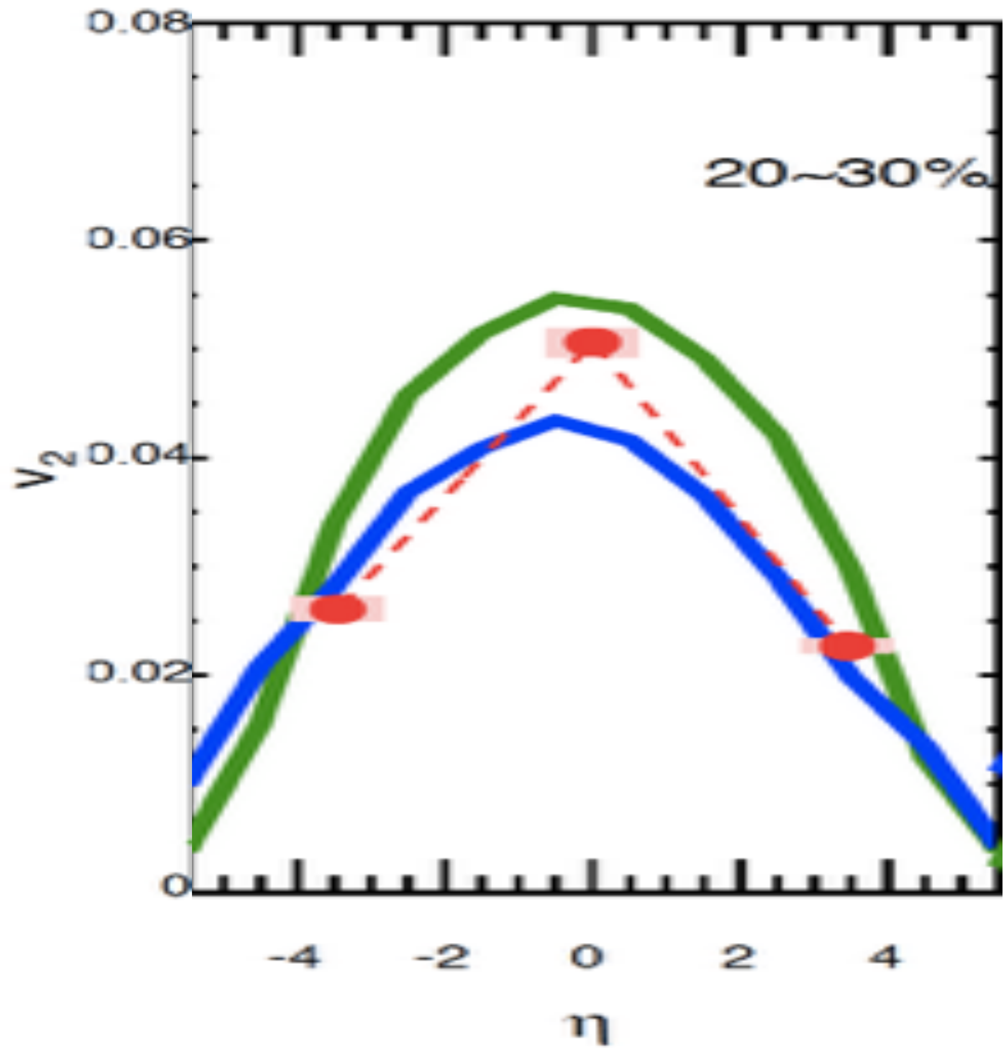

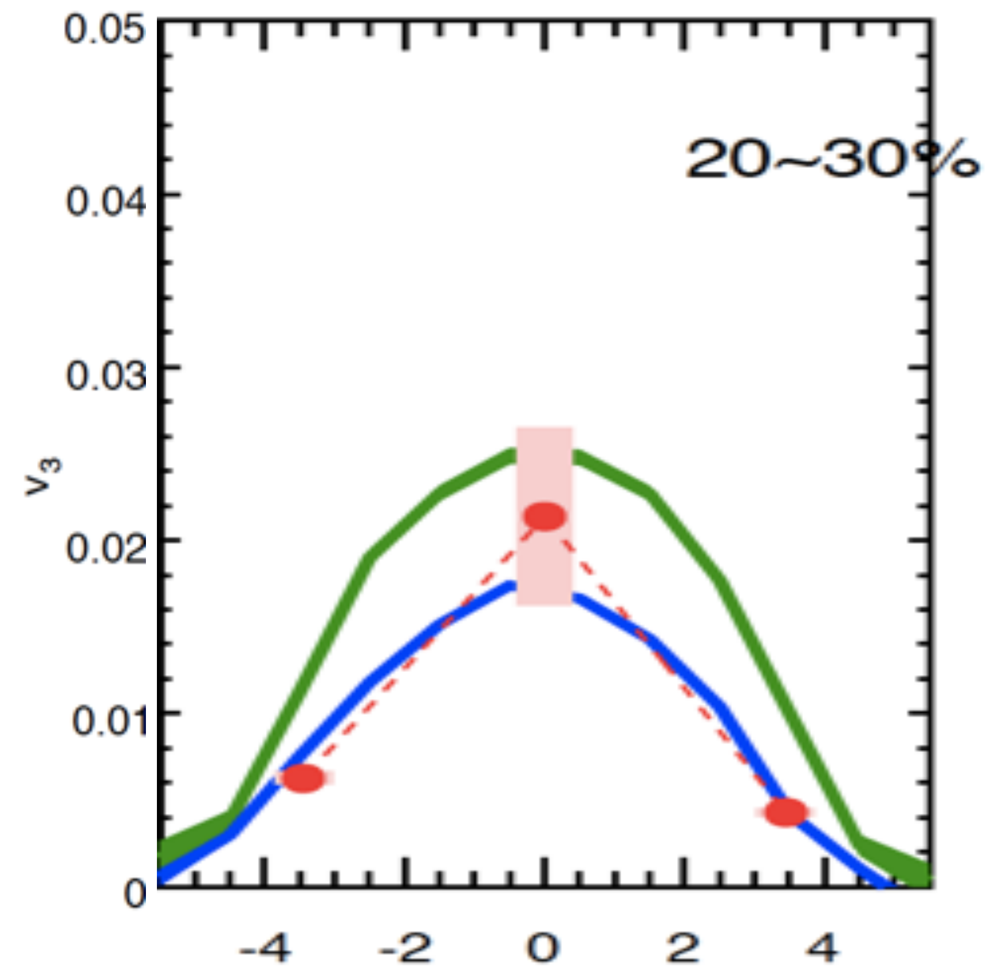

- ✓AMPT and Hydro predict the magnitude of v_2 at F/B rapidity well
- ✓AMPT reproduce the magnitude of v_3 at F/B rapidity well
- ✓Hydro overestimate the magnitude of v_3 at F/B rapidity
  - -Hydro:Smooth longitudinal density+hydro
  - -AMPT:Fluctuated longitudinal density+parton cascade

Results Discussions

- v_1, v_2, v_3 at mid-η
- v_2, v_3 at large-η
- **Initial condition study**
- v_1, v_2, v_3 theory comparison

System size dependence of $v_n(N_{part})$ at F/B rapidity

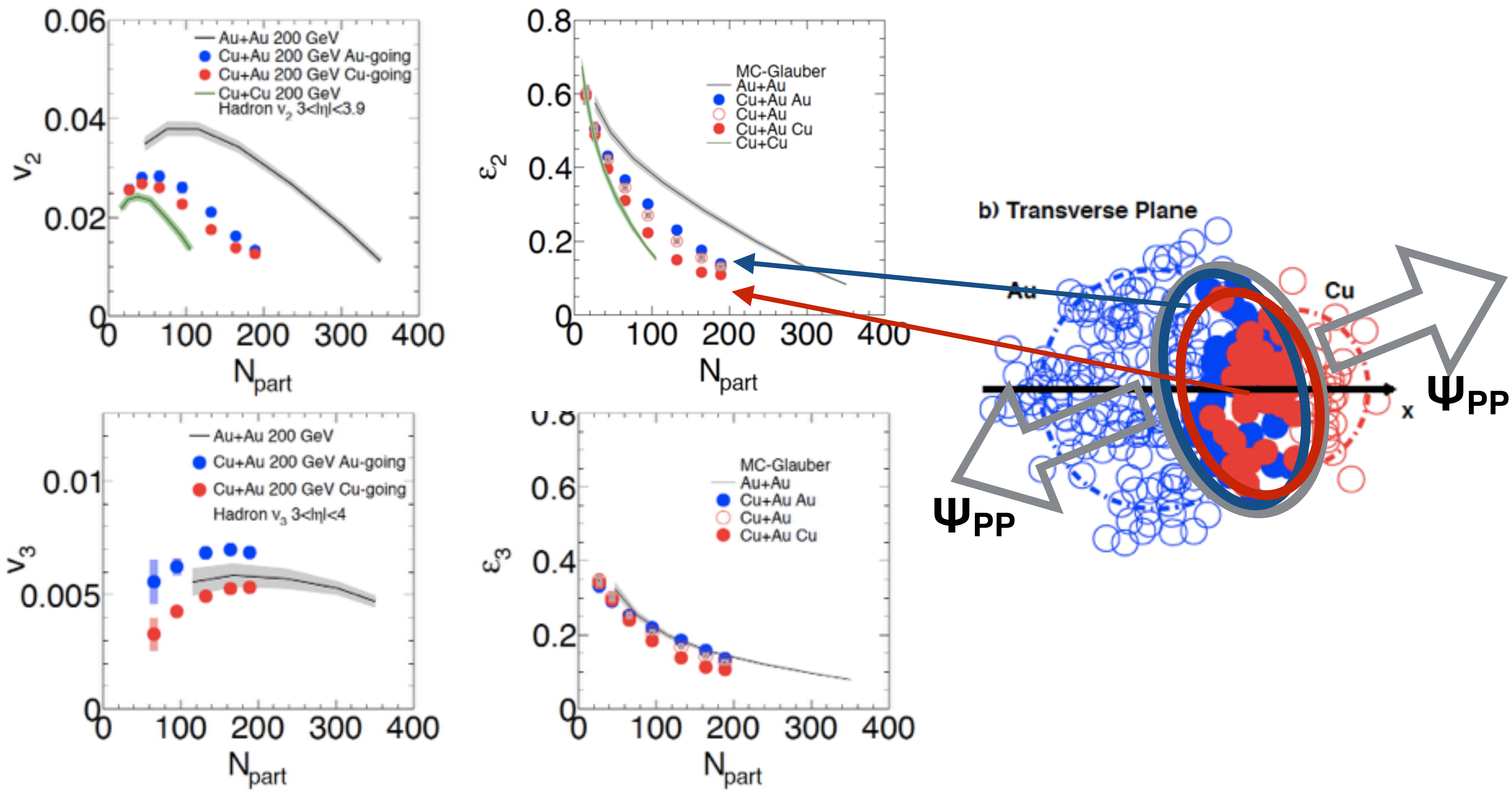

✓F/B asymmetry of v_2 is consistent that of ε_2

-$\varepsilon_{n,Au}$ and $\varepsilon_{n,Cu}$ are estimated from Au and Cu participants separately

$\varepsilon_{n,Au} > \varepsilon_{n,Cu}$ ➡ $v_{n,Au} > v_{n,Cu}$?

v_2/ε_2 scaling with Glauber and IPGlasma

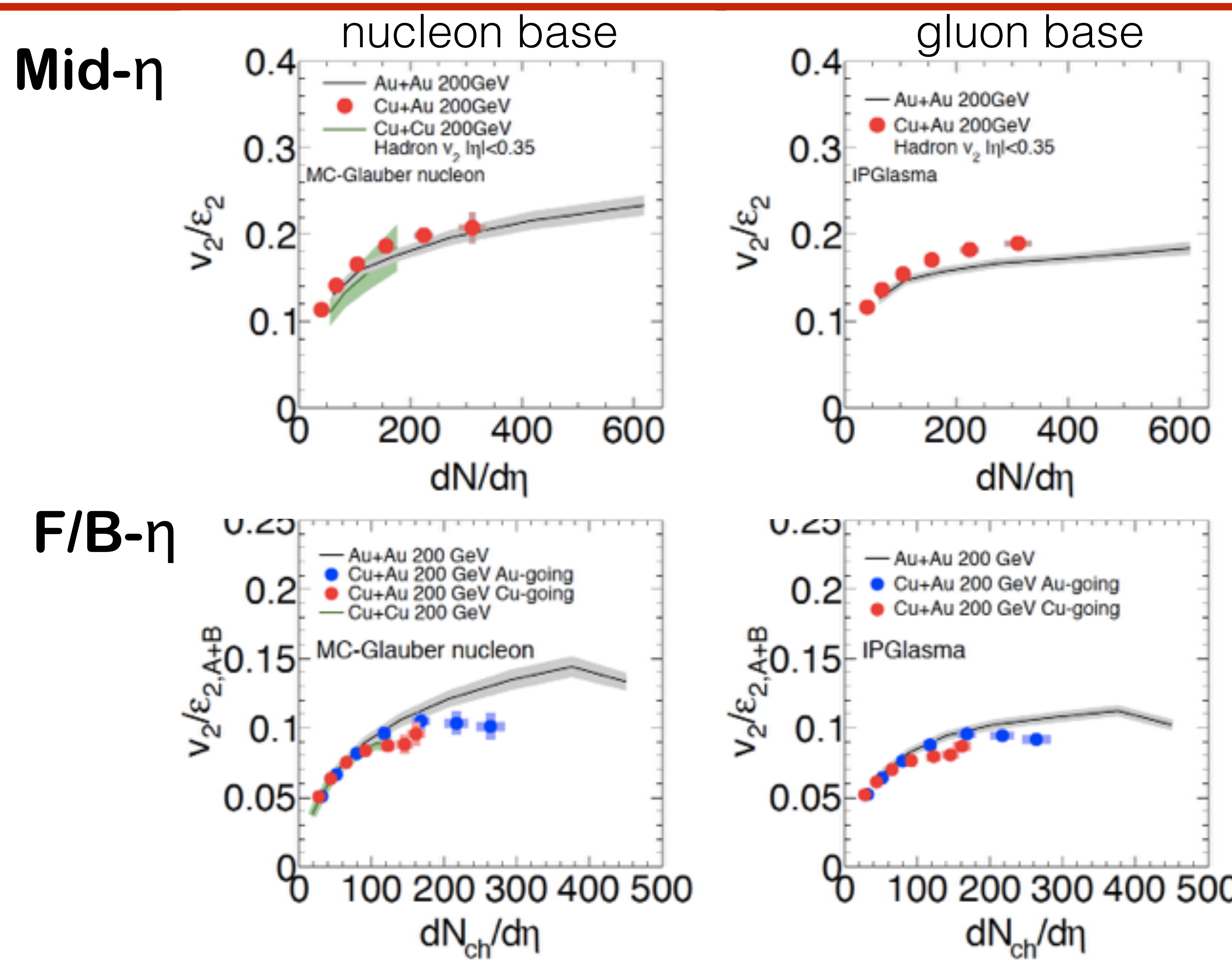

- ✓At-mid η, the v_2 scaled with nucleon base model are consistent among three collision systems
- ✓At-F/B η, the v_2/ε_2 with gluon base model in Cu+Au is closer to that in Au+Au

v_3/ε_3 scaling with Glauber and IPGlasma

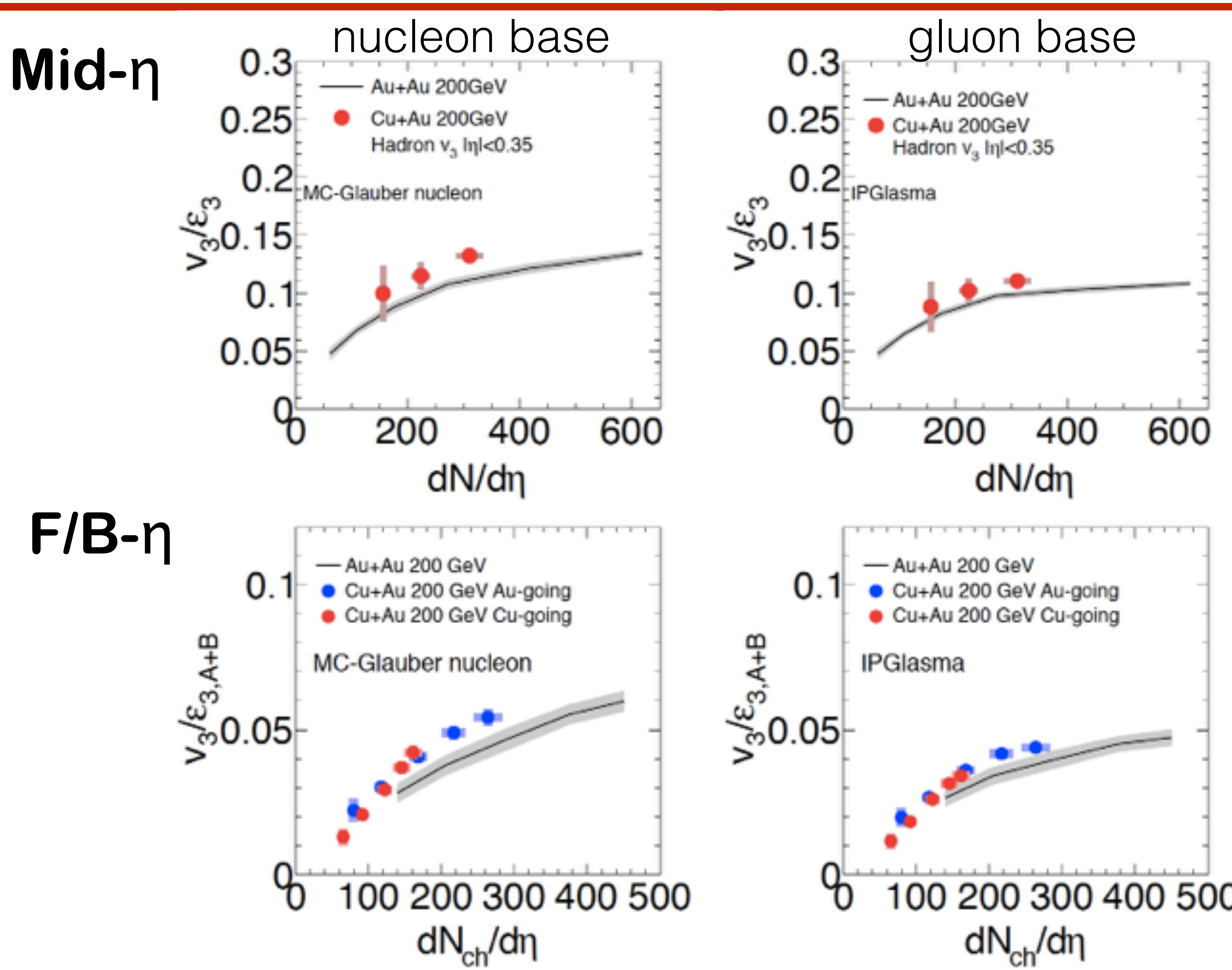

✓**At-mid η, the v_3 scaled with gluon base model in Cu+Au is closer to that in Au+Au**

✓**At-F/B η, the v_3/ε_3 with gluon base model in Cu+Au is closer to that in Au+Au**

η_s dependence of ε_n

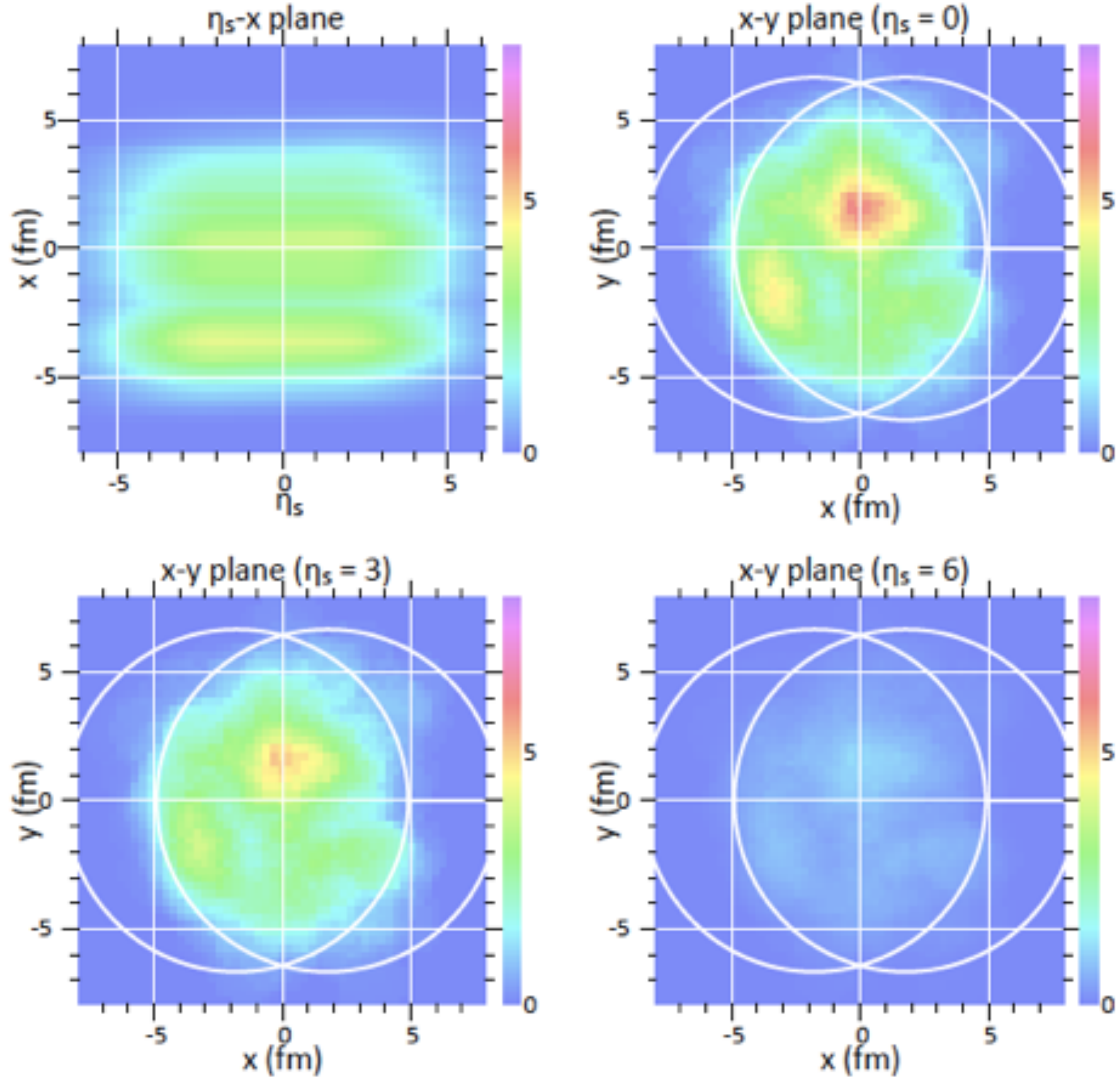

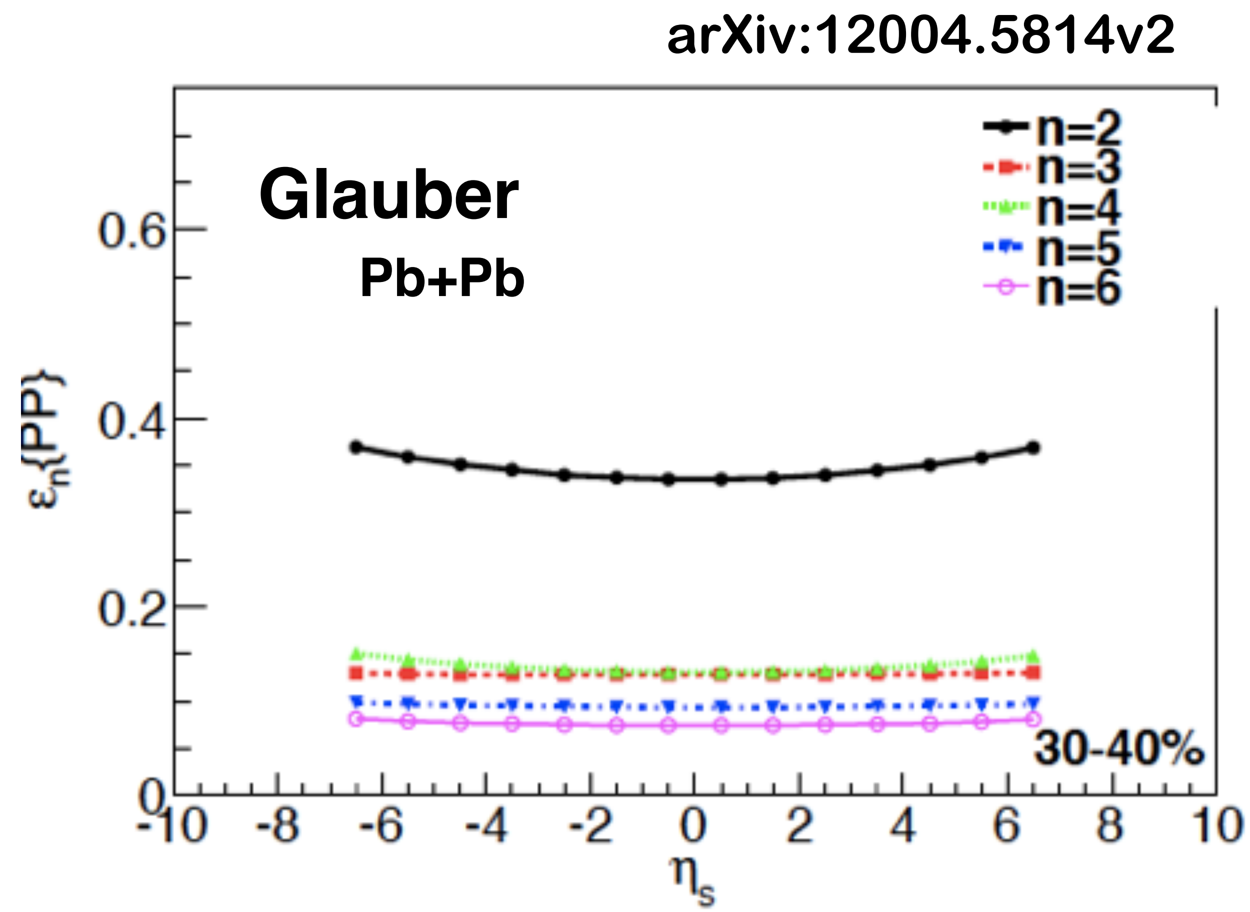

✓Longitudinal structure is less understood
-Transverse direction can be described by Glauber, CGC…

✓Initial spatial geometry $\varepsilon_n(\eta)$ are η symmetric
- Smooth longitudinal density profile, streak-like structure

v_n measurement at Bbc(3<|η|<4)

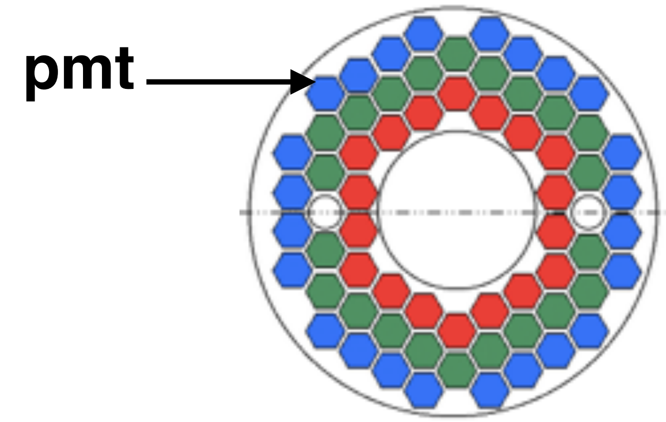

✓v_n is measured using 64 Bbc pmts

- Bbc can't reconstruct tracks
- pmt based v_n include back ground

✓Full Giant simulation with PHENIX configuration

- pmt based v_n -> track based v_n

$$v_n^{track} = R_n * v_n^{pmt} \qquad R_n = \frac{v_{n,input}^{Sim}}{v_{n,output}^{Sim}}$$

$v_{n,input}^{Sim}$
Input v_n from particle simulation

$v_{n,output}^{Sim}$
Output v_n from Giant simulation

✓Correction factor R_n

- R_2 : 0.73
- R_3 : 0.65

✓Systematic study

-dN/deta
- pT spectra
- vn(pt)
- vn(eta)

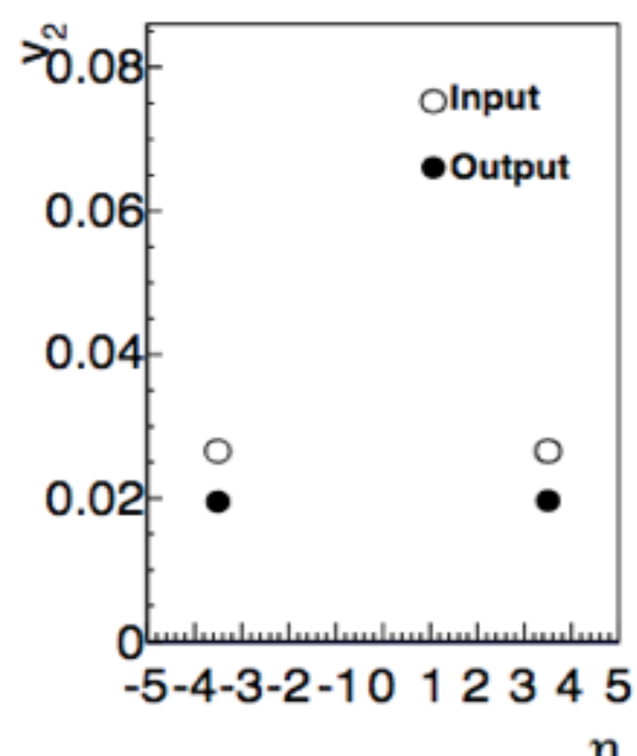

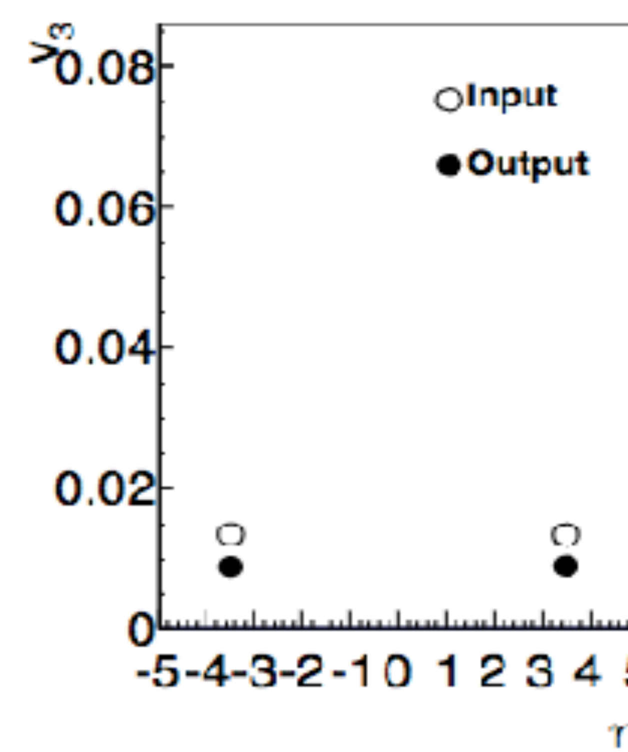

Initial spatial anisotropy

Glauber Monte Carlo simulation

-Wood Saxon density profile

- collision is occurred, if $d < \sqrt{(\sigma_{nn}/\pi)}$

  d:distance between nucleons

  σ_{nn}:total cross section(pp collision)

$$\epsilon_n = \frac{\langle r^2 \cos[n(\phi - \Psi_{n,PP})] \rangle}{\langle r^2 \rangle}$$

$$\Psi_{n,PP} = \frac{1}{n}[\tan^{-1}\frac{\langle r^2 \sin(n\phi)\rangle}{\langle r^2 \cos(n\phi)\rangle} + \pi]$$

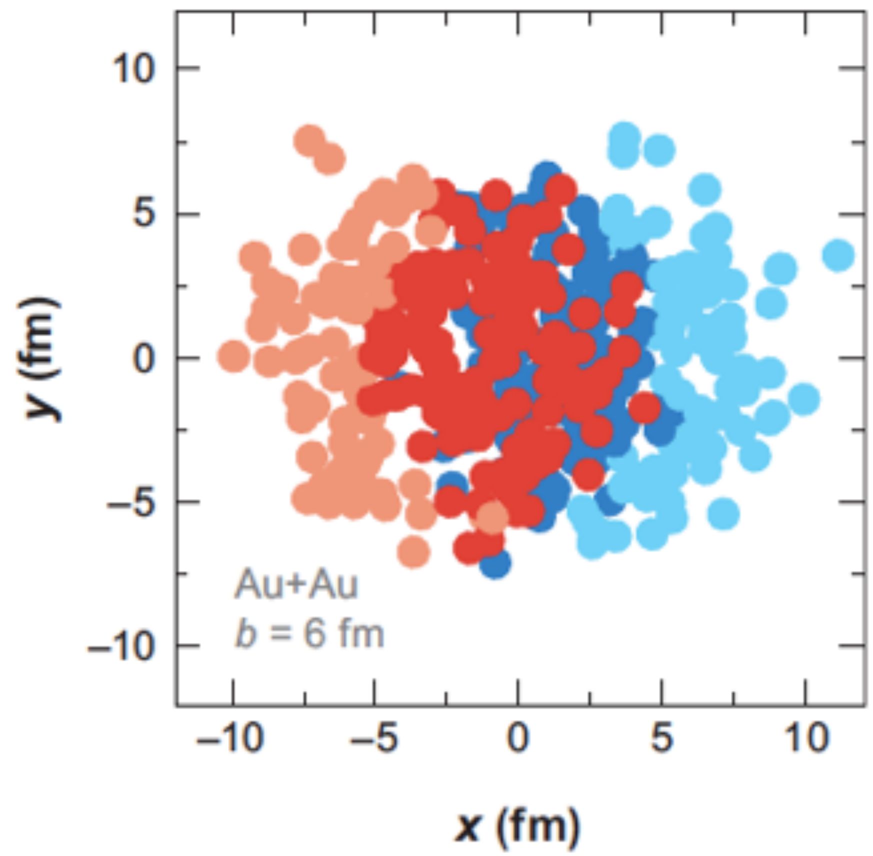

Centrality dependence of ε_n

ε_2:CuCu>CuAu~AuAu

ε_3:CuAu>AuAu

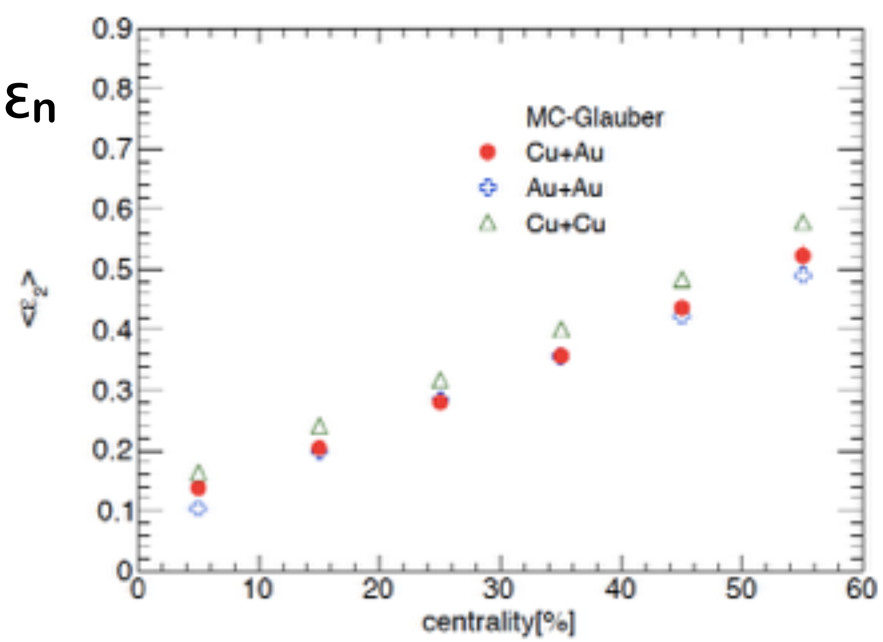

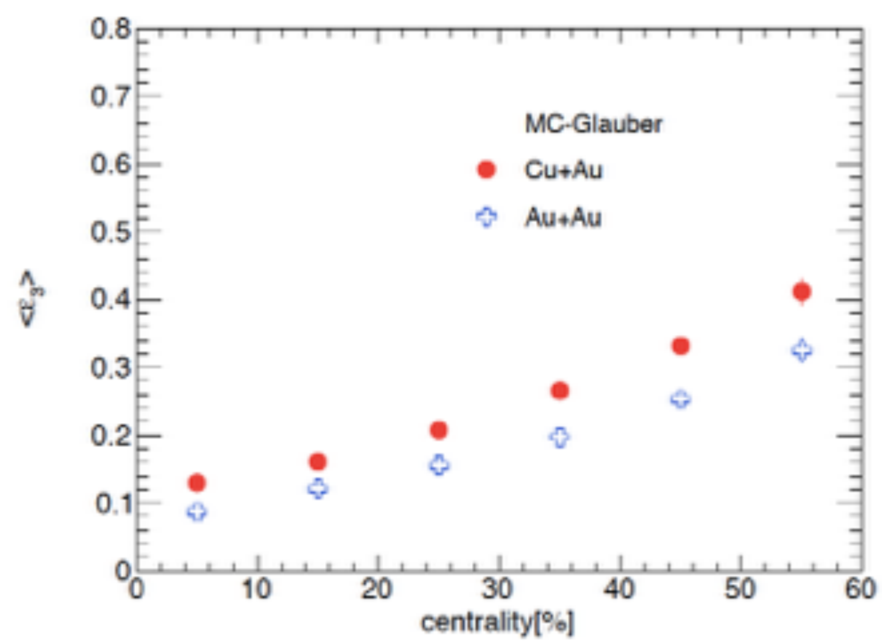

System size dependence of $v_2(N_{part})$ and $\varepsilon_2(N_{part})$

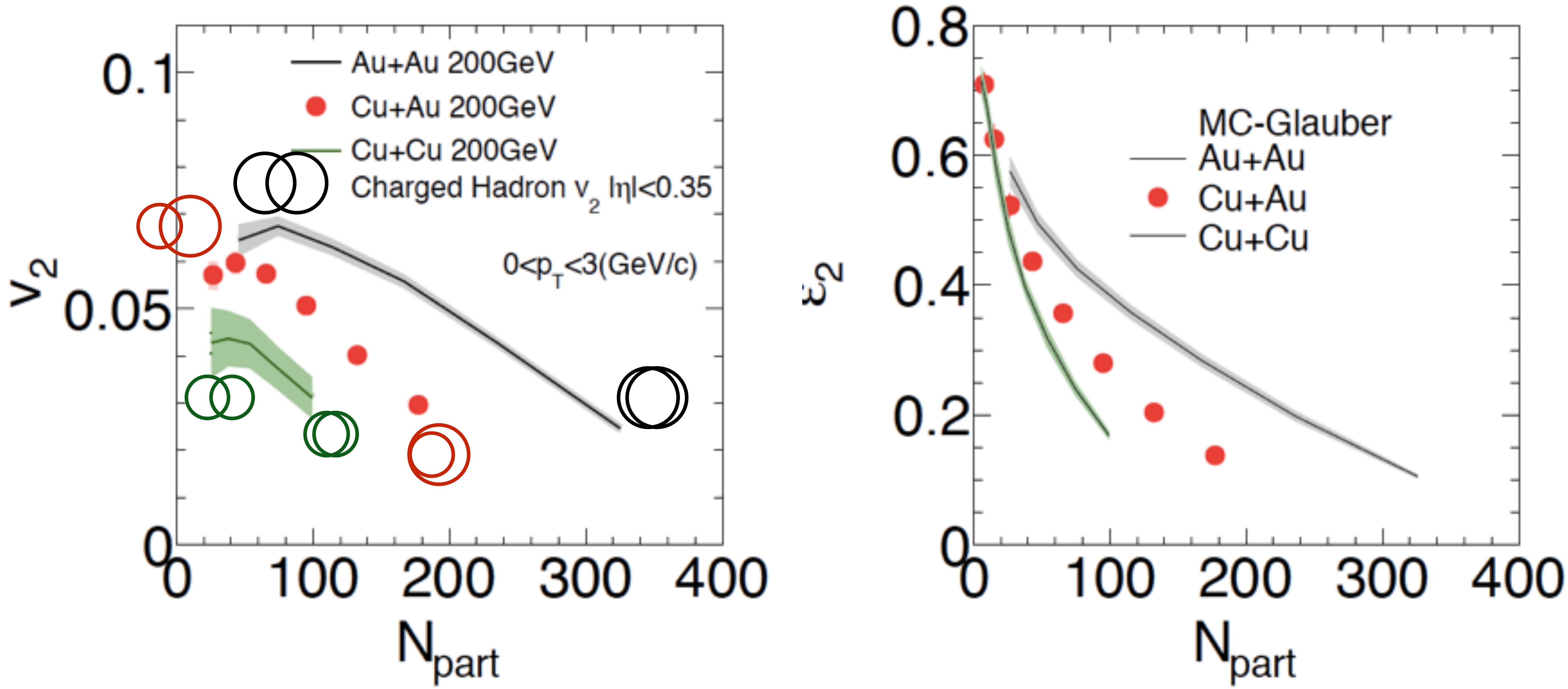

✓ $v_2(N_{part})$ and $\varepsilon_2(N_{part})$ are similar system size dependence

- N_{part}:Number of participants from MC-Glauber
- $v_2(AuAu) > v_2(CuAu) > v_2(CuCu) \sim \varepsilon_2(AuAu) > \varepsilon_2(CuAu) > \varepsilon_2(CuCu)$

System size dependence of $v_3(N_{part})$ and $\varepsilon_3(N_{part})$

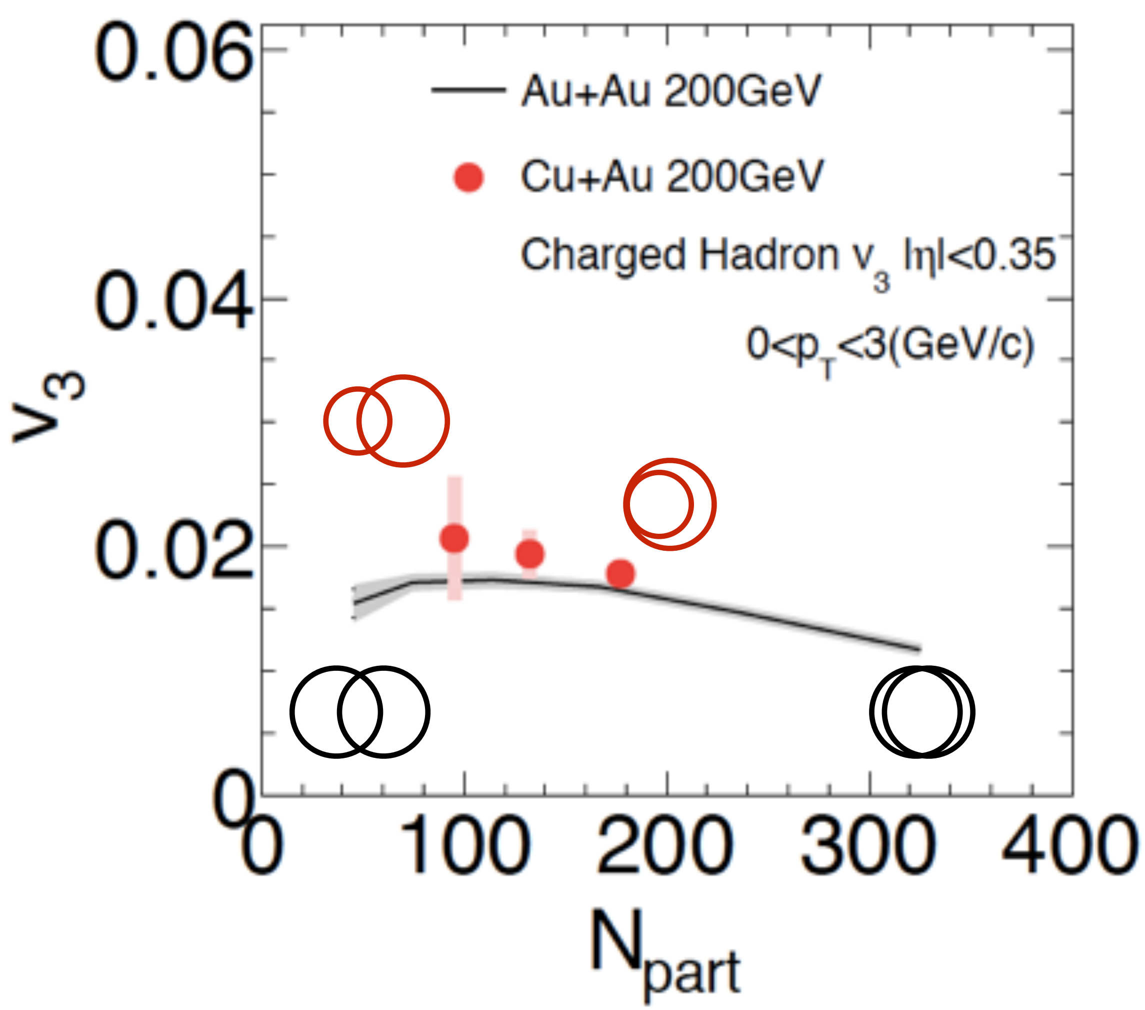

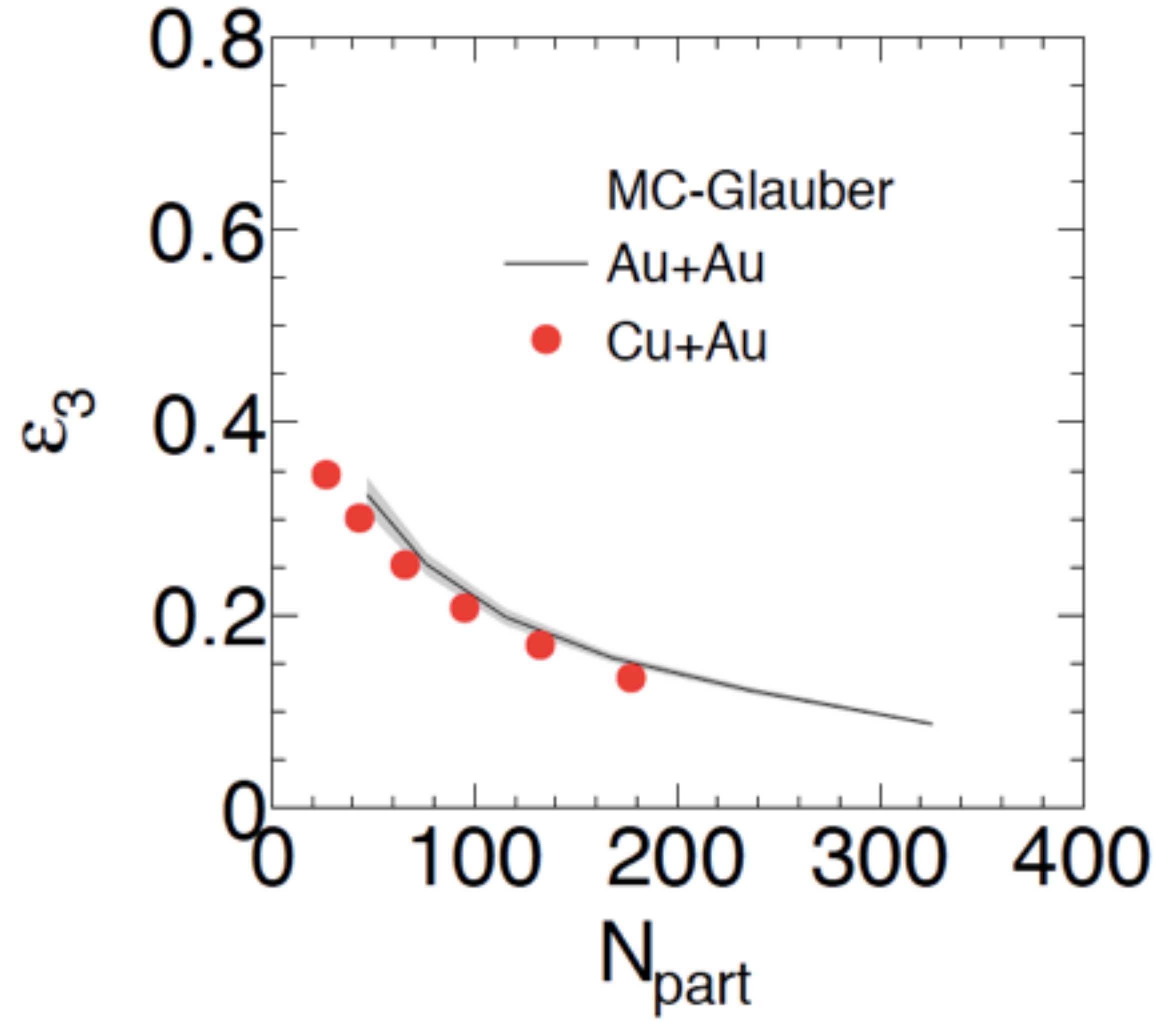

✓Unlike $v_2(N_{part})$, no significant system size dependence of $v_3(N_{part})$ and $\varepsilon_3(N_{part})$

-The ordering of the magnitude of v_3 is reversed with that of ε_3

- v_3 in Cu+Au are almost same or slightly larger than those in Au+Au

-> intrinsic triangularity of asymmetric overlap zone?

System size dependence of v_2 at F/B

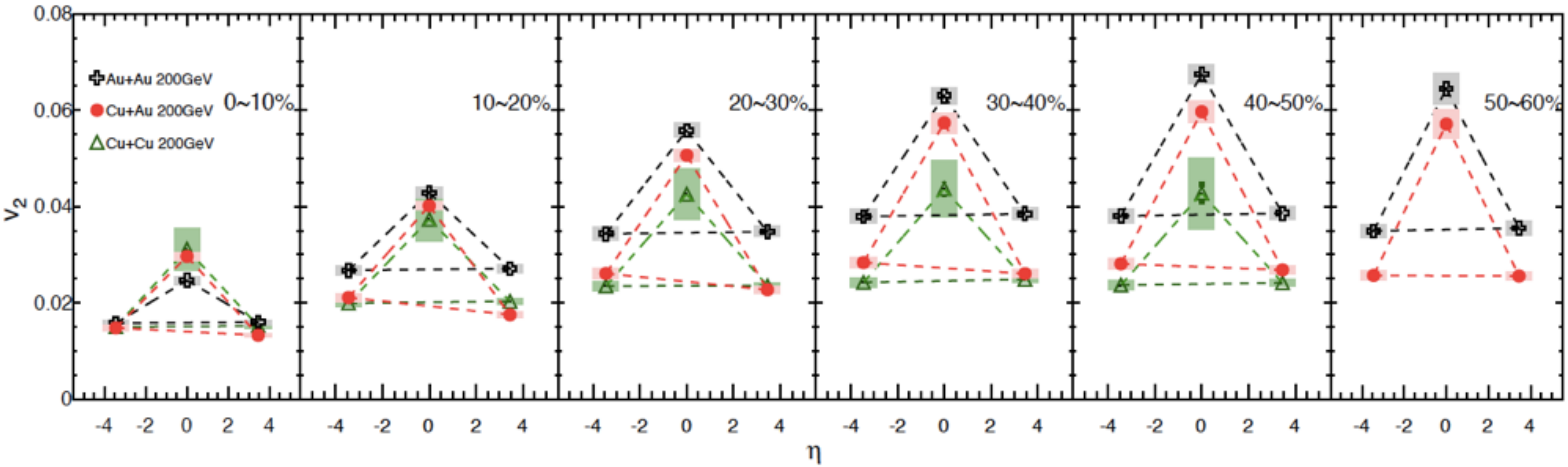

✓In Cu+Au collisions, F/B asymmetry of v_2 is observed.

-central & peripheral collisions: v2(Au-going) ~ v2(Cu-going)

-mid-central collisions : v2(Au-going) > v2(Cu-going)

->caused by different initial geometries in Au and Cu ?

System size dependence of v_3 at F/B

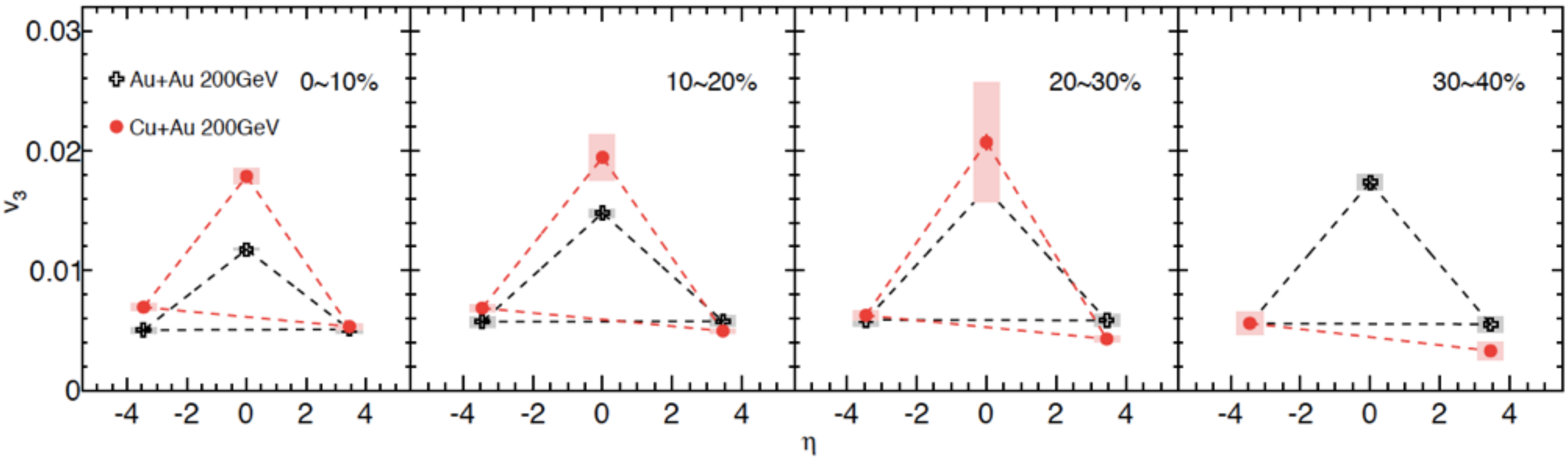

✓Weak centrality dependence of v_3 is seen for all collision systems

- AuAu:same centrality dependence as seen mid η
- CuAu: v_3 decrease as centrality decrease

✓In CuAu collisions, v_3(Au-going) > v_3(Cu-going) for all centrality bins

-> Like v_2, the different initial geometry cause the different v_3 ?

F/B asymmetry of dN/dη

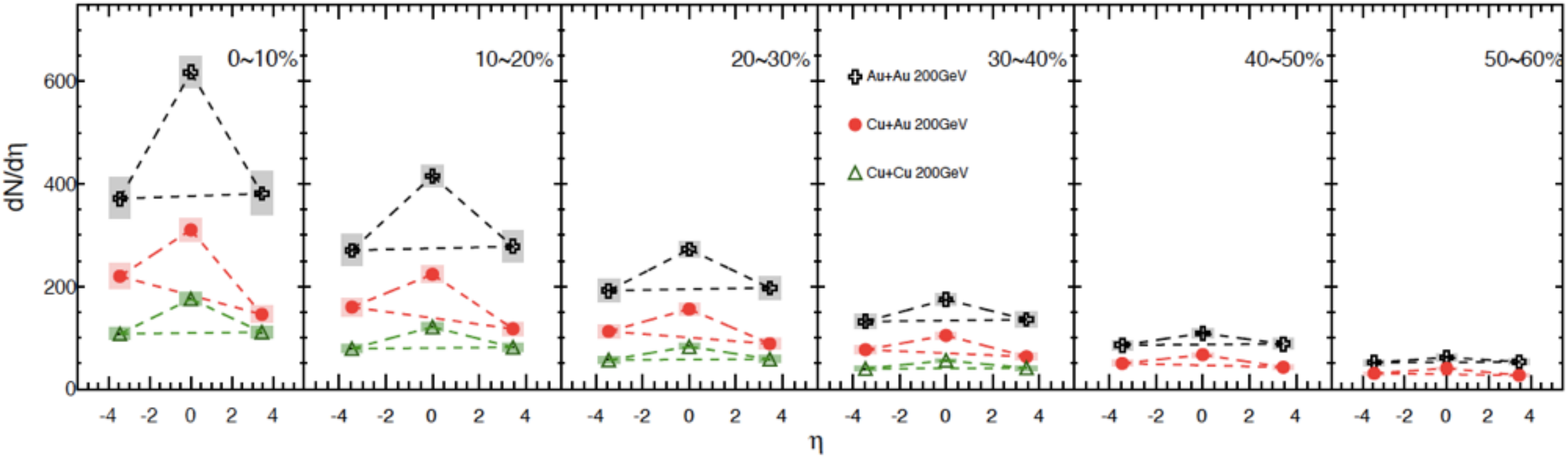

✓Like the v_n, the dN/dη in Au-going side is higher

✓In 50-60%, the dN/dη in Au-going side and Cu-going side are almost same due to similar N_{part}.

Initial geometry model

Glauber nucleon

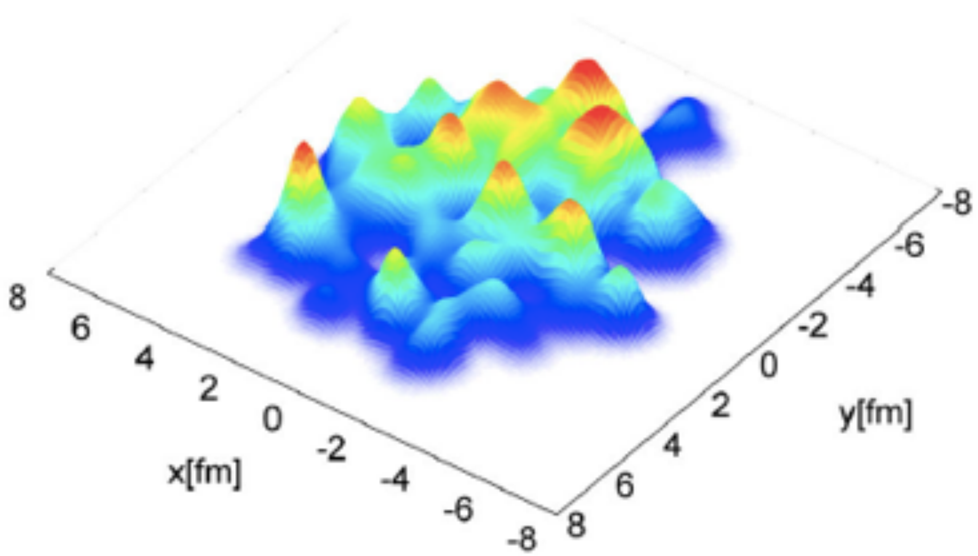

Smooth structure

IPGlasma

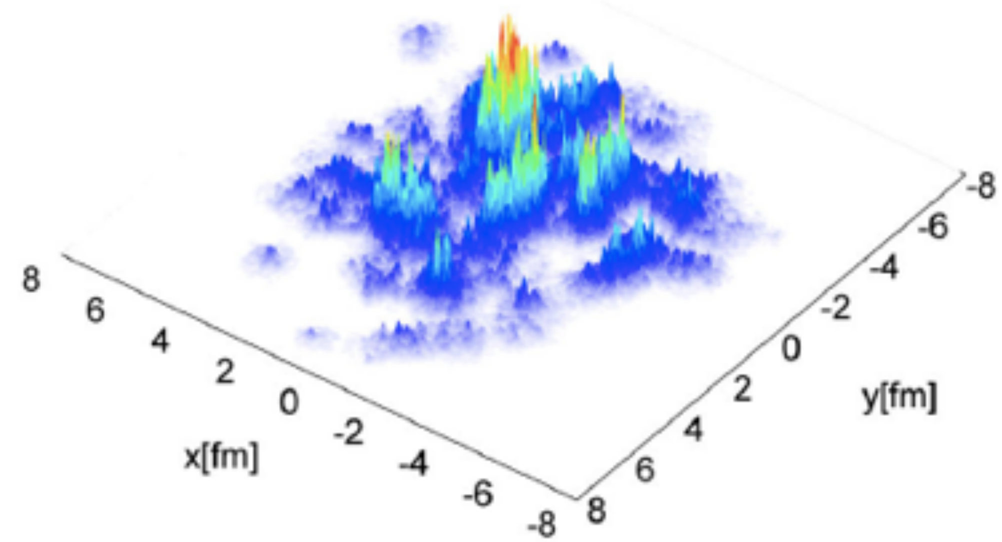

Fine structure

√Glauber Monte Carlo model:nucleon base
√Glauber Monte Carlo model:Constituent quark base
PRC 93 024901
√IPGlasma Model : gluon base(CGC), PRC 89, 064908

->fineness: gluon base>quark base > nucleon base

Model dependence of 2nd and 3rd Eccentricity

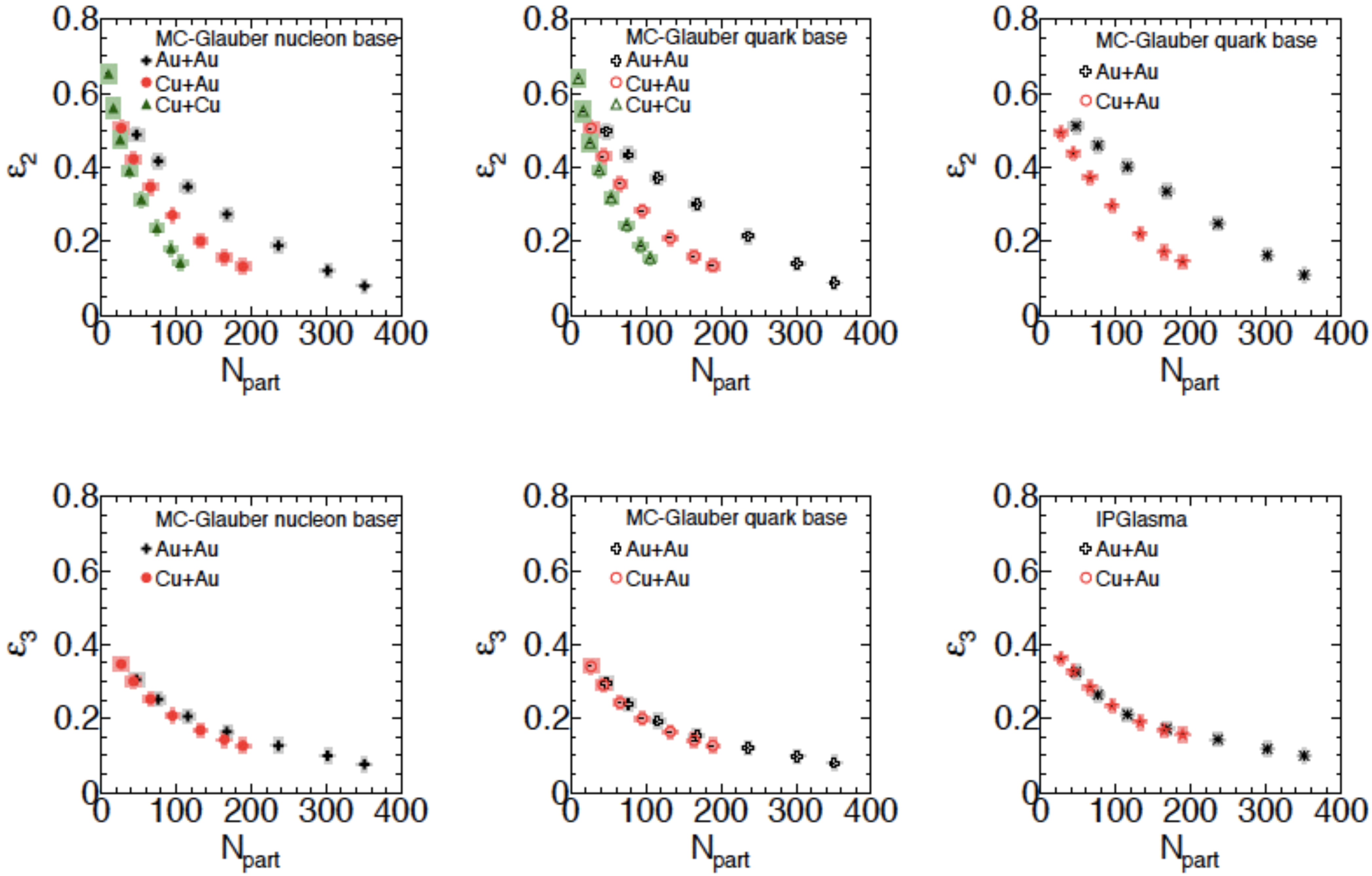

v2/e2 at f/b rapidity vs dN/dy

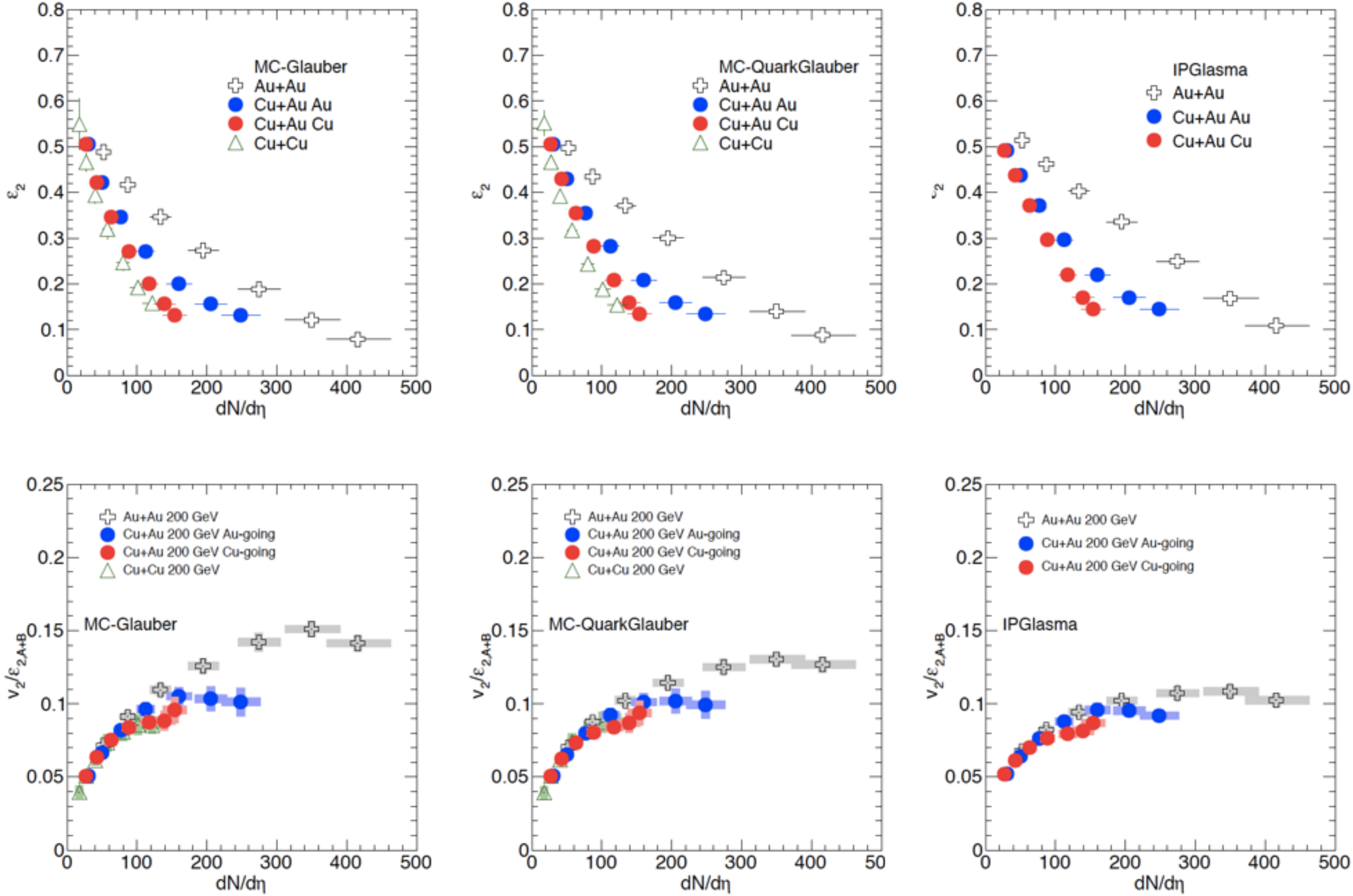

v3/e3 at mid rapidity vs dN/dy

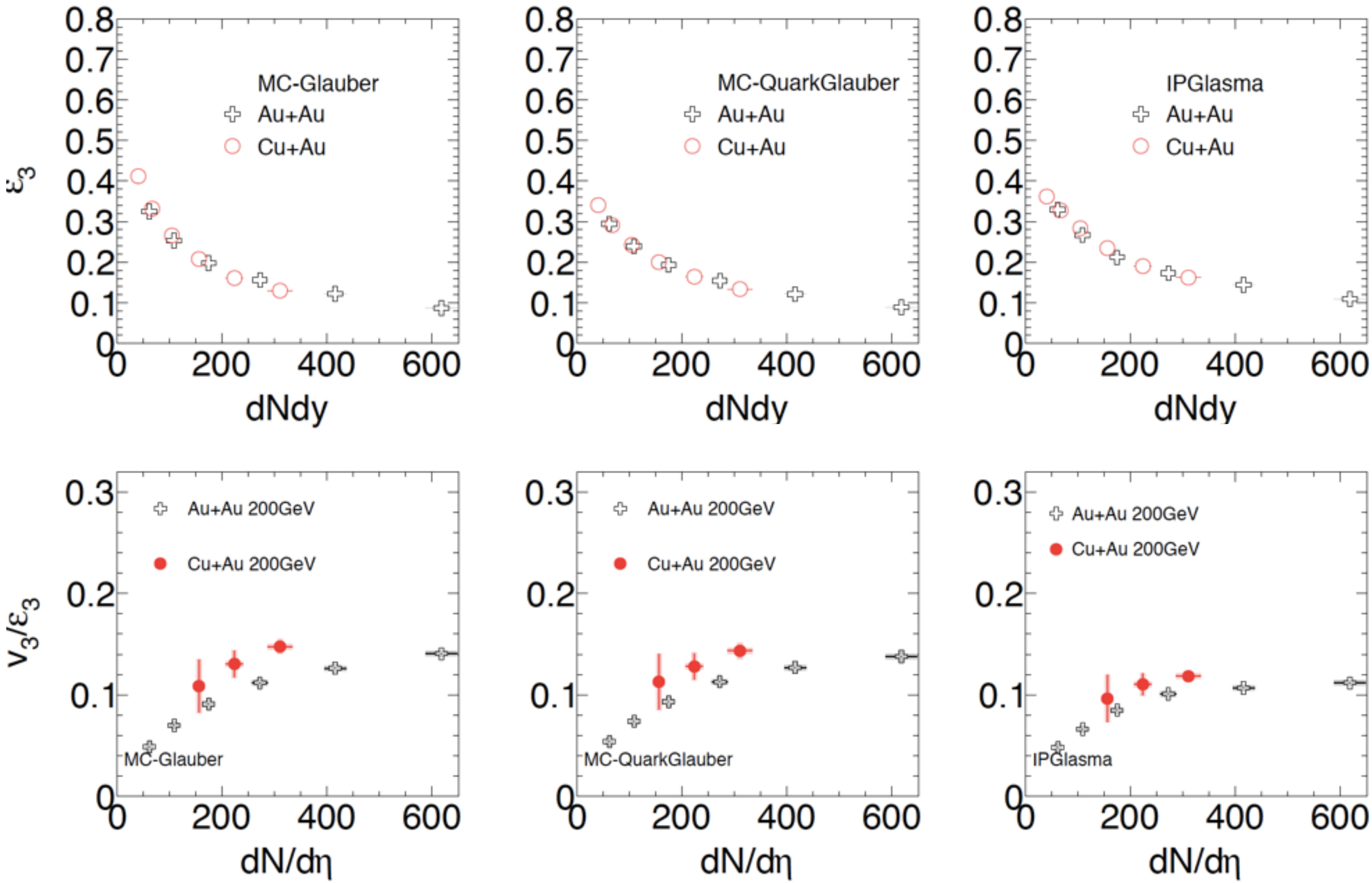

v3/e3 at f/b rapidity vs dN/dy

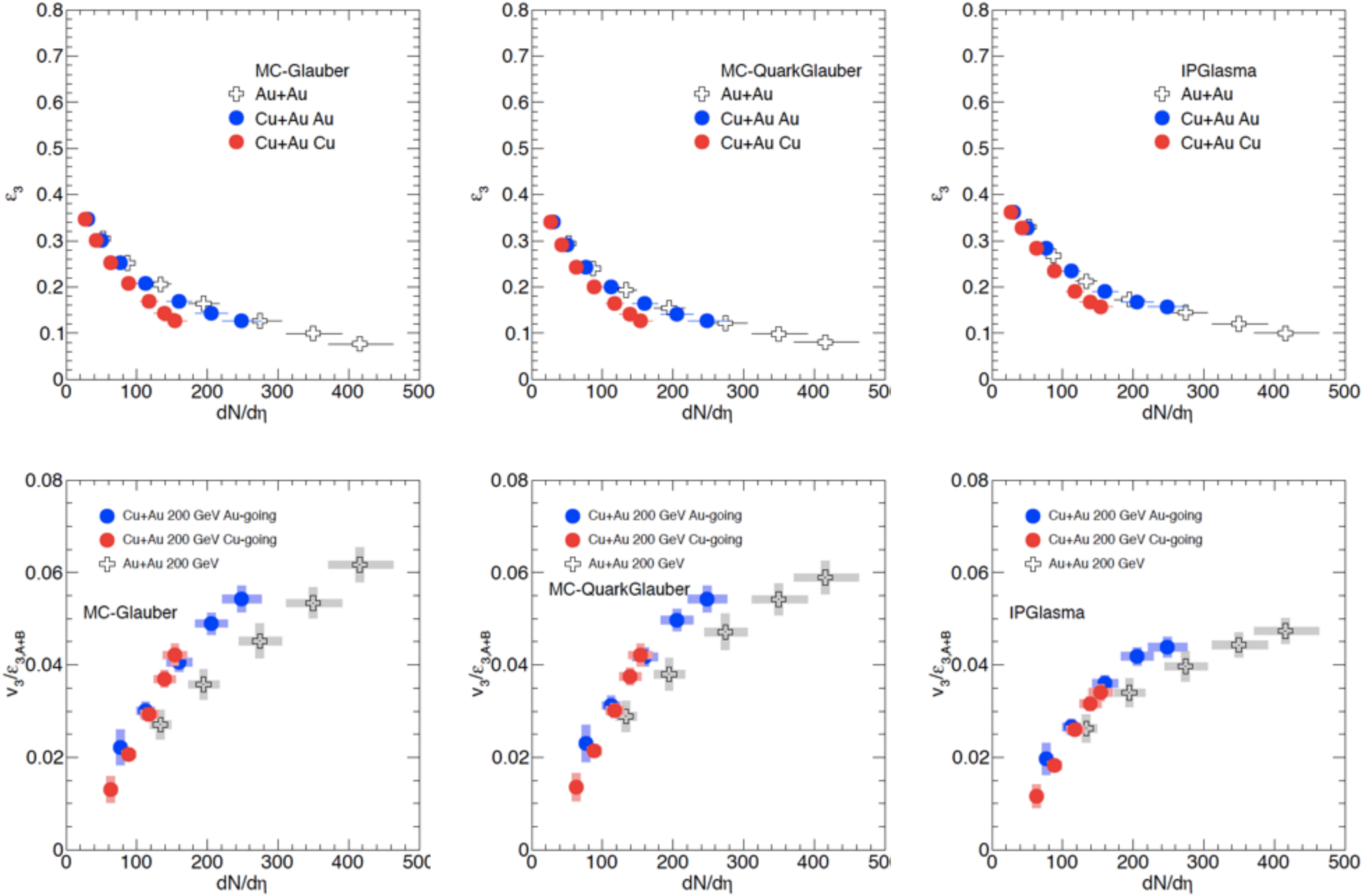

vn vs Npart

v_2/ε_2 scaling at mid-rapidity

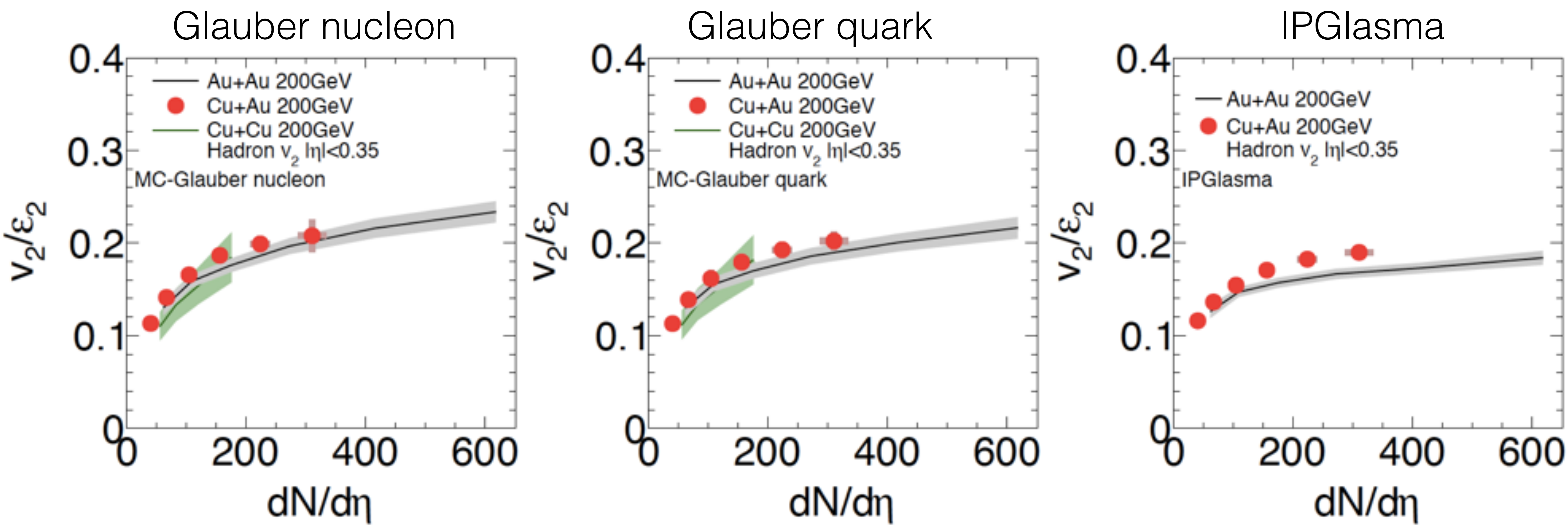

- ✓ v_2 scaled with Glauber model(nucleon,quark) are consistent among three collision systems
- ✓ The deviation is seen in central for IPGlasma model

v_3/ε_3 scaling at mid-rapidity

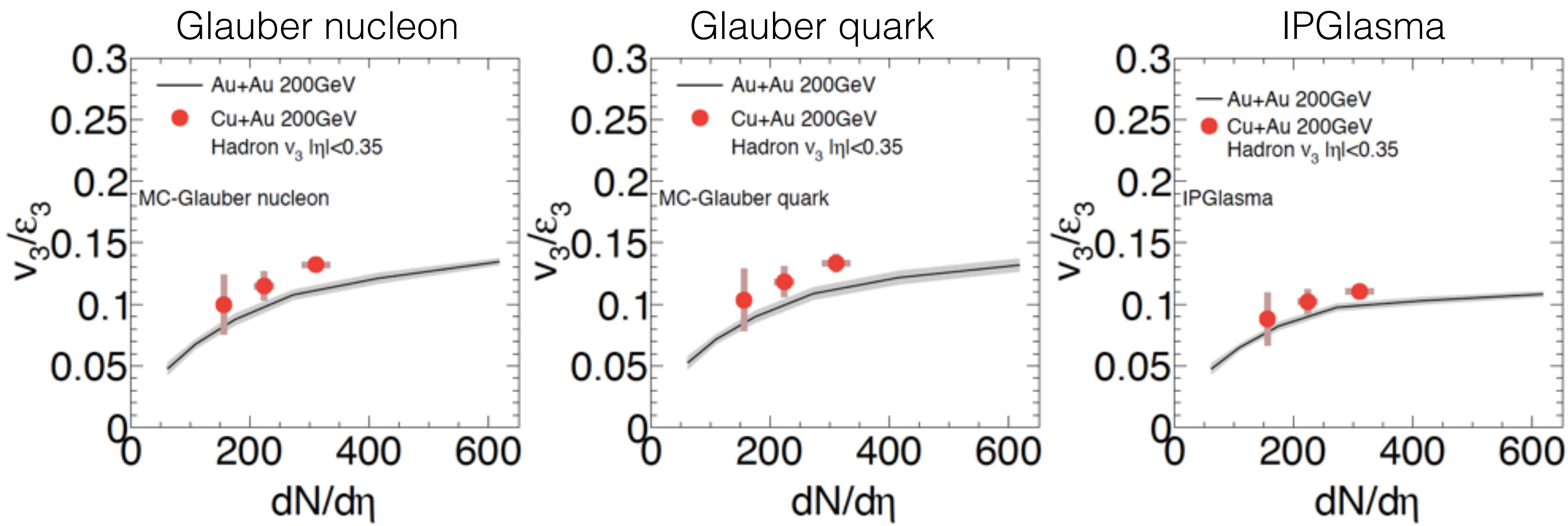

✓In Glauber model(nucleon,quark), the deviation is seen at central bin

✓In IPGlasma model, AuAu v_3/ε_3 and CuAu v_3/ε_3 are close to each other

v_2/ε_2 scaling at f/b-rapidity

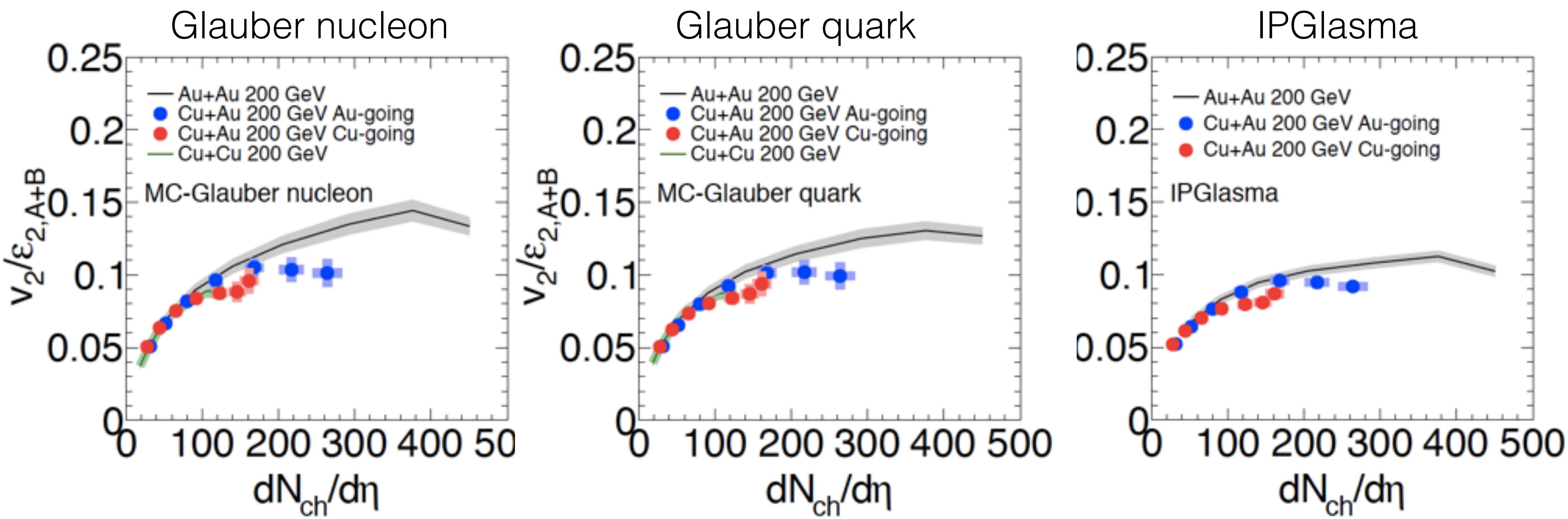

- ✓In Glauber model(nucleon,quark), the deviations between CuAu and AuAu are seen at central bin
- ✓In IPGlasma model, AuAu v_2/ε_2 and CuAu v_2/ε_2 are close to each other

v_3/ε_3 scaling at f/b-rapidity

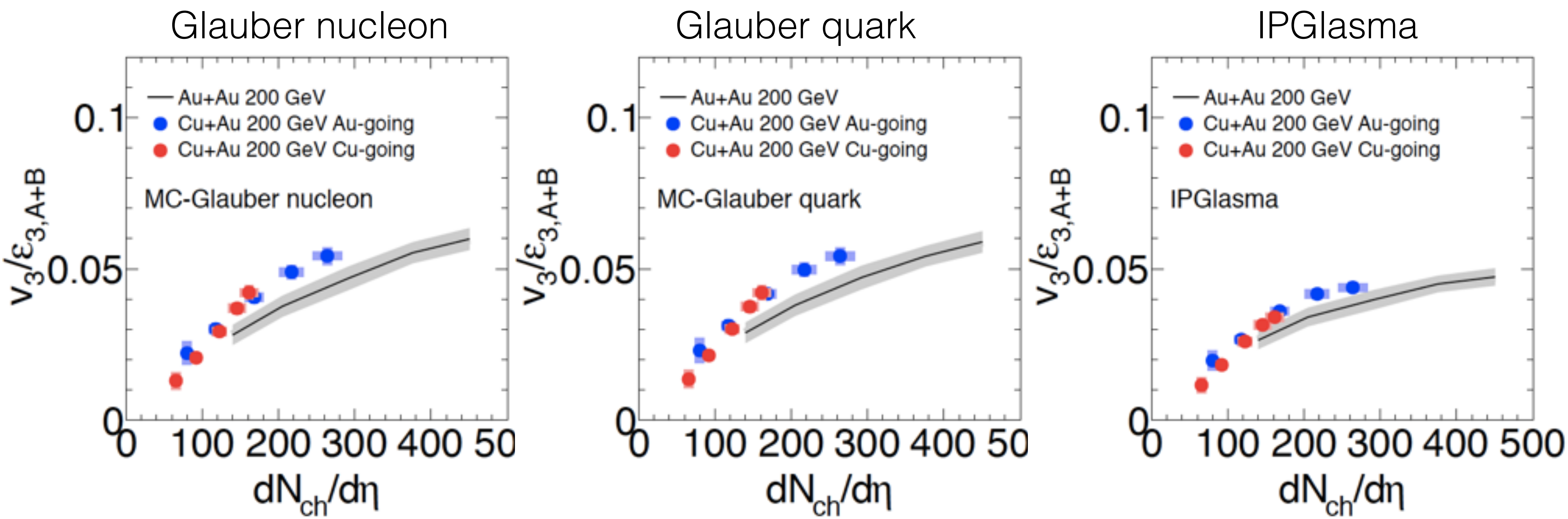

- ✓In Glauber model(nucleon,quark), the deviation is seen from central to mid-central
- ✓In IPGlasma model, AuAu v_3/ε_3 and CuAu v_3/ε_3 are close to each other

Parton cascade and hydro $v_2(\eta)$

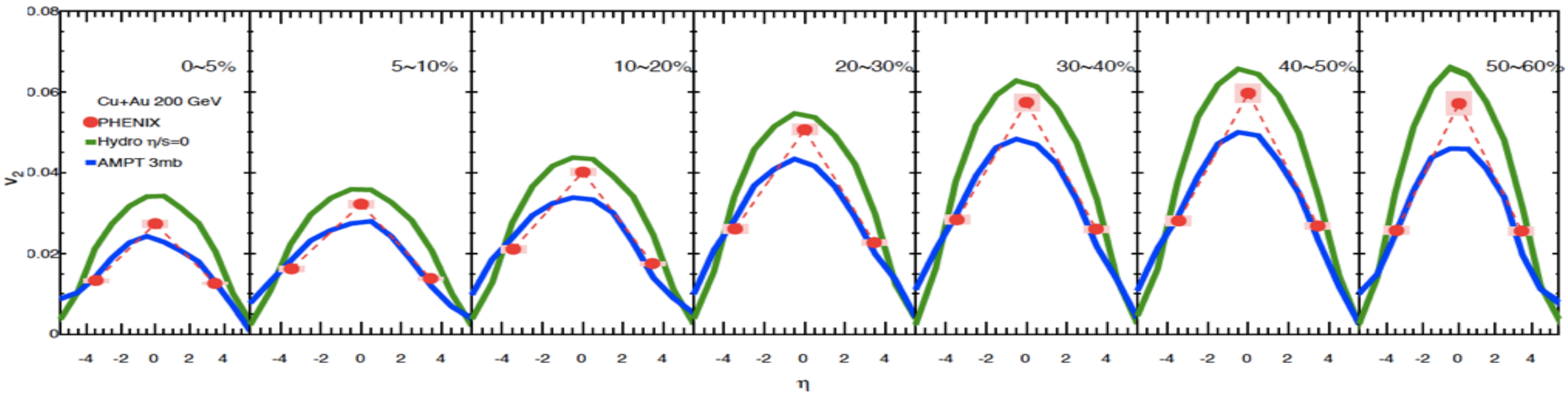

- ✓AMPT and Hydro predict magnitude of v2 at F/B rapidity well
  - -Hydro:Smooth longitudinal density+hydro
  - -AMPT:Fluctuated longitudinal density+parton cascade
- ✓Hydro reproduces the ratio of F/B v2
  - In peripheral collisions, the F/B ratio becomes constant
- ✓AMPT model over-estimate the ratio

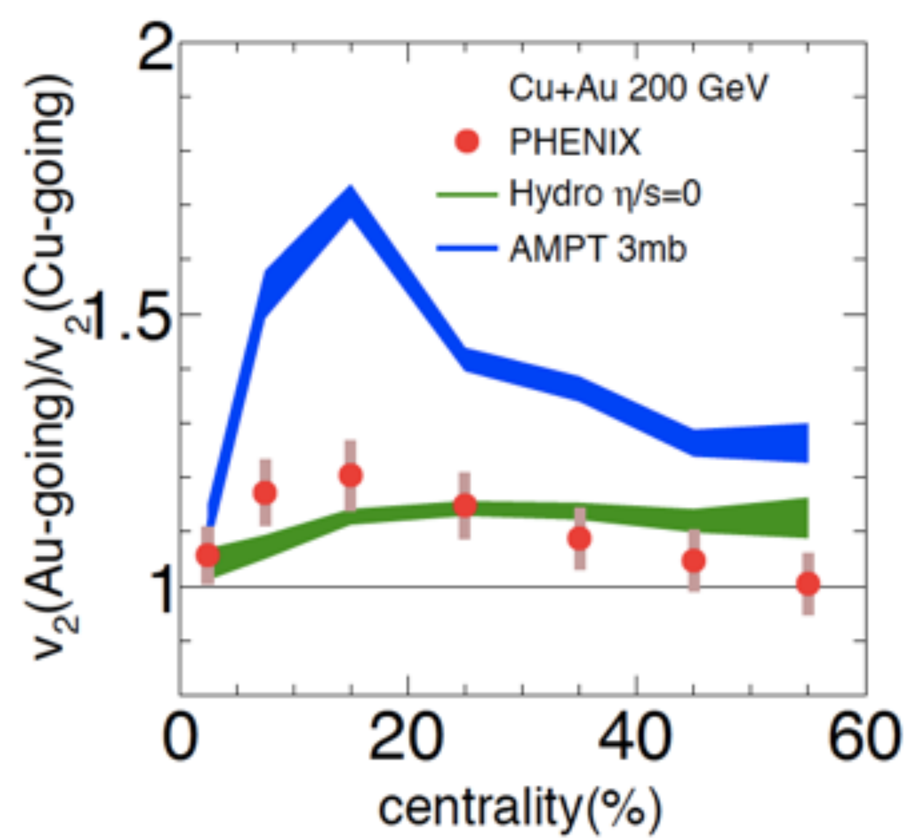

Parton cascade and hydro $v_3(\eta)$

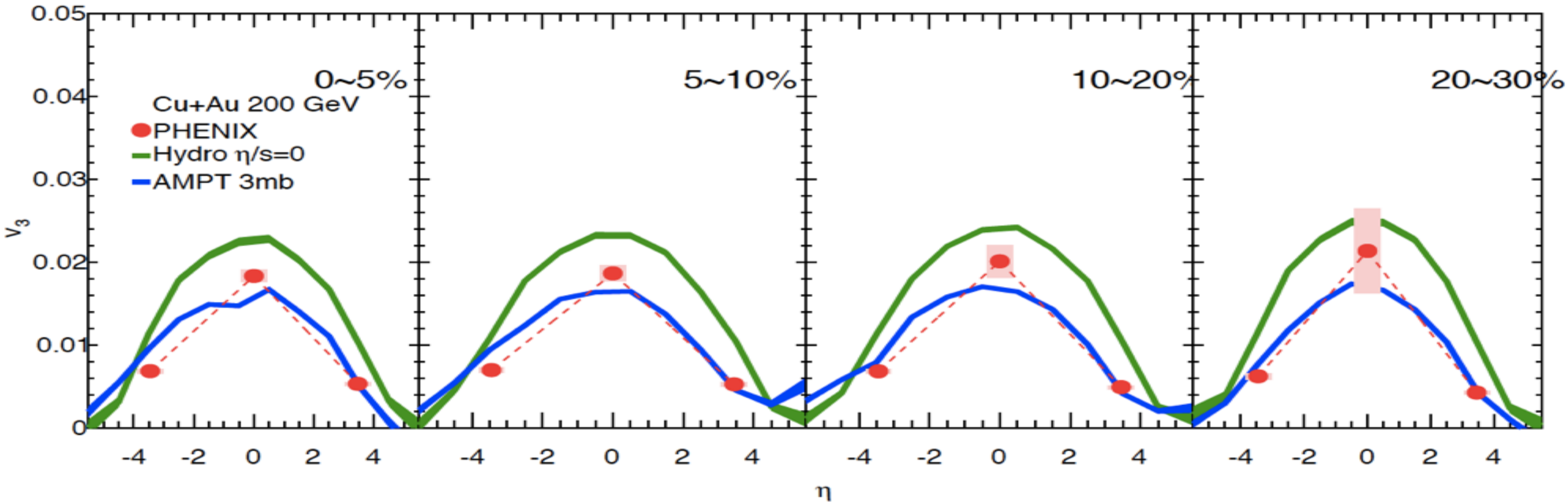

✓AMPT show the F/B asymmetry of v3
- v_3 (Au-going) > v_3(Cu-going)
->Fluctuated longitudinal density show larger F/B asymmetry of v_n

✓Hydrodynamics show weak F/B asymmetry of v3
-v_3(Au-going) ~ v_3(Cu-going)
->Smooth longitudinal density show weaker F/B asymmetry of v_n

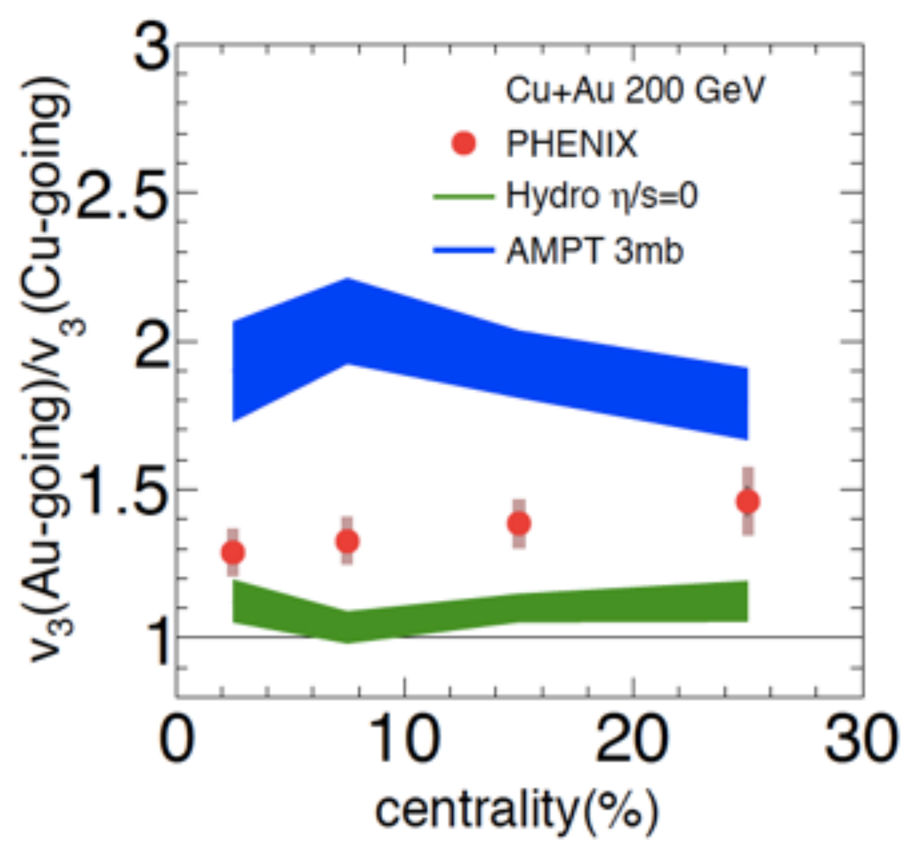

Directed flow in comparison to STAR and ALICE

PRL 111 232302

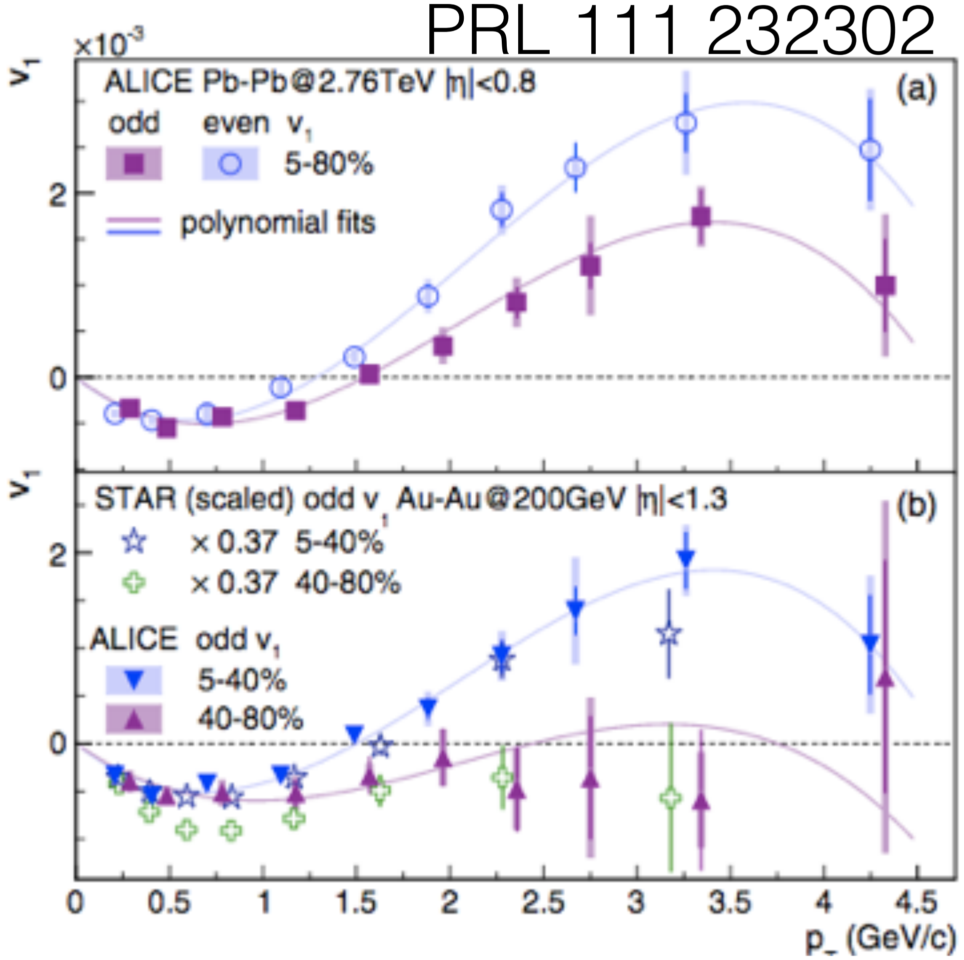

PRL 101 252301

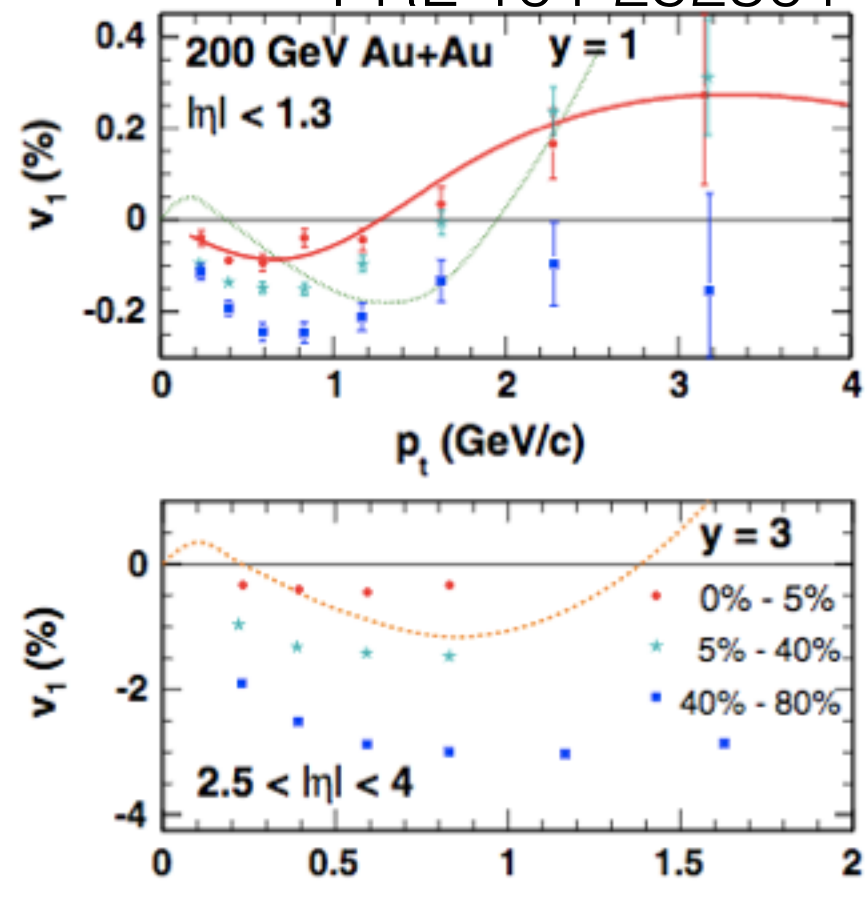

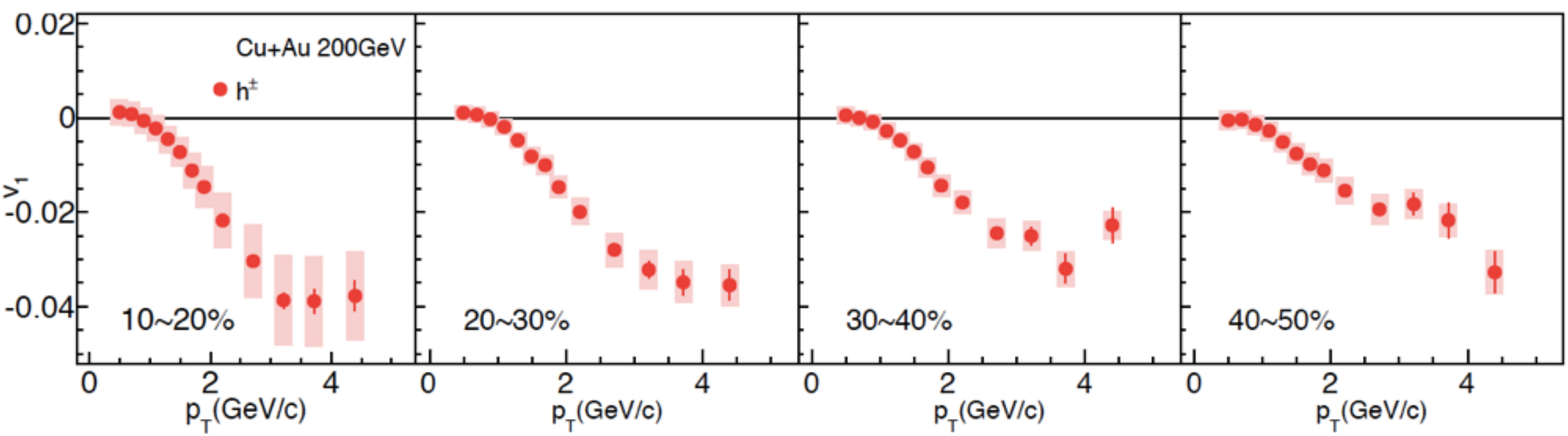

MC-Glauber E-by-E hydro v_2, v_3 at mid-η

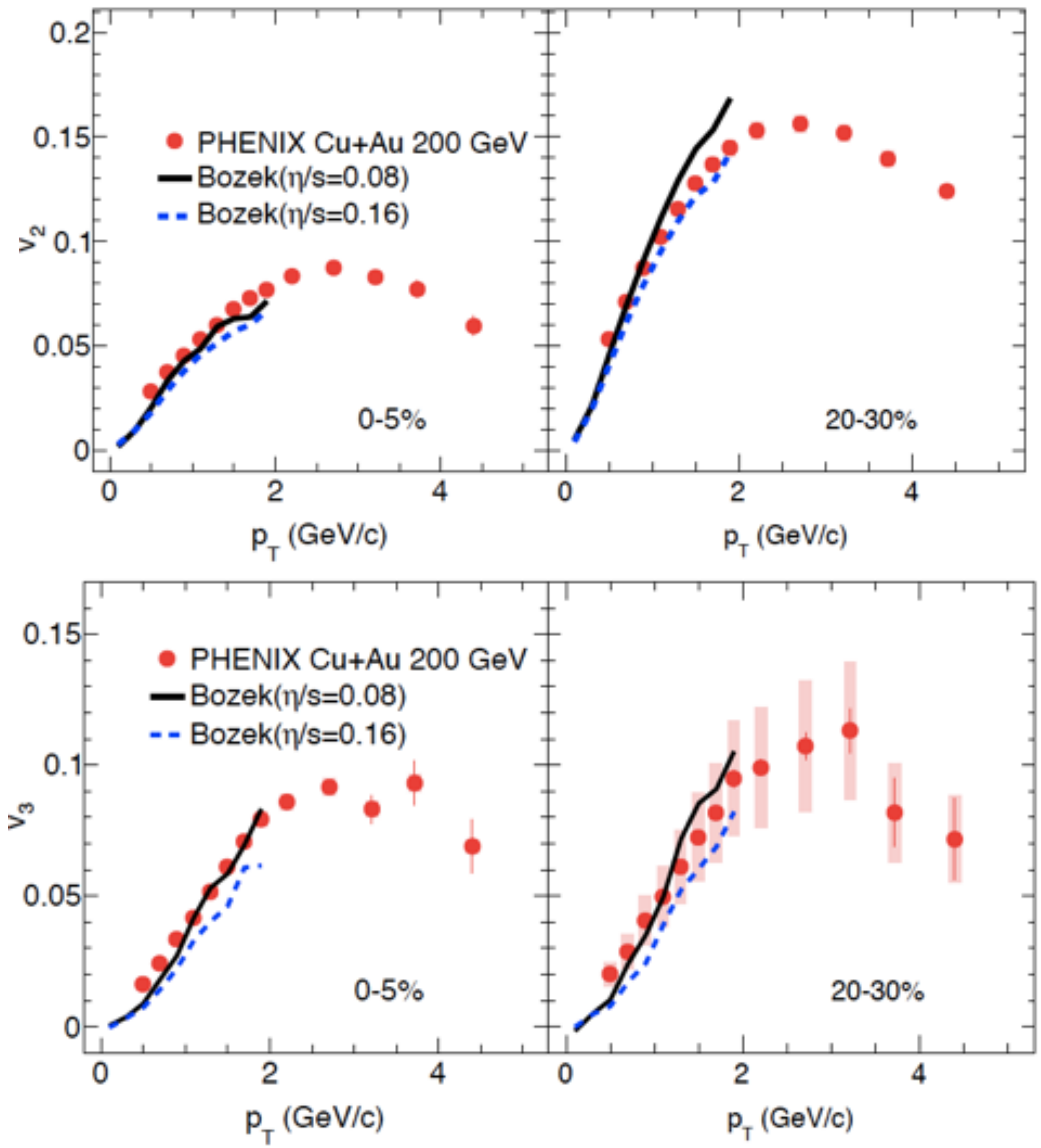

For both centrality, both value of η/s agree with data

v_n:AMPT and Hydrodynamics

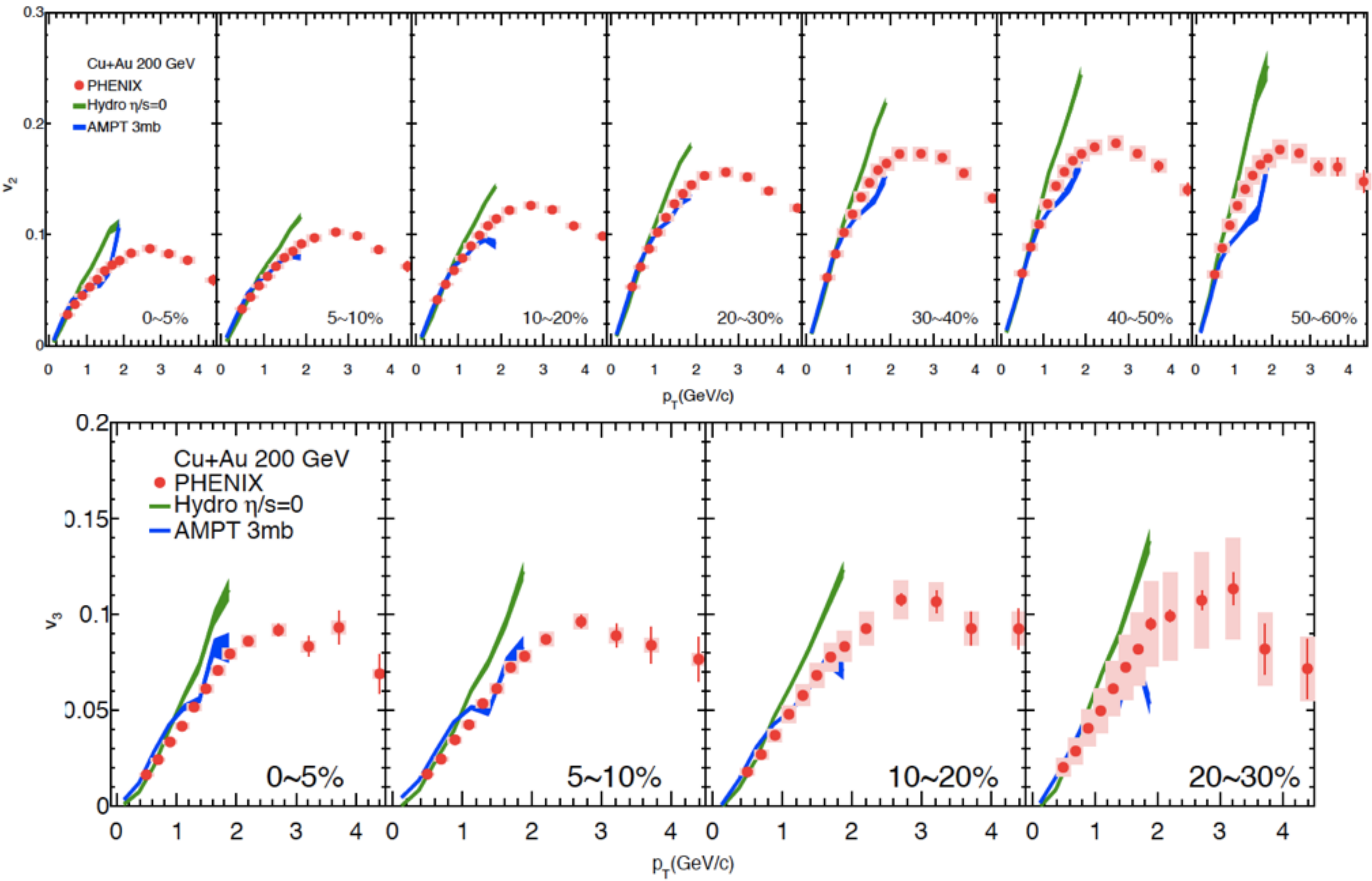

pi, K, p flow

arXiv:1412.1038

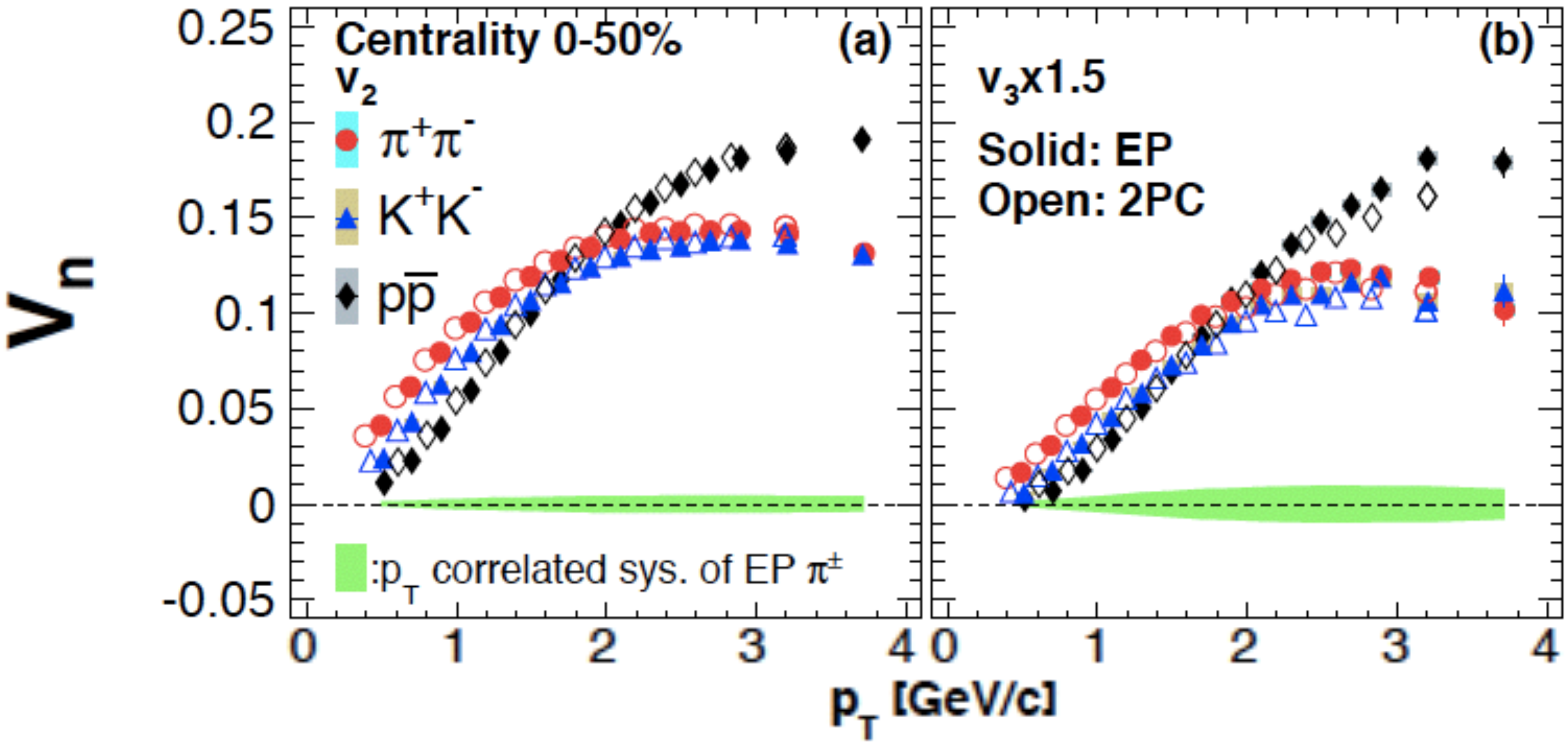

v_2,v_3 have similar particle dependence

v_3 scaled with $n_q^{3/2}$

Scaling property : quark number scaling

arXiv:1412.1038

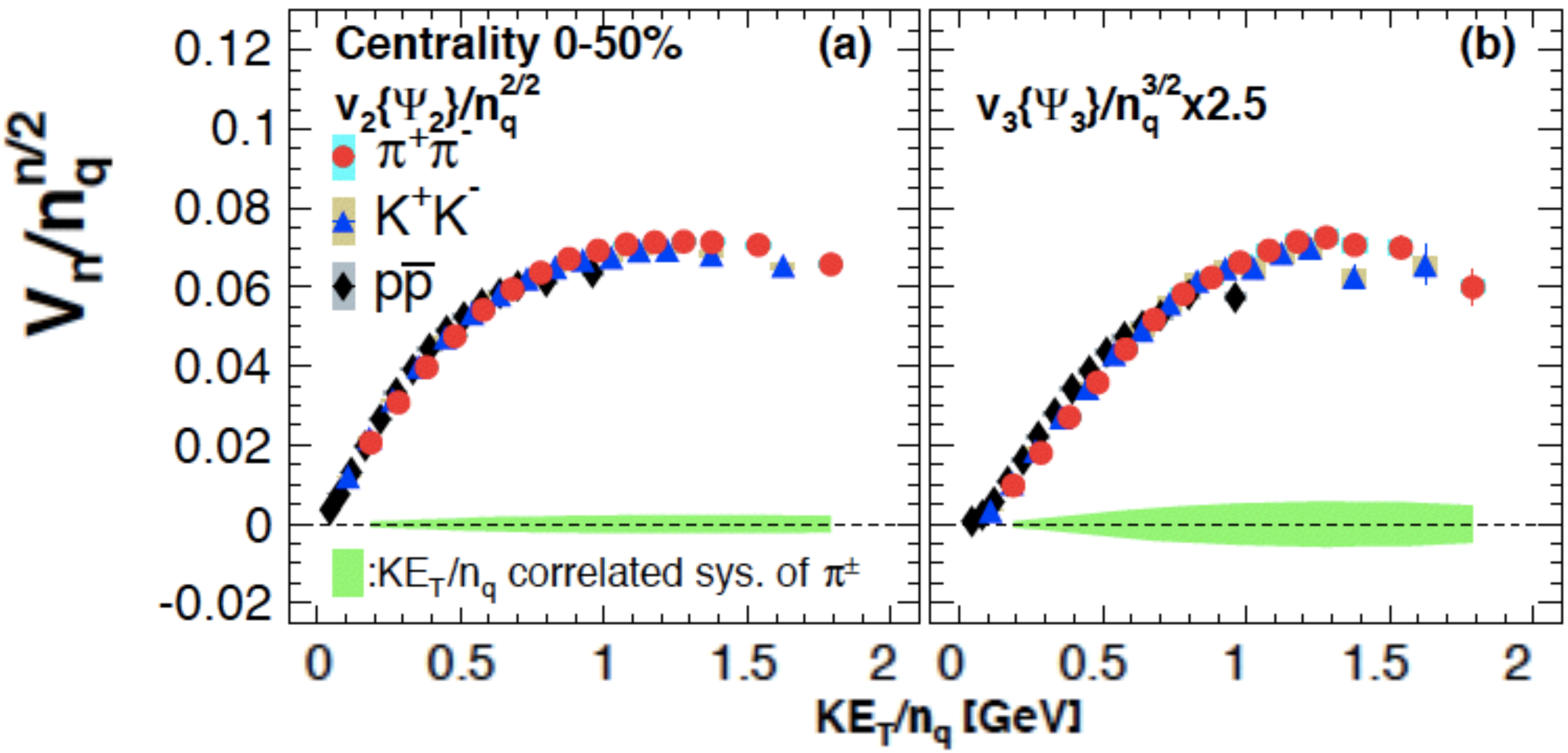

v_2,v_3 have similar particle dependence

v_3 scaled with $n_q^{3/2}$

Track identification at CNT(|η|<0.35)

TOF.E and TOF.W are used

-TOF.E : Scintillation counter 130ps

-TOF.W : MRPC 95ps

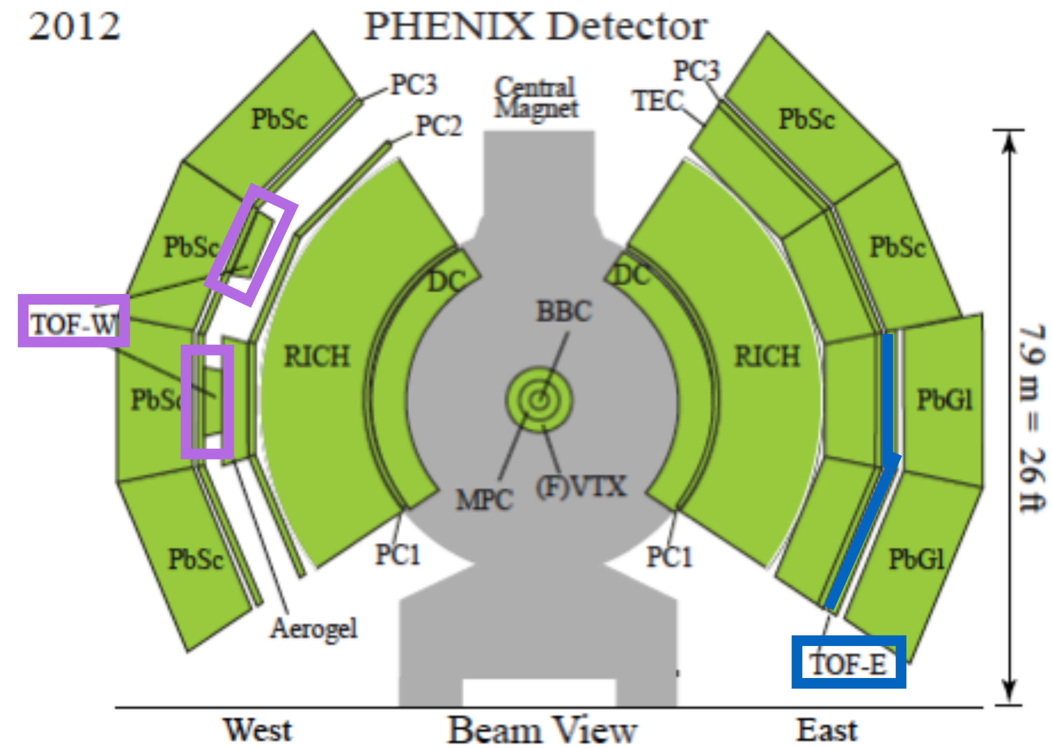

Time of flight method

$$m^2 = p^2\left(\left(\frac{ct}{L}\right)^2 - 1\right)$$

m:particle mass, p:momentum, L:flight pass
c:light velocity, t:time of flight

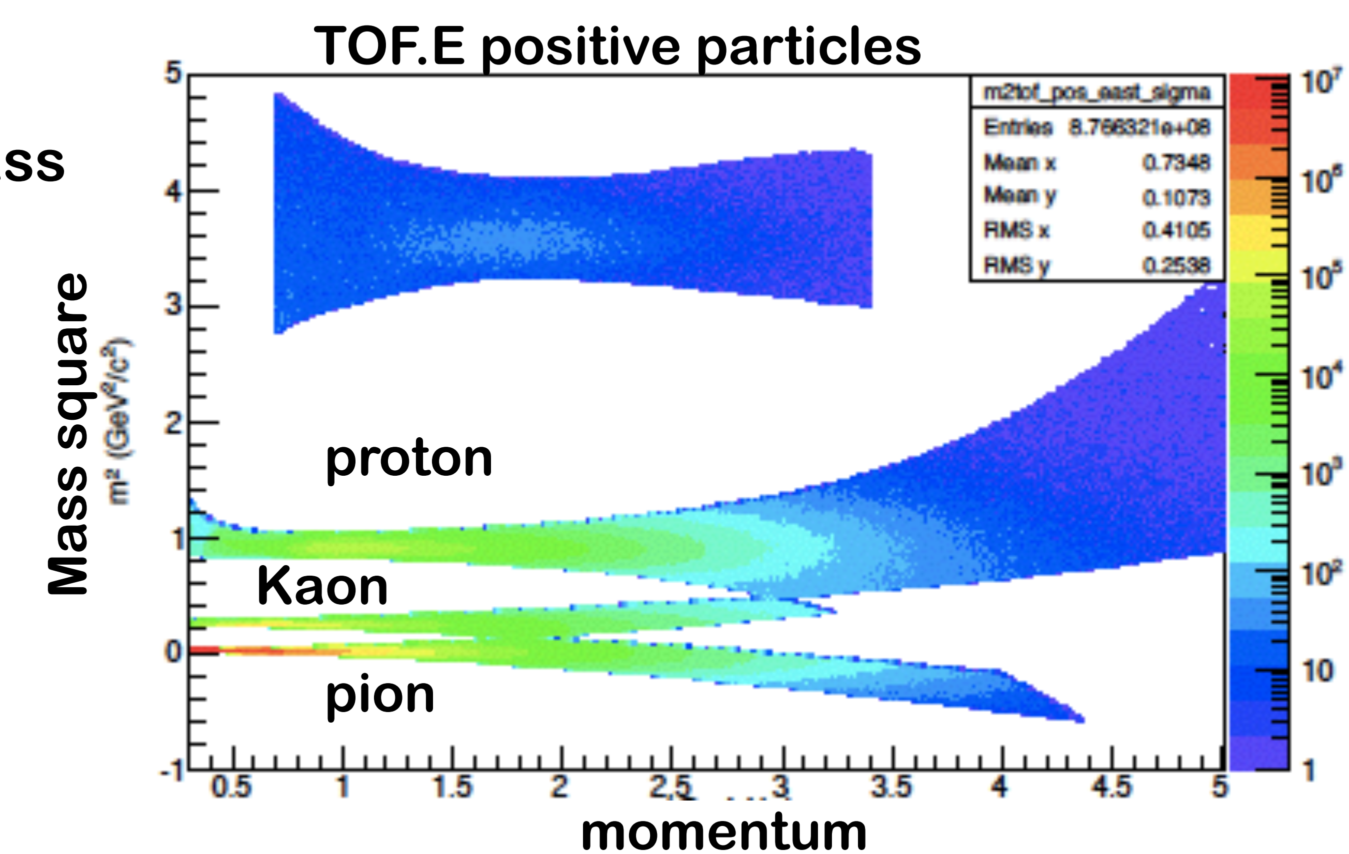

Charged pi,K,p

-pi/K up to 3GeV

-K/p up to 4GeV

Results & Discussions

- System size dependence
- PID v_n
- Rapidity dependence
- Theory comparison

Identified particle v_2 in Cu+Au

arxiv:1509.07784

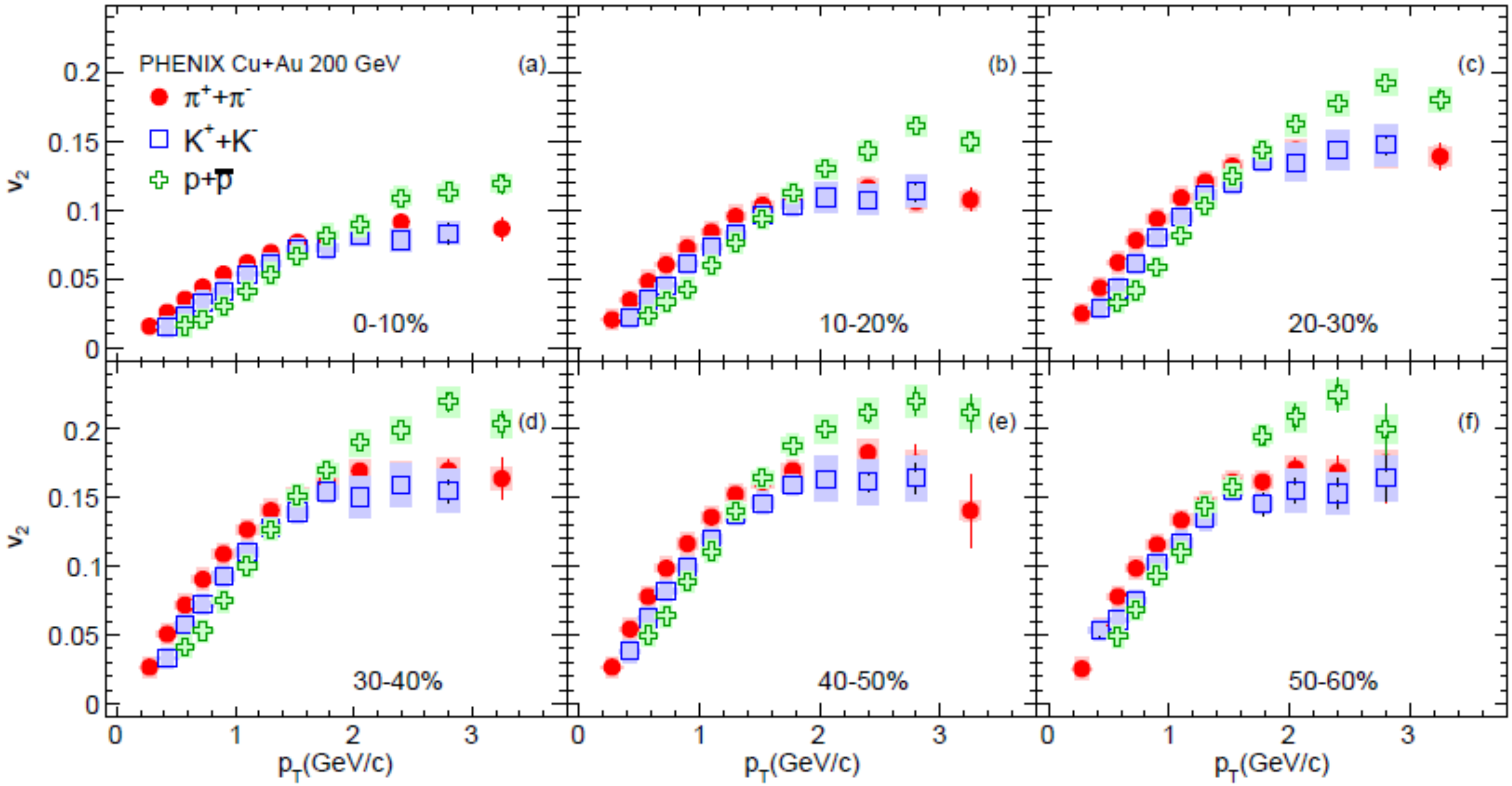

Mass ordering at low p_T for v_2 for all centralities
Baryon and meson splitting at mid-p_T is seen

Identified particle v_1, v_3 in Cu+Au

arxiv:1509.07784

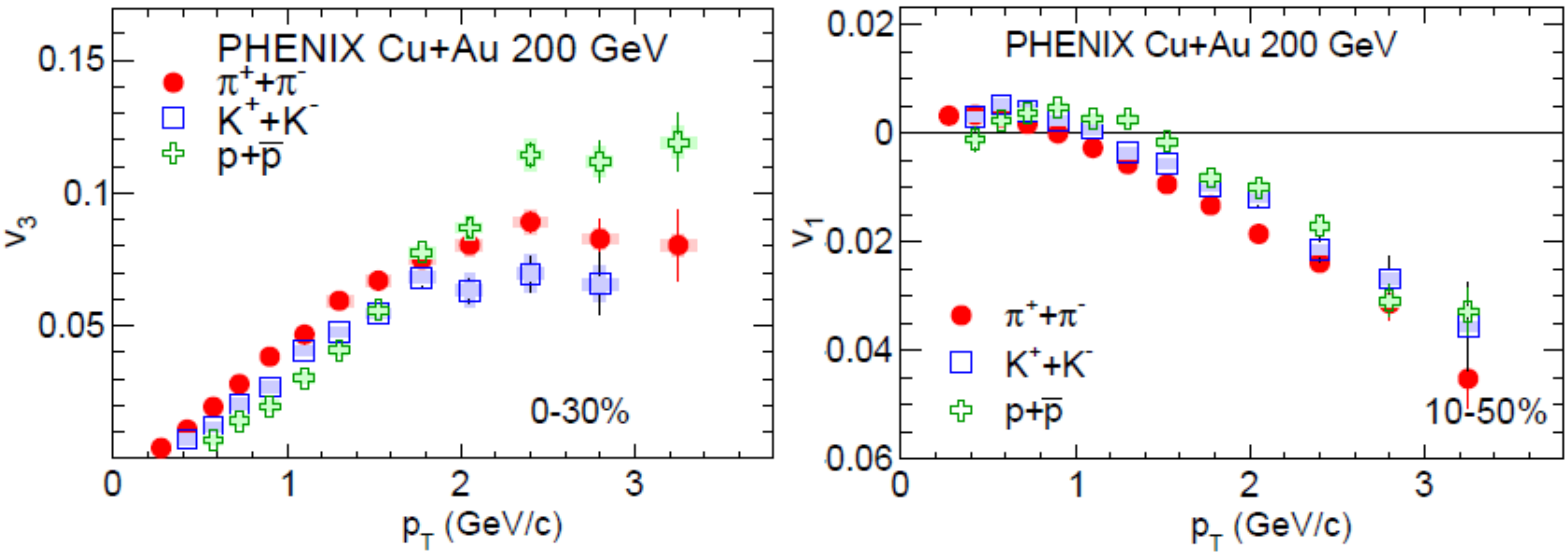

Same particle dependence of v_3 is seen as seen in v_2

Mass ordering is also seen for v_1

- At 1<pT<2.5GeV, Mass ordering is seen

- At low and high pt region, baryon v_1 ~ meson v_1

-Not same trend as seen in v_2, v_3

Quark Number Scaling of v2

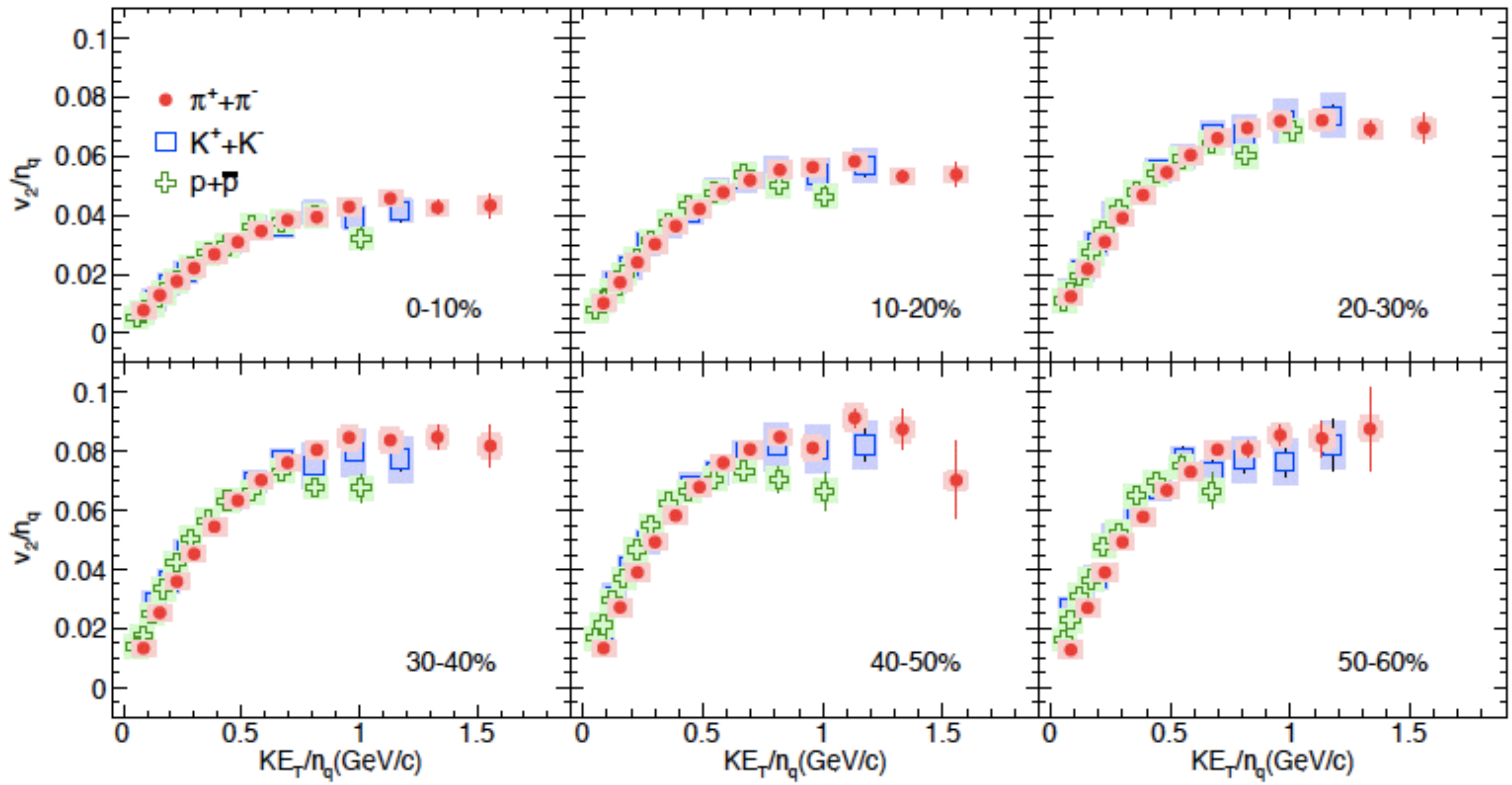

Quark Number Scaling works v2 in CuAu

Quark Number Scaling for v3

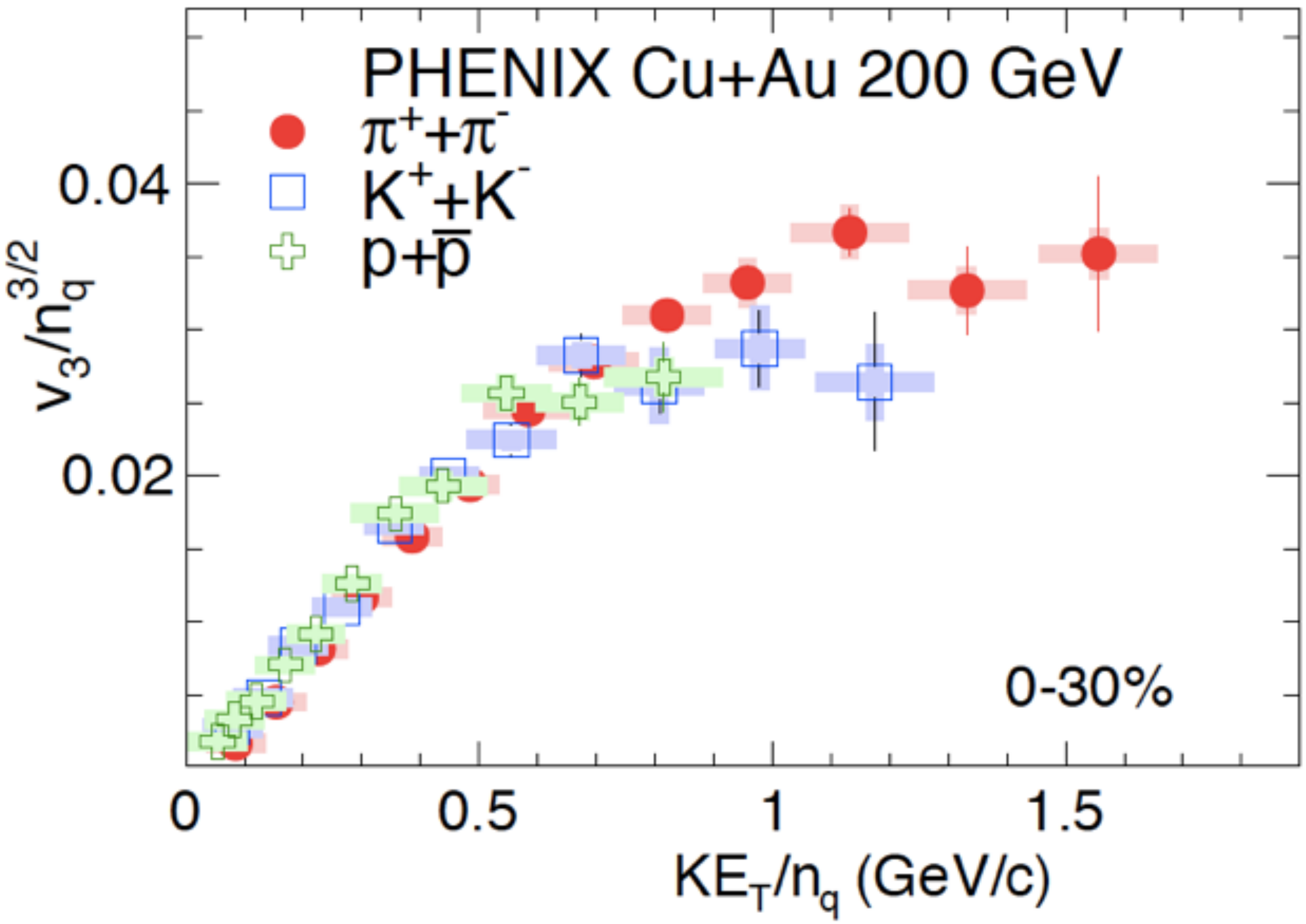

Quark Number Scaling work v3 in CuAu

Comparison to AMPT v2

arxiv:1509.07784

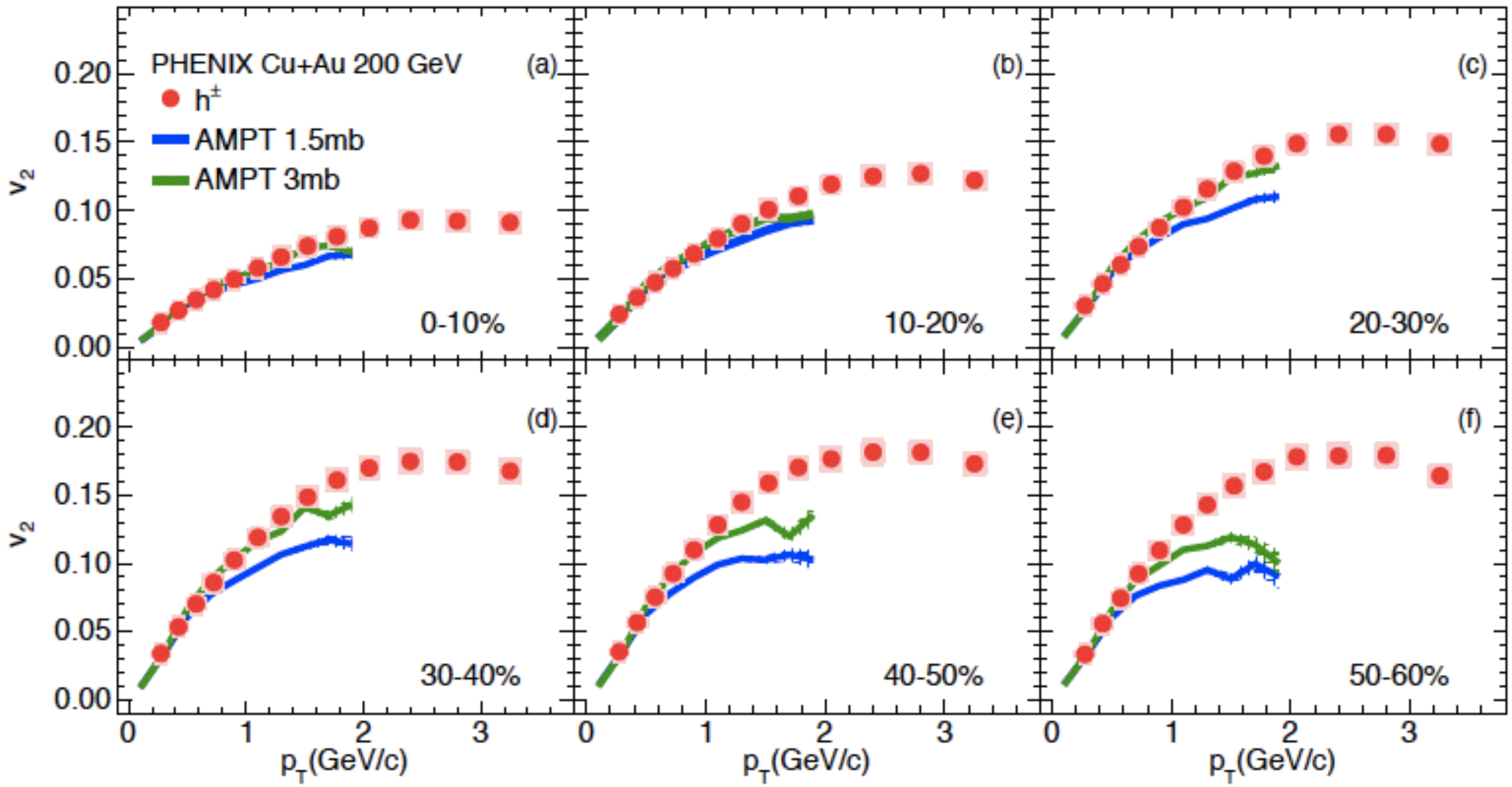

AMPT with 3mb reproduce v2
-In 0-30%, up to 2GeV
-In 30-60%, up to 1GeV

Comparison to AMPT v3

arxiv:1509.07784

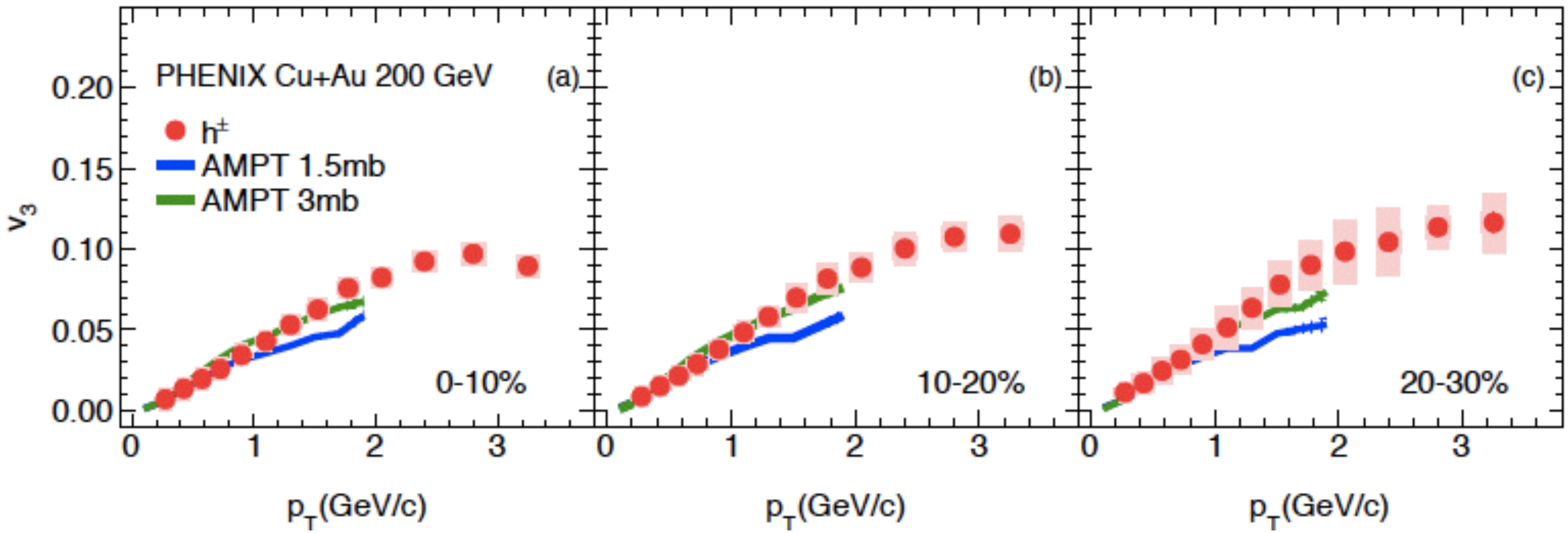

AMPT with 3mb reproduce v3
-In 0-30%, up to 2GeV

Flow in symmetric collisions system

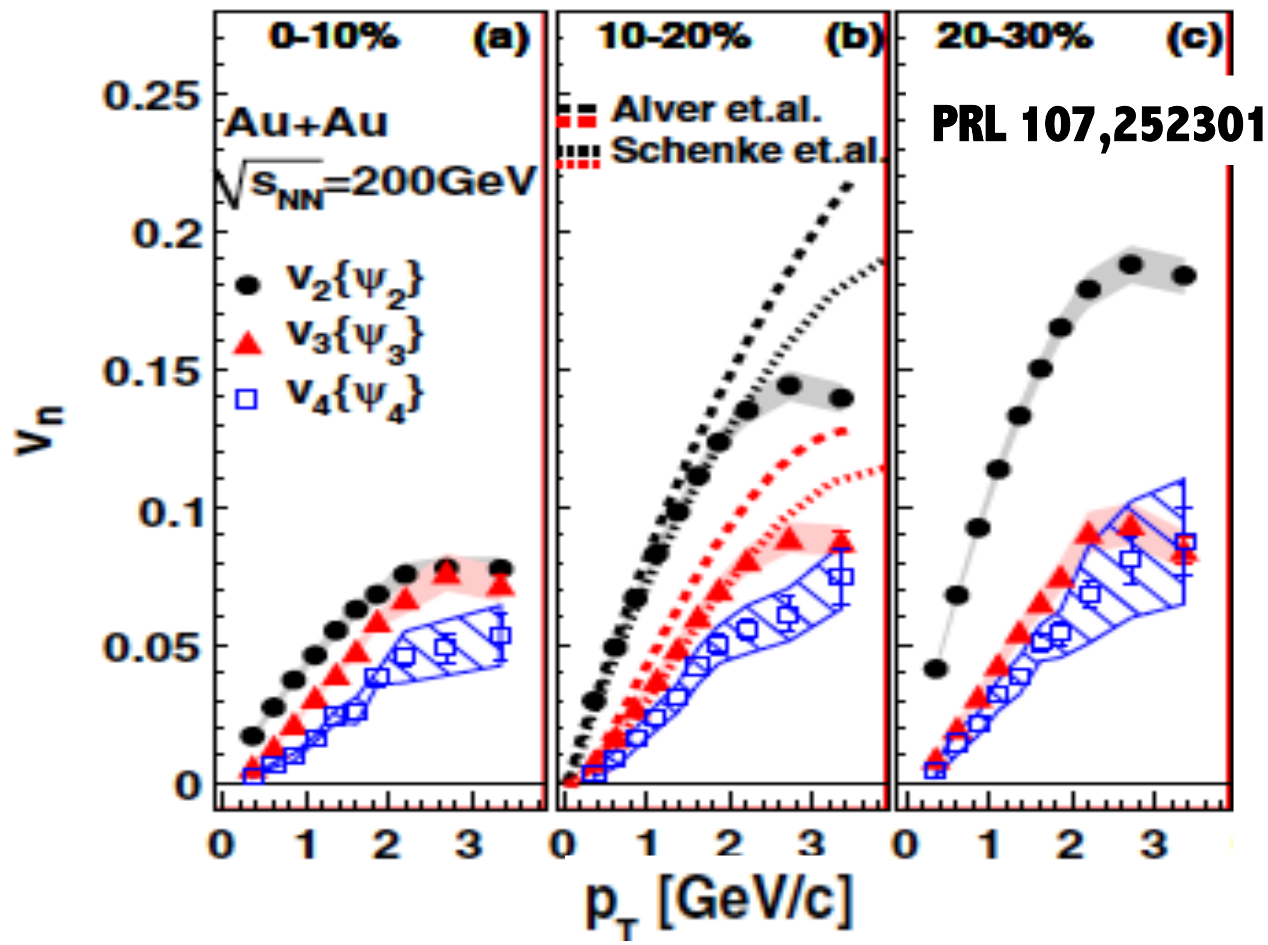

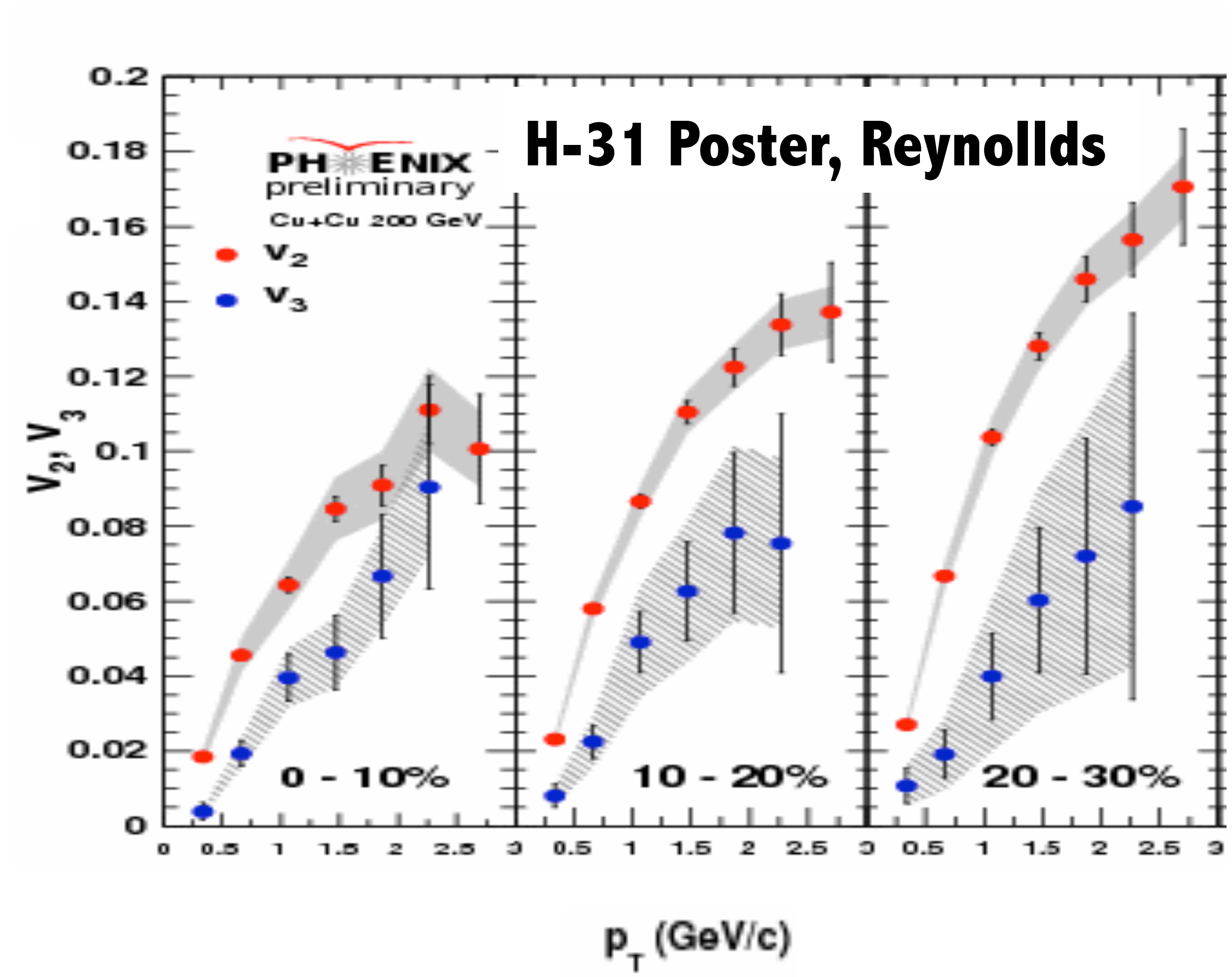

3sub method

Event Plane detectors

- 2nd, 3rd Event plane
  - Bbc, Cnt
- 1st Event plane
  - Bbc, Smd

Event Plane resolution

-Estimated from EP correlations(3sub method)

PHENIX η acceptance

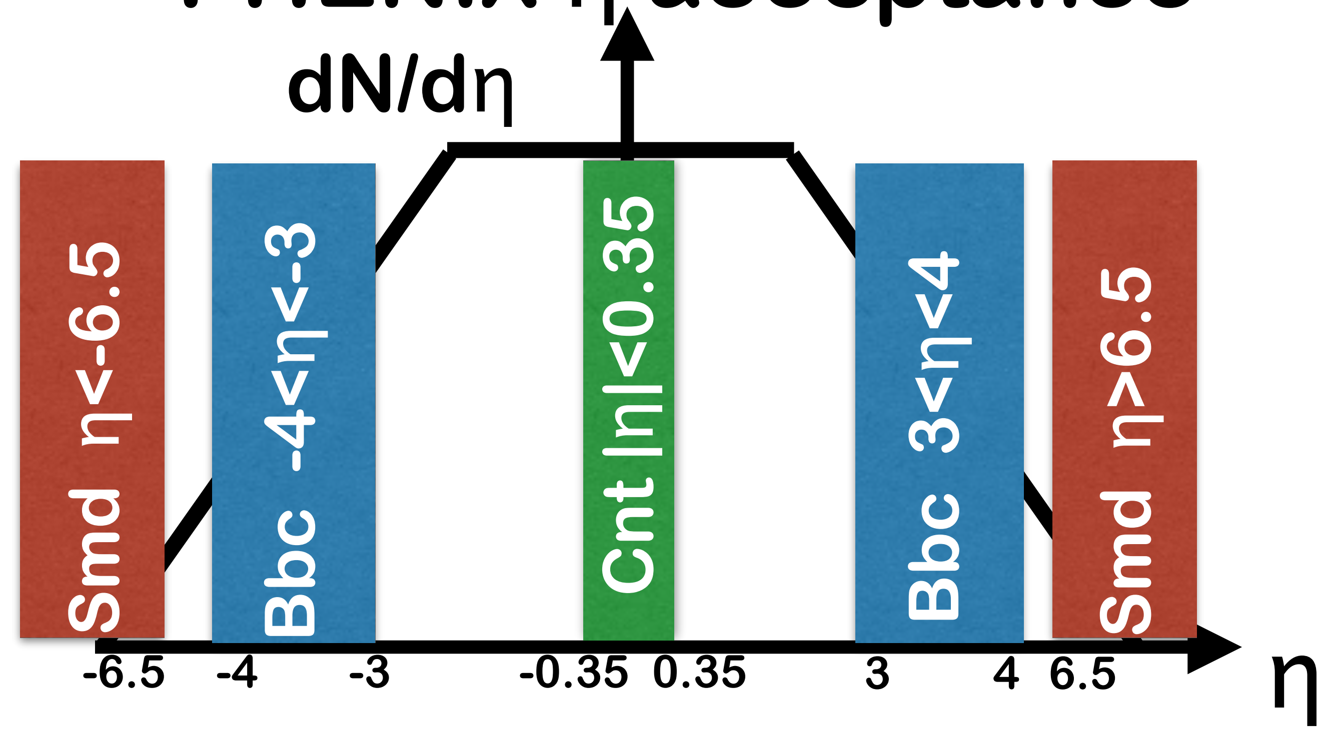

$$Res\{\Psi_{n,A}^{obs}\} = \sqrt{\frac{< cos(n[\Psi_{n,A}^{obs} - \Psi_{n,B}^{obs}]) >< cos(n[\Psi_{n,A}^{obs} - \Psi_{n,C}^{obs}]) >}{< cos(n[\Psi_{n,B}^{obs} - \Psi_{n,C}^{obs}]) >}}$$

$$< \cos(n[\Psi_{n,A}^{obs} - \Psi_{n,B}^{obs}]) >=< \cos(n[\Psi_{n,A}^{obs} - \Psi_{n}^{true} + \Psi_{n}^{true} - \Psi_{n,B}^{obs}]) >$$

$$=< \cos(n[\Psi_{n,A}^{obs} - \Psi_{n}^{true}]) >< \cos(n[\Psi_{n}^{true} - \Psi_{n,B}^{obs}]) >$$

$$= Res\{\Psi_{n,A}\}Res\{\Psi_{n,B}\}$$

Average v_n at Mid-rapidity

How to integrate vn(pT)

Weighted average using pT spectra as weights

-pT spectra: PHENIX AuAu (ppg023)

-vn : PHENIX AuAu,CuAu,CuCu(ppg124,132,183)

$$< v_n >= \frac{\sum_i \frac{dN}{dp_{T,i}} v_n(p_{T,i})}{\sum_i \frac{dN}{dp_{T,i}}}$$

-vn(pT,i) and dN/dpT,i values are obtained from fitting functions

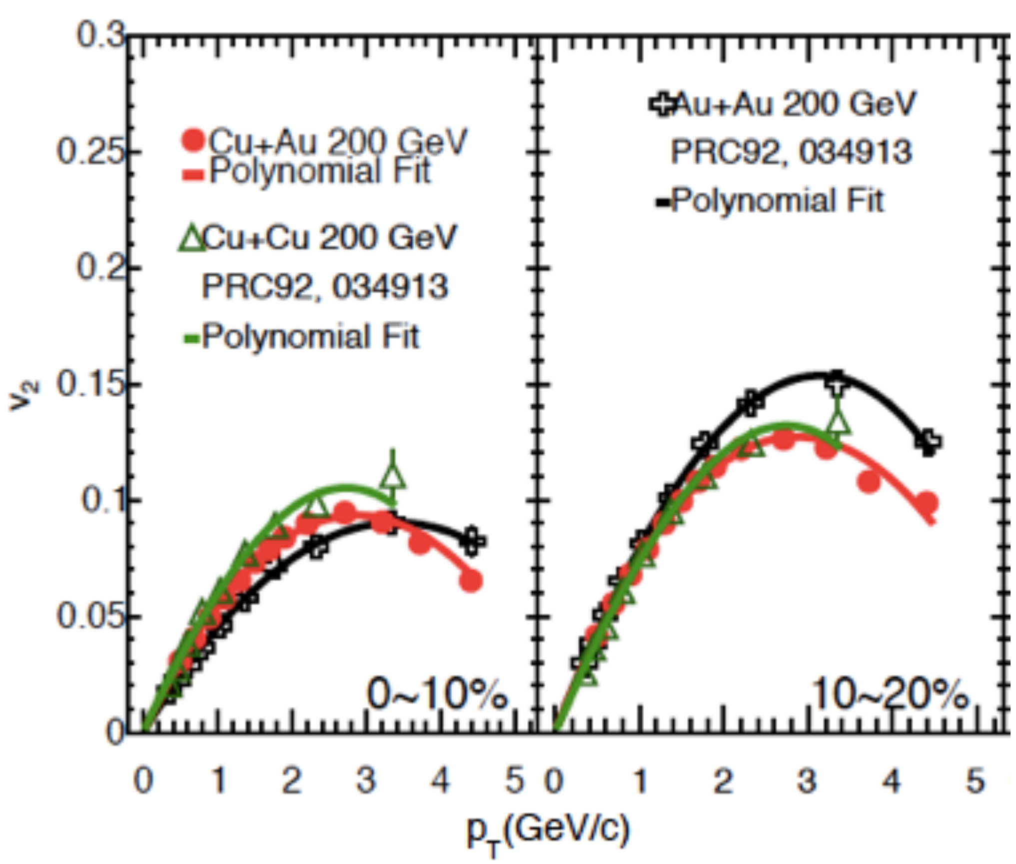

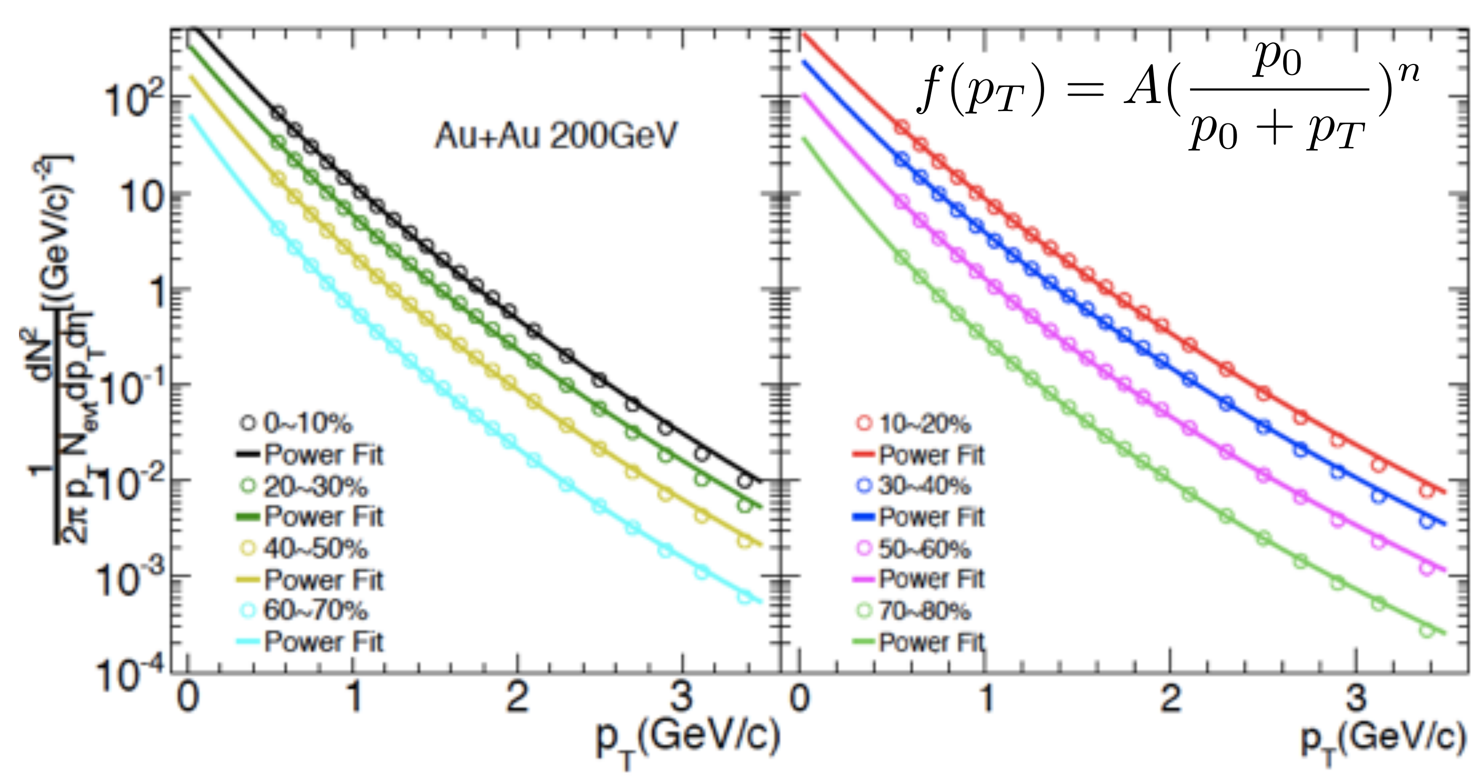

Determination of pT spectra in Cu+Cu and Cu+Au

Cu+Cu and Cu+Au spectra are assumed using Au+Au spectra
-There no published Cu+Cu and Cu+Au spectra
-$dN_{ch}/d\eta$ and <pT> depends on Npart

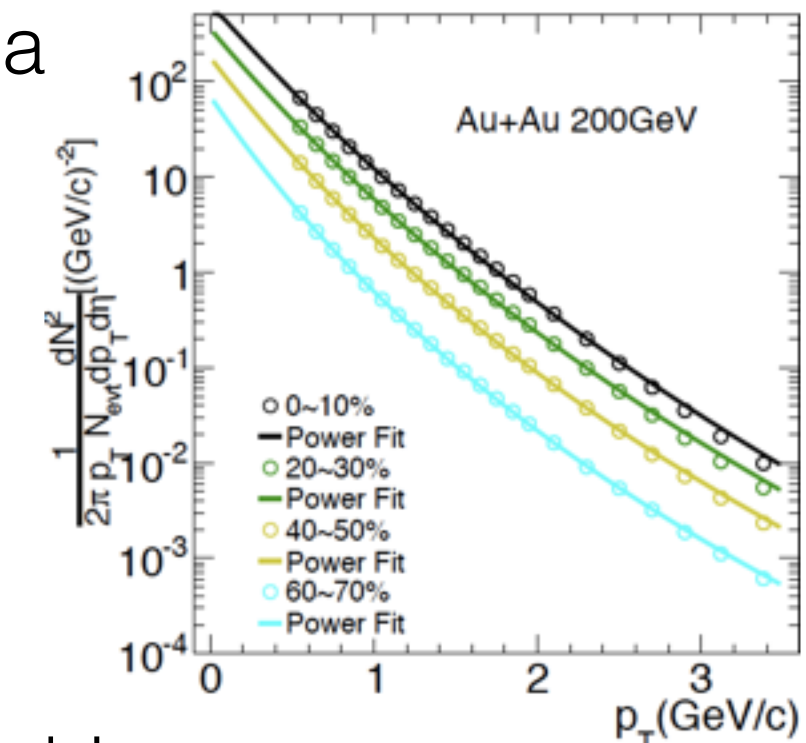

Procedure

1. Fit Au+Au spectra with $f(p_T) = A(\frac{p_0}{p_0 + p_T})^n$
   p_0 and n are free parameter
2. Obtain p_0 and n as a function of Npart
3. Make pT spectra for Cu+Cu and Cu+Au
   using $p_0(N_{part})$ and $n(N_{part})$ for corresponding N_{part} bins

$$f(p_T, N_{part}) = (\frac{p_0(N_{part})}{p_0(N_{part}) + p_T})^{n(N_{part})}$$

$p_0(N_{part})$

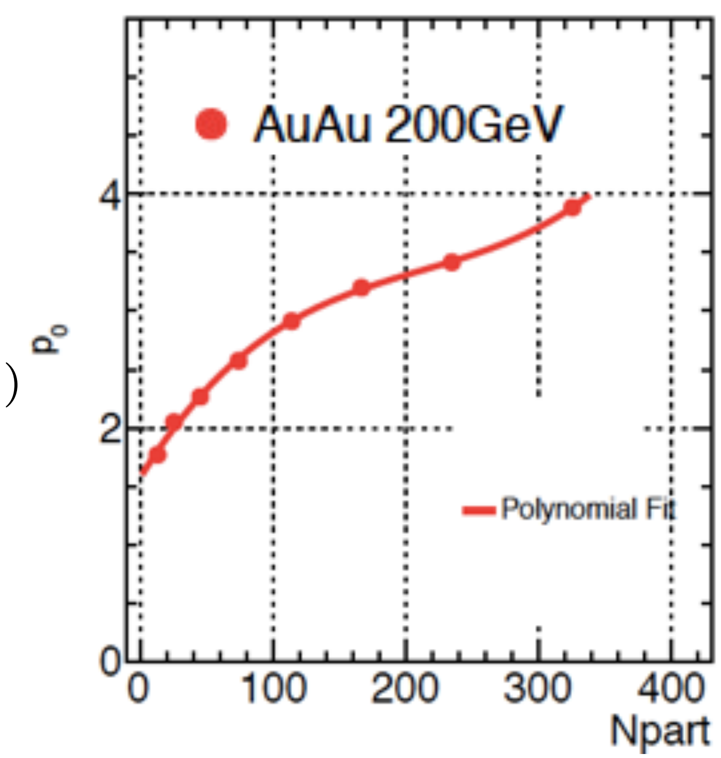

$n(N_{part})$

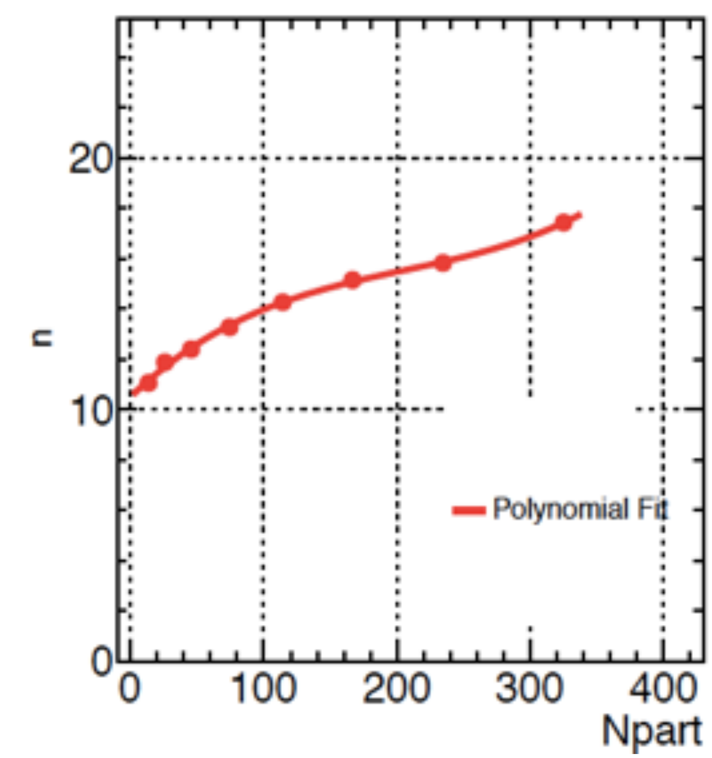

Comparison to PHOBOS

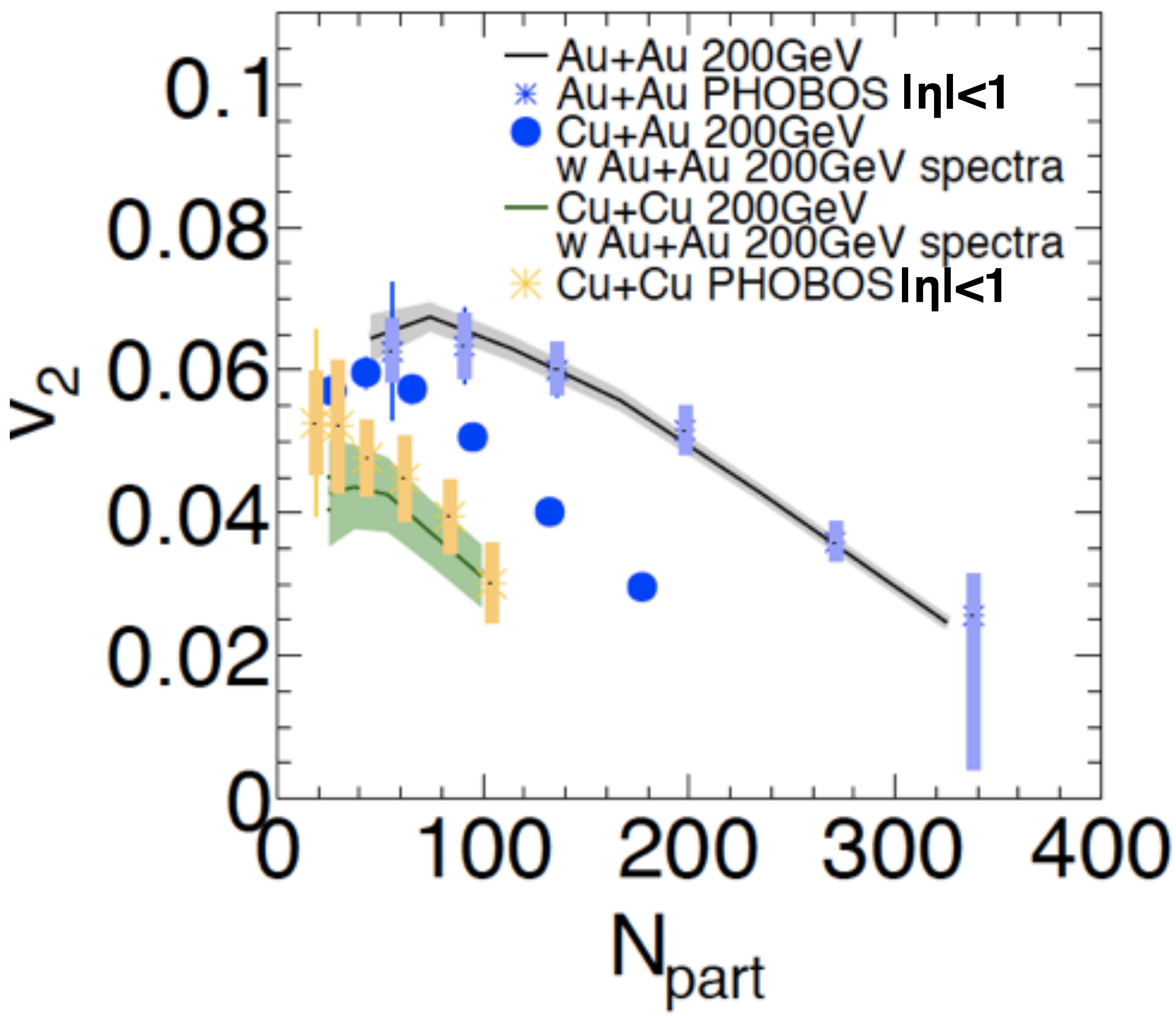

My results are consistent with PHOBOS within the error

-η range is different, PHOBOS's results are obtained wider range

pT integration is successfully done